Master's thesis

NTNU
Norwegian University of Science and Technology
Faculty of Natural Sciences
Department of Chemistry

Mari Rødseth

Chemoenzymatic synthesis of (*S*)-carteolol

Kinetic resolution by transesterification of precursors with *Candida antarctica* Lipase B

Master's thesis in Chemical Engineering and Biotechnology
Supervisor: Associate Professor Elisabeth Egholm Jacobsen

June 2021

NTNU
Norwegian University of
Science and Technology

Mari Rødseth

Chemoenzymatic synthesis of (*S*)-carteolol

Kinetic resolution by transesterification of precursors with *Candida antarctica* Lipase B

Master's thesis in Chemical Engineering and Biotechnology
Supervisor: Associate Professor Elisabeth Egholm Jacobsen
June 2021

Norwegian University of Science and Technology
Faculty of Natural Sciences
Department of Chemistry

NTNU

Kunnskap for en bedre verden

Preface

This thesis was written by Mari Rødseth as part of the two-year master program Industrial Chemistry and Biotechnology, with a specialization in Organic Chemistry. All experiments were performed at the Department of Chemistry at the Norwegian University of Science and Technology (NTNU) under the supervision of associate professor Elisabeth Egholm Jacobsen. The work was performed between January and June 2021, and built on work performed between August and December 2020. Part of the results from this project have also been published [1].

Firstly, I would like to thank Dr. Egholm Jacobsen for her guidance, interesting conversation and encouragement throughout this project. Her advice has been invaluable, as has her support of us students and willingness to answer emails at odd hours. Staff engineer Roger Aarvik is thanked for his prompt delivery of any needed supplies and lively conversation. Head engineer Julie Asmussen is thanked for her endless patience in training me, and her flexibility regarding scheduling times. Head engineers Susana Villa Gonzalez and Torun Margreta Melø are both thanked for their help regarding mass spectrometry and nuclear magnetic resonance spectroscopy experiments respectively.

I would also like to thank my fellow students Anna Tennfjord, Raymond Trohjell and Kristoffer Klungseth for being both willing and eager to exchange ideas. Their support, help and company has made late nights working significantly more enjoyable.

Lastly, I would like to thank my friends and family for their support. They have kept my spirits up through all my mistakes, of which there has been a fair amount. A special thanks to my partner, Bjørn Ole Kosberg Fuglseth, who means more to me than anything and has been completely content with late night dinners after exhausting laboratory endeavors.

Abstract

There has been an increased focus on synthesis of enantiopure active pharmaceutical ingredients in the last few decades. Combined with the growing demand for environmentally friendly chemistry, it is of great interest to explore biocatalytic synthesis and resolution of biologically active compounds. As a contribution to the further examination of such processes, this project focused on the chemoenzymatic synthesis of β-blocker (*S*)-carteolol ((*S*)-**4**).

The synthesis was carried out in four steps, indicated with reaction conditions and yields in Scheme 0.1. In the first synthesis step, 5-(3-chloro-2-hydroxypropoxy)-3,4-dihydroquinolin-2(1H)-one (**2a**) and 5-hydroxy-(2,3-epoxypropoxy)-3,4-dihydroquinolin-2(1H)-one (**2b**) were formed by an S_N2 substitution of epichlorohydrin with 5-hydroxy-3,4-dihydroquinolin-2(1H)-one (**1**) in a basic environment. The reaction was performed with 2 equivalents epichlorohydrin and 0.3 equivalents sodium hydroxide dissolved in a water- and dimethyl sulfoxide solution [3:2], at room temperature for 24 hours. A **2a**:**2b** [75:24] product mixture was obtained in 91% of the expected amount when adjusted for product composition.

In the second synthesis step, epoxide **2b** was opened with lithium chloride in an acidic environment, forming chlorohydrin **2a**. The reaction was performed with 2 equivalents lithium chloride and 2 equivalents acetic acid dissolved in acetonitrile, at room temperature for 24 hours. Chlorohydrin **2a** was obtained in 83% of the expected amount when adjusted for the composition of starting material, and in 76% total yield across both steps.

Chlorohydrin (*R*)-**2a** was obtained by enzymatic kinetic resolution in the third synthesis step. Racemic **2a** underwent an enantioselective transesterification reaction with vinyl butanoate, forming ester (*S*)-1-chloro-3-((2-oxo-1,2,3,4-tetrahydroquinolin-5-yl)oxy)propan-2-yl butanoate ((*S*)-**3**). The reaction was performed with 5 equivalents vinyl butanoate and *Candida antarctica* Lipase B (1.0 g / 1.0 mmol **2a**) in dry acetonitrile, at 37 °C and with 200 rpm for 74 hours. Chlorohydrin (*R*)-**2a** was obtained in 38% yield and 97% *ee*. Ester (*S*)-**3** was obtained in 43% yield and 77% *ee*. An enantiomeric ratio of 27 was calculated.

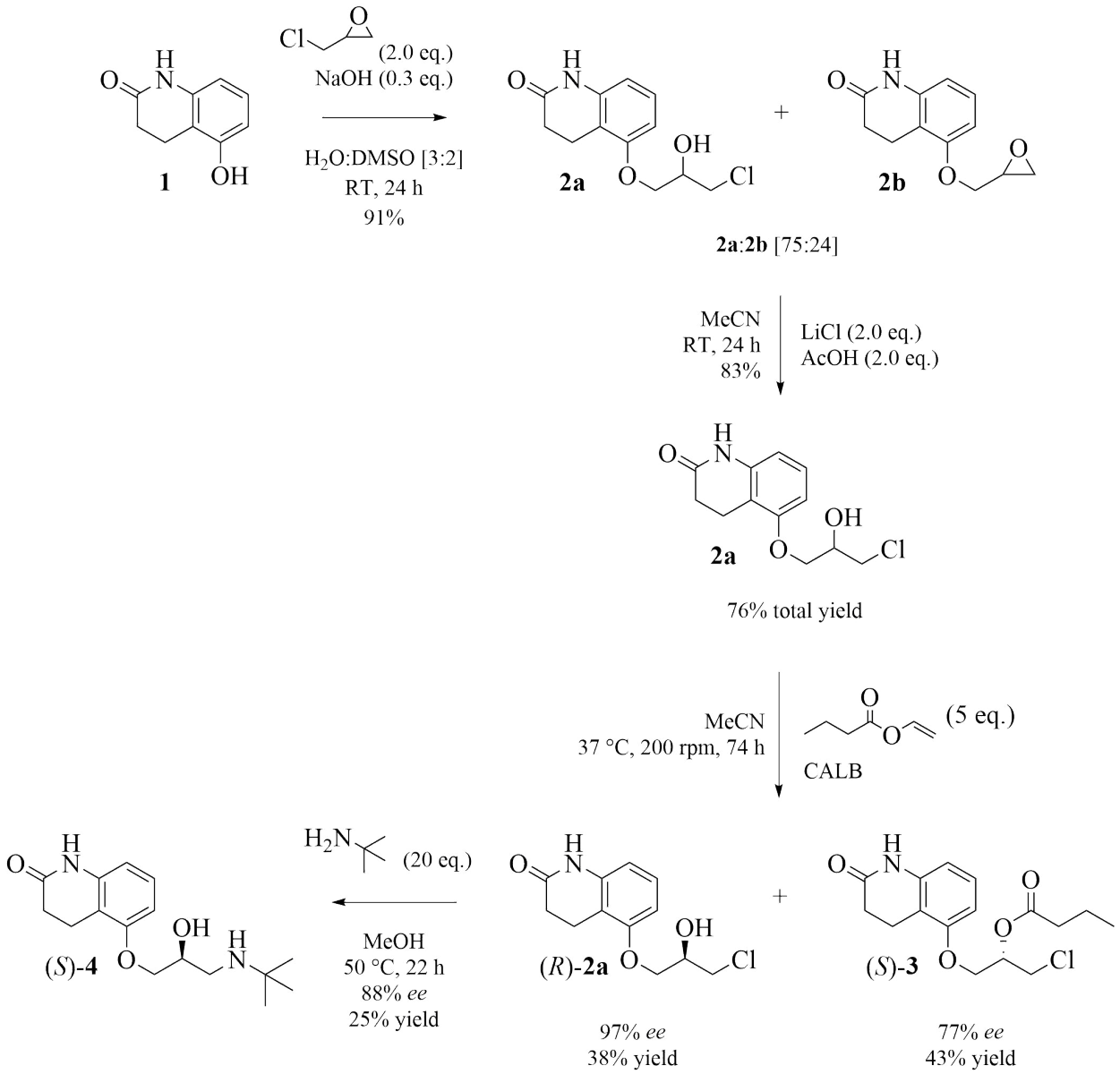

Scheme 0.1: Synthesis of (*S*)-carteolol ((*S*)-**4**) from alcohol **1** *via* kinetic resolution of chlorohydrin **2a**.

In the fourth and final synthesis step, (*S*)-**4** was formed by alkylation of *tert*-butylamine with chlorohydrin (*R*)-**2a**. The reaction was performed with 20 equivalents *tert*-butylamine in methanol, at 50 °C for 22 hours. The product was extracted and purified by flash chromatography (*iso*-propanol:*n*-hexane:diethylamine [80:20:3]). (*S*)-**4** was obtained in 25% yield and with 88% *ee*.

Synthesis of racemic **4** was performed with the same reaction conditions, see Scheme 0.2. After extraction, racemic **4** was obtained in 77% yield.

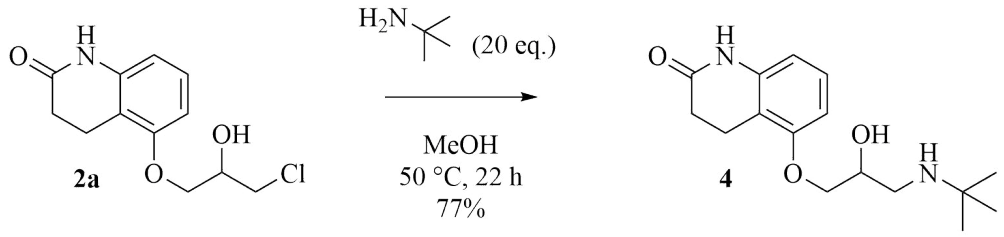

Scheme 0.2: Synthesis of carteolol (**4**) by alkylation of *tert*-butylamine with racemic chlorohydrin **2a**.

Synthesis of 5-(3-fluoro-2-hydroxypropoxy)-3,4-dihydroquinolin-2(1H)-one (**2d**) was also explored. The reaction was performed with 2 equivalents epifluorohydrin and 0.3 equivalents sodium hydroxide, at room temperature for 24 hours, see Scheme 0.3. Fluorohydrin **2d** was obtained in a 75% yield.

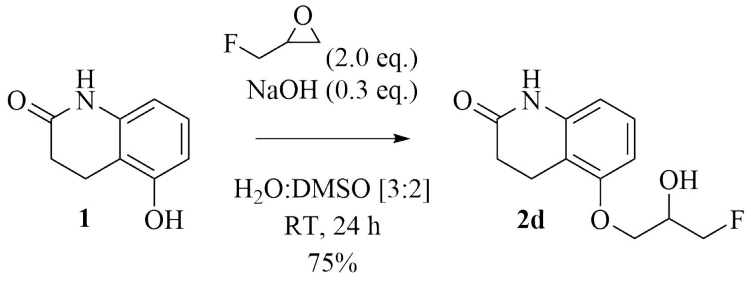

Scheme 0.3: Synthesis of fluorohydrin **2d** from alcohol **1** by use of epifluorohydrin in alkaline conditions.

Sammendrag

Det har vært et økt fokus på syntese av enantiomert rene aktive farmasøytiske ingredienser de siste tiårene. Kombinert med et økende behov for miljøvennlig kjemi så er det av stor interesse å utforske biokatalytisk syntese og oppløsning av biologisk aktive stoffer. Som et bidrag til videre forskning på slike prosesser vil dette prosjektet fokusere på kjemoenzymatisk syntese av β-blokker (*S*)-carteolol ((*S*)-**4**).

Syntesen gikk over fire trinn, som er vist med reaksjonsbetingelser og utbytter i Skjema 0.4. I det første syntesetrinnet dannes 5-(3-kloro-2-hydroksypropoksi)-3,4-dihydroquinolin-2(1H)-on (**2a**) og 5-hydroksy-(2,3-epoksypropoksi)-3,4-dihydroquinolin-2(1H)-on (**2b**) ved en S_N2 substutisjon av epiklorhydrin med 5-hydroksy-3,4-dihydroquinolin-2(1H)-on (**1**) i basisk miljø. Reaksjonen ble utført med 2 ekvivalenter epiklorhydrin og 0.3 ekvivalenter natriumhydroksid løst i en vann- og dimetylsulfoksidløsning [3:2], ved romtemperatur i 24 timer. En **2a**:**2b** [75:24] produktblanding ble oppnådd i 91% av forventet mengde etter justering for produktkomposisjon.

I det andre syntesetrinnet ble klorhydrin **2a** formet ved åpning av epoksid **2b** med litiumklorid i surt miljø. Reaksjonen ble utført med 2 ekvivalenter litiumklorid og 2 ekvivalenter eddiksyre løst i acetonitril, ved romtemperatur i 24 timer. Klorhydrin **2a** ble oppnådd i 83% av forventet mengde etter justering for komposisjonen av startmaterialet, og i 76% totalt utbytte over begge trinn.

Klorhydrin (*R*)-**2a** ble oppnådd ved enzymatisk kinetisk oppløsning i det tredje syntesetrinnet. Rasemisk **2a** ble enantioselektivt omestret med vinylbutanoat og formet ester (*S*)-1-kloro-3-((2-okso-1,2,3,4-tetrahydroquinolin-5-yl)oksy)propan-2-ylbutanoat ((*S*)-**3**). Reaksjonen ble utført med 5 ekvivalenter vinylbutanoat og *Candida antarctica* Lipase B (1.0 g / 1.0 mmol **2a**) i tørr acetonitril, ved 37 °C og 200 rpm i 74 timer. Klorhydrin (*R*)-**2a** ble oppnådd i 38% utbytte og 97% *ee*. Ester (*S*)-**3** ble oppnådd i 43% utbytte og 77% *ee*. En enantiomerisk ratio på 27 be kalkulert.

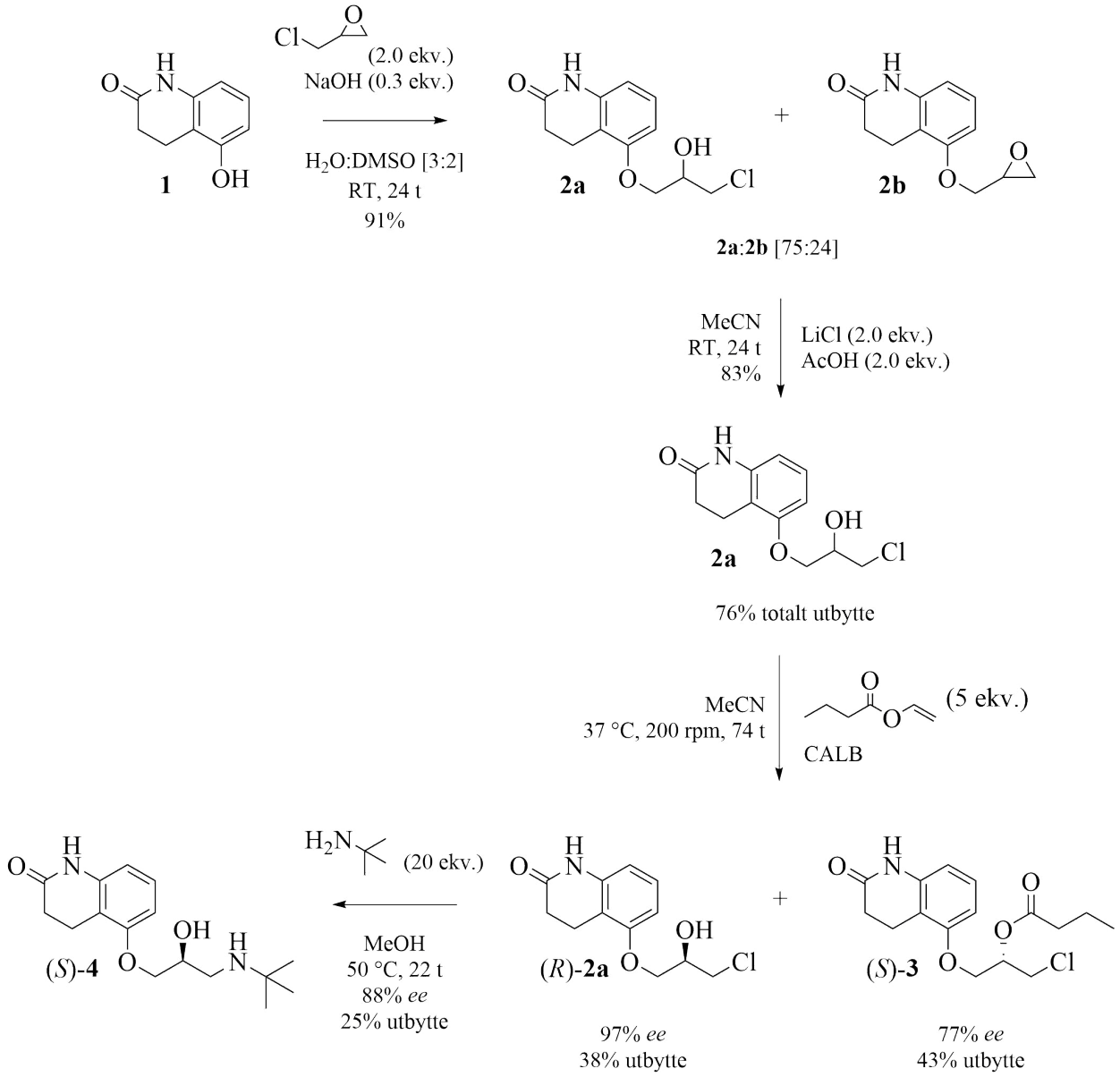

Scheme 0.4: Syntese av (*S*)-carteolol ((*S*)-**4**) fra alkohol **1** *via* kinetisk oppløsning av klorhydrin **2a**.

I det fjerde og endelige syntesetrinnet ble (*S*)-**4** dannet ved alkylering av *tert*-butylamin med klorhydrin (*R*)-**2a**. Reaksjonen ble utført med 20 ekvivalenter *tert*-butylamin løst i metanol, ved 50 °C i 22 timer. Produktet ble ekstrahert og renset ved flash kromatografi (*iso*-propanol:*n*-heksan:dietylamin [80:20:3]). (*S*)-**4** ble oppnådd i 25% utbytte og 88% *ee*.

Syntese av rasemisk **4** ble utført under de samme reaksjonsbetingelsene, se Skjema 0.5. Etter ekstraksjon ble rasemisk **4** oppnådd i 77% utbytte.

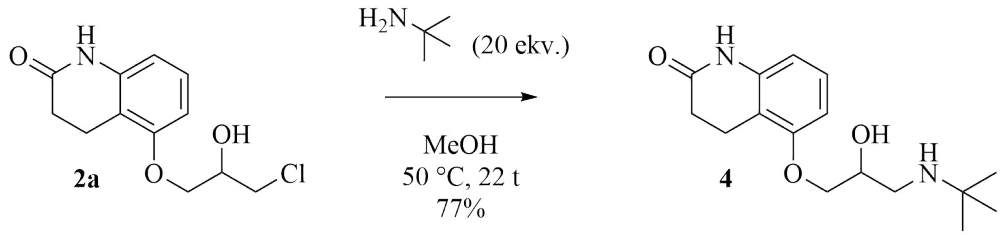

Scheme 0.5: Syntese av carteolol (**4**) ved alkylering av *tert*-butylamin med rasemisk klorhydrin **2a**.

Syntese av 5-(3-fluoro-2-hydroksypropoksi)-3,4-dihydroquinolin-2(1H)-on (**2d**) ble utforsket. Reaksjonen ble utført med 2 ekvivalenter epifluorhydrin og 0.3 ekvivalenter natriumhydroksid løst i en vann- og dimetylsulfoksidløsning [3:2], ved romtemperatur i 24 timer, se Skjema 0.6. Fluorhydrin **2d** ble oppnådd i et 75% utbytte.

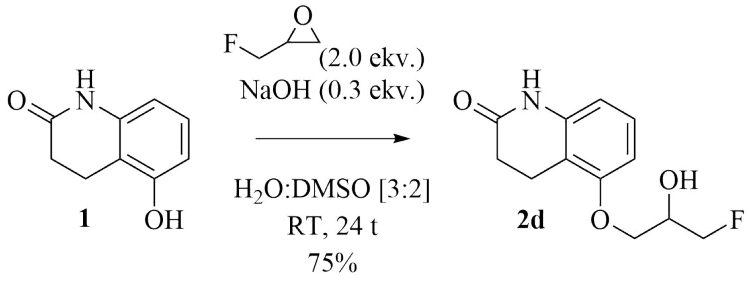

Scheme 0.6: Syntese av fluorhydrin **2d** fra alkohol **1** ved bruk av epifluorhydrin i basisk miljø.

Compound Overview

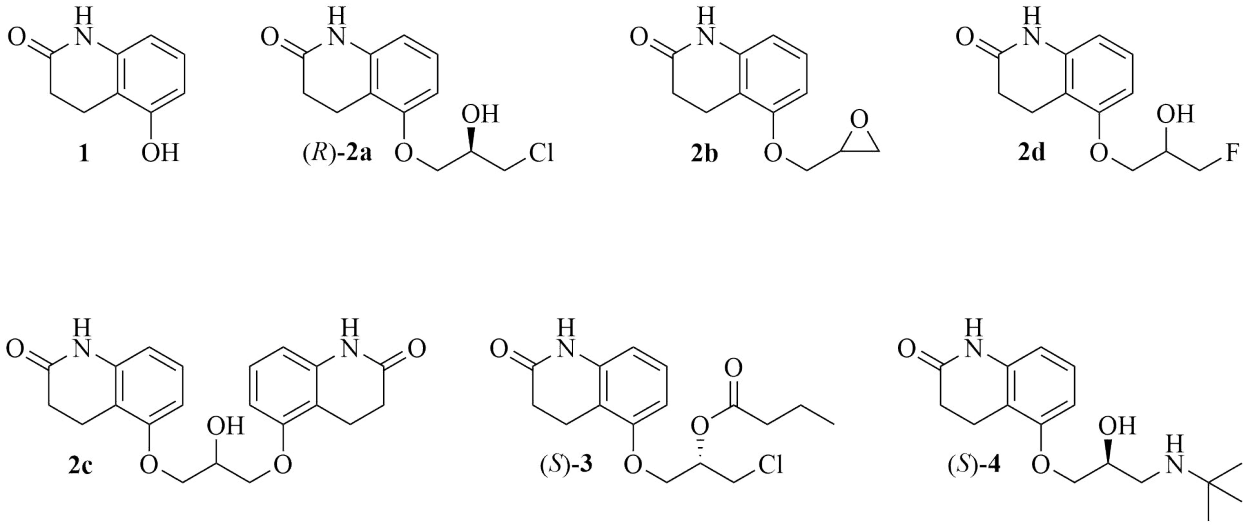

Figure 0.1: An overview presenting the starting material, intermediate products, byproducts and the final product.

Contents

1 Introduction

1.1 Primary open-angle glaucoma

Glaucoma is the term for an eye condition caused by intraocular pressure (IOP) that result in nerve damage and reduced sight [2]. In 2013, patients diagnosed with glaucoma were estimated to comprise 3.5% of the world population aged 40 to 80 [3]. In 2020, glaucoma was reported as the second leading cause to blindness, with 3.6 million people going irreversibly blind from the condition [4]. This constitutes 11% of all global cases of blindness in that year. Similarly, 4.1 million people suffered moderate- to severe vision impairment due to glaucoma in the same period.

Different types of glaucoma are classified by their respective structural changes in the eye, where the most common type is primary open-angle glaucoma (POAG) [2]. For patients diagnosed with POAG, damage to the optical nerve is caused by elevated IOP from an imbalance in secretion of aqueous humor and outflow. The condition often has a slow onset without pain, and is therefore not diagnosed until an advanced stage, where the patient experiences gradual blindness. In 2013, 3.0% of the world population aged 40 to 80 suffered from POAG [3]. Early discovery and proper treatment of its effects is integral for the reduction of patient blindness associated with the condition [2].

Topical application of β-adrenergic antagonists, widely known as β-blockers, has become a common treatment of open-angle glaucoma [2]. The β-antagonists diminish the production of aqueous humor in the eye by targeting β-receptors in the ciliary epithelial [5]. This alleviates IOP. Many commercially available ophthalmic drugs therefore employ β-antagonists like carteolol, timolol and betaxolol as the active pharmaceutical ingredient [2].

1.2 β-Adrenergic receptors and antagonists

The effect of drugs are transmitted by the binding of their active pharmaceutical ingredient (API) to certain receptors. The API of a drug is the ingredient with biological impact, and

relayed effects depend on the kind of receptor targeted. Compounds with high affinity for the receptor will incite strong biological responses.

β-Adrenergic antagonists are a group of biologically active compounds that target the β-adrenergic receptors. There are primarily three types of β-adrenergic receptors: β1-, β2- and β3-receptors. It has been shown that both β1- and β2-receptors affect the production of humor in the ciliary epithelial of rabbits [5].

β-receptors are essential to the sympathetic nervous system as they also mediate the effect of β-adrenergic agonists such as the catecholamines epinephrine (adrenaline) and norepinephrine [6]. Inhibition of agonist-binding to the receptors induces effects such as a decrease in heart rate, prompting use of β-blockers in e.g. treatment of chronic heart failure [7, 8]. The involvement of norepinephrine dysregulation in anxiety and depression also suggests that β-blockers may contribute positive effects in medical regulation of related mental health conditions [9].

1.3 β-Blocker carteolol

Carteolol (Figure 1.1) has been shown to alleviate IOP in patients with POAG [10], and is the API in commercially available ophthalmic drugs like Ocupress (US) [11] and Teoptic (UK) [12]. It is generally sold as 1% or 2% solutions that are topically applied twice daily [13]. One study [14] reported a reduction in formation of aqueous humor by 20.4% in patients with elevated IOP who were treated with carteolol [13].

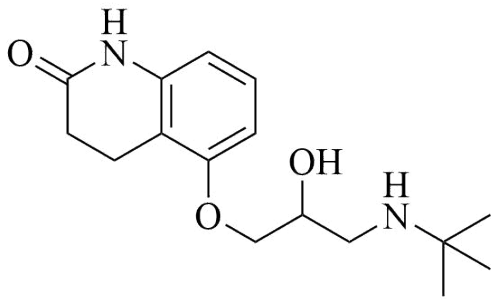

Figure 1.1: The chemical structure of β-blocker and ophthalmic drug carteolol.

Compared with β-antagonists like timolol, fewer ocular symptoms were experience during treatment with carteolol [13]. Especially burning of the eyes was reported [15]. One study has also reported fewer incidents of adverse cardiovascular effects with carteolol than with timolol [16]. Timolol was found to cause lower heart rates and more nocturnal bradycardia than carteolol. It is believed that these effects are caused by the intrinsic sympathomimetic activity of carteolol, an ability to stimulate β-adrenergic receptors in addition to blocking β-agonists.

The β-antagonistic abilities of carteolol are categorized as non-selective, meaning it inhibits activity of all three known β-receptor types. No difference in effect on IOP has been reported between selective and non-selective β-blockers [17]. Carteolol has also shown antagonistic action against β-agonists such as isoprenaline [18].

1.3.1 Synthesis of racemic carteolol

Carteolol has commonly been synthesized as a racemate from 5-hydroxy-3,4-dihydroquinolin-2(1H)-one in two steps. First, an S_N2 substitution of an epihalogenohydrin with the alcohol is performed in alkaline conditions. This forms the epoxide precursor 5-hydroxy-(2,3-epoxypropoxy)-3,4-dihydroquinolin-2(1H)-one, which is further employed in the alkylation of *tert*-butylamine where carteolol is formed.

Deprotonation of the starting material was performed by *in situ* generation of methoxide by Nakagawa *et al.* [18]. They obtained the epoxide precursor in 55% yield. After alkylation of *tert*-butylamine, carteolol was obtained in 58% yield. Tamura *et al.* [19], who patented their method in 1975, performed the same synthesis in a sodium hydroxide solution (1.5%). No additional solvent was added, and the epoxide was obtained in 53% yield. Carteolol was obtained in 53% yield after the amine alkylation step. Both research groups performed these reactions at elevated temperatures and with reagents in excess.

Mangishi *et al.* [20] performed the first synthesis step with sodium hydroxide in a water- and dimethyl sulfoxide solution, see Scheme 1.1. They used catalytic amounts of sodium

hydroxide and ran the reaction at room temperature for 24 hours. The epoxide was obtained in 80% yield with this method. This suggests that use of dimethyl sulfoxide and lower temperatures was beneficial. After alkylation of *tert*-butylamine at elevated temperatures, carteolol was obtained in 80% yield.

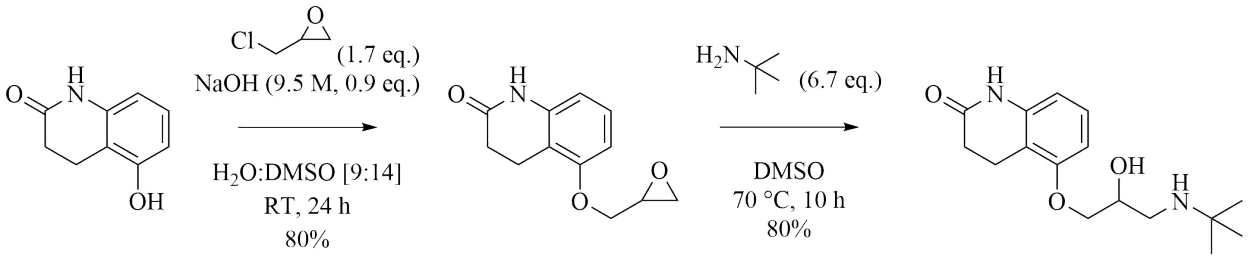

Scheme 1.1: Synthesis of racemic carteolol by alkylation of 5-hydroxy-3,4-dihydroquinolin-2(1H)-one with epichlorohydrin in a basic environment, and alkylation of *tert*-butylamine with the epoxide precursor 5-hydroxy-(2,3-epoxypropoxy)-3,4-dihydroquinolin-2(1H)-one [20].

1.3.2 S_N2 substitution reactions

Substitution reactions are a class of reactions in which an electronegative group of the substrate is replaced by a another nucleophile [21]. There are two mechanisms involved, the S_N1- and S_N2 mechanisms, where the first is unimolecular and the second bimolecular. These terms refer to the number of involved components during the rate determining step, which means there are two molecules involved in an S_N2 reaction. The S_N2 mechanism occurs in one step with simultaneous nucleophilic back-side attack on the electrophilic reaction center and displacement of the leaving group. In reactions with asymmetric substrates, a back-side attack will lead to an inversion in stereochemistry, see Scheme 1.2.

The reaction rate, r, of an S_N2 reaction depends on the concentration of substrate $[S]$ and nucleophile $[Nu]$, see Equation (1.1) [21]. Either can be increased to promote faster reaction times. Other factors, such as steric hindrance and basicity of the leaving group, also affect reactivity of a compound.

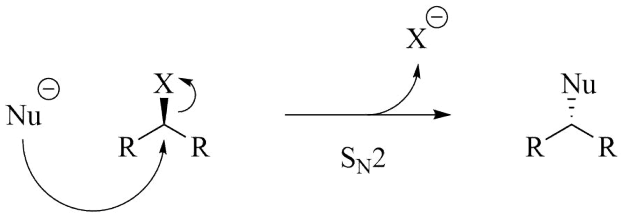

Scheme 1.2: Illustrated mechanism of an S_N2 reaction where the leaving group (X^-) is displaced simultaneously as the nucleophilic (Nu^-) attack. This mechanism was proposed by Edward Hughes and Christopher Ingold in 1937 [21].

$$r = k \times [S] \times [Nu] \tag{1.1}$$

Steric hindrance at the reaction site has an adverse effect on S_N2 mechanisms as it prevents sufficient access for the concurrent insertion of nucleophile and displacement of leaving group [21]. Heavily substituted reaction sites will thus process under an S_N1 mechanism. Similarly, the basicity of the leaving group will determine the ease with which a substitution can proceed. Polar aprotic solvents facilitate S_N2 substitutions as there is less coordination between solvent and nucleophile [21].

Many substitution reactions are performed by *in situ* generation of the nucleophile, often by deprotonation of an alcohol with a proton acceptor [21]. A common example of an S_N2 reaction is the Williamson ether synthesis, in which the nucleophile is an alkoxide displacing the halide ion from an alkyl halide to form an ether [21].

1.3.3 Alkylation of primary amines

Amines are good nucleophiles and will readily react with alkyl halides in nucleophilic aliphatic substitution reactions, see Scheme 1.3 [21]. As discussed in Section 1.3.2, a primary alkyl halide will more readily follow an S_N2 mechanism than an S_N1 mechanism.

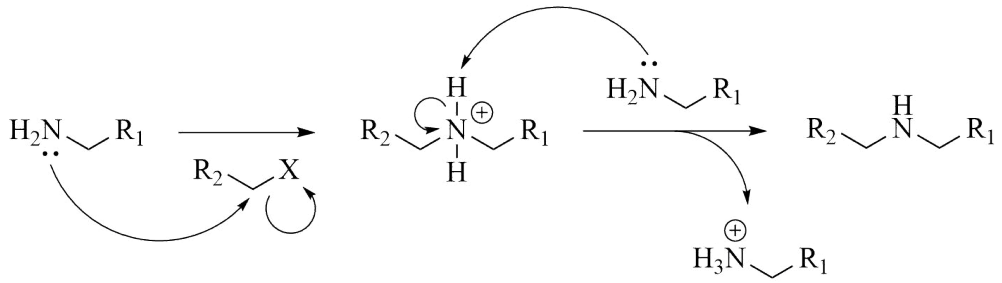

Scheme 1.3: Alkylation of a primary amine by S_N2 reaction with an alkyl halide. The protonated intermediate is deprotonated by the starting amine [21, 22].

The alkylated amine is often just as reactive as the starting amine, if not even more so [22]. For this reason, the alkylation of the product may compete with that of the starting material to form tetra-alkylated salts, see Scheme 1.4. This can be circumvented by using a sterically hindered amine, such as *tert*-butylamine. The steric hindrance of the tert-butyl group will prevent further alkylation.

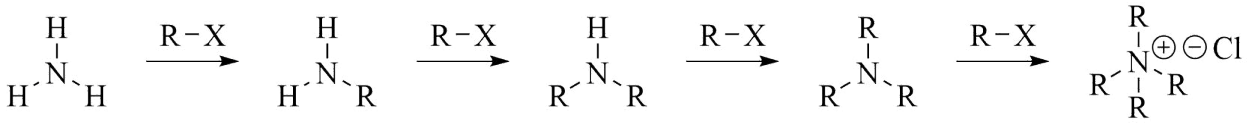

Scheme 1.4: Formation of a tetra-substituted amine salt by multiple alkylations of the amine [22].

1.4 Importance of enantiopure APIs

A chiral compound is considered enantiomerically pure when it consists of only one of its enantiomers. Synthesis of enantiopure APIs has become increasingly important since discovering that one of the enantiomers may have no- or even adverse effects. (*S*)-Thalidomide is the most famous example of this. The U.S. Food and Drug Administration (FDA) issued a guidance document in 1992, where they urged pharmaceutical companies to focus their efforts on single-enantiomer APIs above racemic ones [23]. Since then, drugs with single-enantiomer ingredients have dominated an increasingly large part of the pharmaceutical marked. Some are launched as novelty drugs and others as chiral switches. Where novelty drugs contain only novelty APIs, chiral switches are single-enantiomer relaunches of existing

pharmaceuticals [24]. The concept of chirality is further elaborated in the section below.

1.4.1 The biological effect of chirality

Chirality is a geometric property of a molecule caused by an asymmetric center [21]. This is a form of stereochemistry, and each steric center forms two different stereoisomers: the (R)-enantiomer and the (S)-enantiomer, see Figure 1.2. Each enantiomer is the non-superimposable mirror-image of the other, and may have vastly different biological effects.

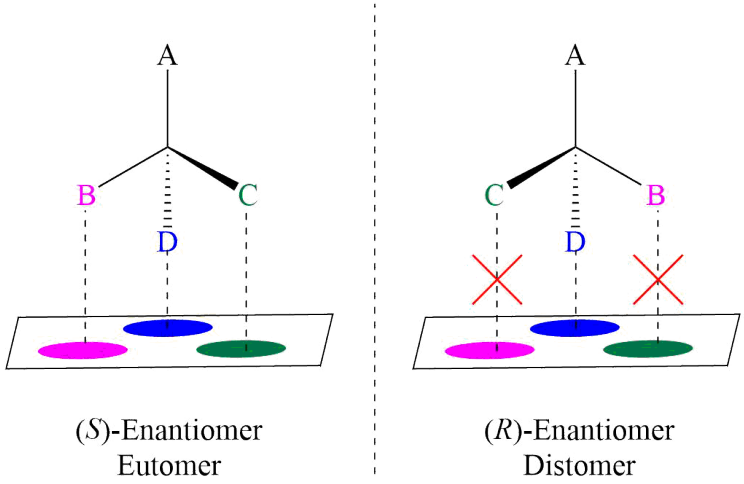

Figure 1.2: Illustration of the difference in compatibility between enantiomers and the associated chiral receptor. For the eutomer there is full compatibility, while the distomer is incompatible with the same receptor [25].

The enantiomers of a chiral compound will not exhibit distinctive chemical or physical properties until they are placed in chiral environments. As the chemical processes in living organisms are chiral, this can induce a difference i biological activity. The dissimilar three-dimentional structures may for example cause incompatibility with the binding cite of an enzyme, see Figure 1.2 [25]. The biologically active enantiomer is called an eutomer, while the enantiomer with no or adverse pharmacological effects is called the distomer [26]. Scientific ascertainment of the two is commonly achieved by chiral chromatography or polarimetry, see Section 1.9.

There are many examples of biologically active compounds where one enantiomer induces different effects than the other. A significant difference in effect between enantiomers has been reported for carteolol [27]. The binding sites of β-receptors in guinea-pig tissue discriminate stereochemically between the (R)- and (S)-enantiomers. While there is no discernible difference in inhibition of β-receptors in the ciliary body of guinea-pigs, the (S)-enantiomer was found to have 10 times the β-antagonistic activity of the (R)-enantiomer in atria- and trachea tissues.

Another example is citalopram, which is a seretonin reuptake antagonist prescribed for depression [28]. The (S)-enantiomer of citalopram holds 30 times the potency of the (R)-enantiomer and is commercially sold under the name Lexapro. Similarly, the effects of atenolol, a β-blocker prescribed for blood-pressure related ailments such as arrhythmia and angina, are only contributed to by the (S)-enantiomer [29, 30]. Many β-blockers are only biologically active in their (S)-enantiomeric form.

1.4.2 Single-enantiomer synthesis

Enantiopure APIs can either be synthesized enantioselectively or separated by chiral resolution techniques after synthesis. There are primarily three forms of enantioselective synthesis: chiral pool synthesis, chiral auxiliary synthesis and enantioselective catalysis [31].

In chiral pool synthesis, the stereochemistry of a chiral reactant is retained during reaction [31]. An example is the synthesis of (2S,3S)-3-hydroxyproline from a pyroglumatic acid derivative [32]. This method is effective when synthesis can be performed from naturally occurring starting materials such as sugars. As many pharmaceutical ingredients require long and convoluted synthesis pathways with this strategy, they produce low yields.

Chiral auxiliaries may be used for addition to- and asymmetric induction of a racemic starting material [31]. It requires stochiometric amounts of the auxiliary, as well as an addition and elimination step. As with chiral pool synthesis, the extra steps may negatively impact product yield and synthesis cost-efficiency.

Enantioselective catalysis requires only catalytic amounts of the enantiopure compound. The most important catalysts used for this purpose are metal-ligand complexes with chiral ligands, chiral organocatalysts and biocatalysts [31]. An example is the method of catalytic asymmetric dihydroxylation developed by Sharpless *et al.* [33].

1.4.3 Chiral resolution

Resolution of enantiomers after synthesis of a racemic mixture is a much used approach to obtaining single-enantiomer compounds. Diastereomeric salt formation is a strategy where the racemic target compound is treated with an enantiopure resolving agent [34]. This forms two diastereomers that can then be separated by crystallization, filtration or achiral chromatography. Depending on the target enantiomer, decomposition of the salt may be necessary.

Of more modern techniques, chromatography is often used, see Section 1.9.1. The compounds are either separated indirectly through derivatization, or directly by use of chiral stationary- or mobile phases [31].

Kinetic resolution is another viable strategy for separation of enantiomers. A chiral catalyst reacts selectively with one of the compound enantiomers, leaving the other unreacted. As one enantiomer predominantly exists in the derivatized form, separation of the two can be performed by achiral methods [35]. Both chemical and enzymatic catalysts are much used, and enzymatic kinetic resolution will be further discussed in Section 1.7.1.

1.5 Synthesis of (*S*)- and (*R*)-carteolol

Synthesis of (*S*)-carteolol from 5-hydroxy-3,4-dihydroquinolin-2(1H)-one has previously been performed by use of chiral reagents, see Scheme 1.5. The method was patented by Wei *et al.* [36] in 2008, who obtained (*R*)-epichlorohydrin commercially. They deprotonated the starting material with sodium hydroxide and alkylated it with (*R*)-epichlorohydrin. From this they obtained the epoxide precursor (*S*)-5-hydroxy-(2,3-epoxypropoxy)-3,4-dihydroquinolin-

2(1H)-one in an 80% yield and with 99.5% *ee*. *tert*-Butylamine was then alkylated with the epoxide precursor, forming (*S*)-carteolol in a 72% yield, also with 99.5% *ee*. This method is simple and effective, but requires the use of commercially available, single-enantiomer reagents.

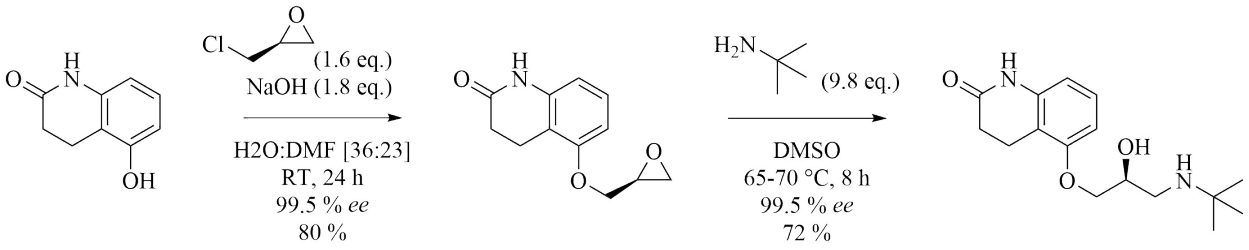

Scheme 1.5: Synthesis of (*S*)-carteolol by alkylation of 5-hydroxy-3,4-dihydroquinolin-2(1H)-one with (*R*)-epichlorohydrin in a basic environment, and alkylation of *tert*-butylamine with the epoxide precursor (*S*)-5-hydroxy-(2,3-epoxypropoxy)-3,4-dihydroquinolin-2(1H)-one [36].

Chiral pool synthesis of (*S*)- and (*R*)-carteolol has also been performed using D-mannitol as starting material. The experiment was conducted by Tsuda *et al.* [37], who synthesized the (*S*)-enantiomer in a 6% yield and the (*R*)-enantiomer in a 14% yield. The low output was due to the number of steps required to convert D-mannitol to carteolol, a prevalent problem with chiral pool synthesis of complex compounds.

1.6 Green Chemistry

In the field of sustainable chemistry, the principles of green chemistry and synthesis design have become increasingly important. The approach is founded in reduction or elimination of the use and generation of environmentally hazardous chemicals, often with an associated increase in long-term profits [38, 39]. From this concept, twelve principles were formulated to provide a guideline for product- and process design, commonly shared under the acronym PRODUCTIVELY. The principles revolve around waste reduction and prevention of hazardous byproduct formation, as well as general points of environmental impact reduction such as increased energy efficiency and use of renewable materials.

The principles of green chemistry should be applied as a cohesive system of design across all stages of chemical syntheses that strive towards a more sustainable process [38, 39]. This often requires redesign of products and processes at the molecular level. Incorporation of chemical properties relevant to health and environment into product development and processing is therefore necessary.

While one would think that large-scale production of harsh chemicals is the worst perpetrator of green chemistry principles, the pharmaceutical industry is often considered worse [40]. That is because small amounts of product require large amounts of waste during their syntheses, leading to massive environmental footprints. For these reasons, the use of biocatalysis in the synthesis of pharmaceutical ingredients is viewed as an industrial process concurrent with the principles of green chemistry. Biocatalysis affords high yield and purity, while simultaneously avoiding other, more harmful catalytic agents and permitting milder reaction conditions than otherwise required.

1.7 Biocatalysis in organic chemistry

Enzymes are found in all living organisms - small as large - and are complex proteins that catalyze the chemical processes necessary for life. They were used for commercial production of alcoholic beverages from barley as early as 6000 BC [41]. In the current century, enzymes are used in everything from the food industry to the fashion industry [42].

Enzymes are natural catalysts, which mean that they lower the activation energy of a reaction and increase reaction rate. As all living things are chiral, enzymes often also express a preference for one enantiomer of a chiral compound. This enantioselectivity, together with the general chemoselectivity enzymes possess, has inspired the industrial use of enzymes for a wide variety of chiral syntheses and -resolutions [43].

The benefit of using enzymes over chemical catalysts are many. Reactions catalyzed by enzymes can proceed 10^8 to 10^{10} times faster than when unassisted [44], which is much faster than rates achieved with chemical catalysts [43]. Enzymes may also be used in concentrations

down to 10^{-4} m%, while chemical catalysts often require concentrations of 0.1 to 1.0 m% [43]. As enzymes are biodegradable and chemical catalysts often are not, the benefit of superior sustainability should also be considered. Enzymes are also often the most efficient under mild reaction conditions, like pH ranges of 5 to 8 and temperatures of 20 to 40 °C [43]. However, in cases where tougher reaction conditions are needed, or enzymes with the required selectivity cannot be obtained, chemical catalysts may be the only reasonable option.

1.7.1 Enzymatic kinetic resolution

Enzymatic kinetic resolution is the separation of enantiomers based on the enantioselectivity an enzyme displays for the substrate. The enantiomer of preferred stereochemistry will more readily be transformed into the product. [35] The first enzymatic kinetic resolution was performed by Pasteur [45] on ammonium sodium tartrate with mold from *Penicillium galucum* in 1858 [35]. The bacteria metabolized (*R*,*R*)-tartrate selectively, leaving an excess of (*S*,*S*)-tartrate. The experiment was conducted by Louis Pasteur, who then discovered that (*S*,*S*)-tartrate was optically active (-).

As mentioned, enzymes catalyze reactions by lowering the activation energy. This is generally attributed to a stabilization of the substrate transition state by the enzyme [43]. If the substrate is chiral, the transition state-enzyme complex formed for each enantiomer will have different free energies (ΔG), see Figure 1.3. This causes a difference in activation energy ($\Delta\Delta G^{\neq}$) and therefore a difference in rate of transformation.

Even with perfect enzyme enantioselectivity, the product yield of a classical kinetic resolution will never surpass 50%. This is because half of the starting material in a racemic mixture is of the wrong stereochemistry. A solution to this issue is combination of kinetic resolution reactions with *in situ* racemization of the starting material [46]. This approach is known as dynamic kinetic resolution (DKR), and can increase the yields up to a full 100%. DKR is only a valid approach if the enzyme exhibits high enantioselectivity for the substrate,

the enzyme and racemization catalyst are compatible and the rate of racemization is at least ten times faster than the kinetic resolution reaction [47]. It is also important that the racemization catalyst doesn't interfere with the formed product. Dynamic kinetic resolution of various secondary alcohols has been achieved with Lipase B from *Candida antarctica* and Shvo's dimeric ruthenium complex [48]. Enantiopure acetates were obtained in high yields and with 99% enantiomeric excess.

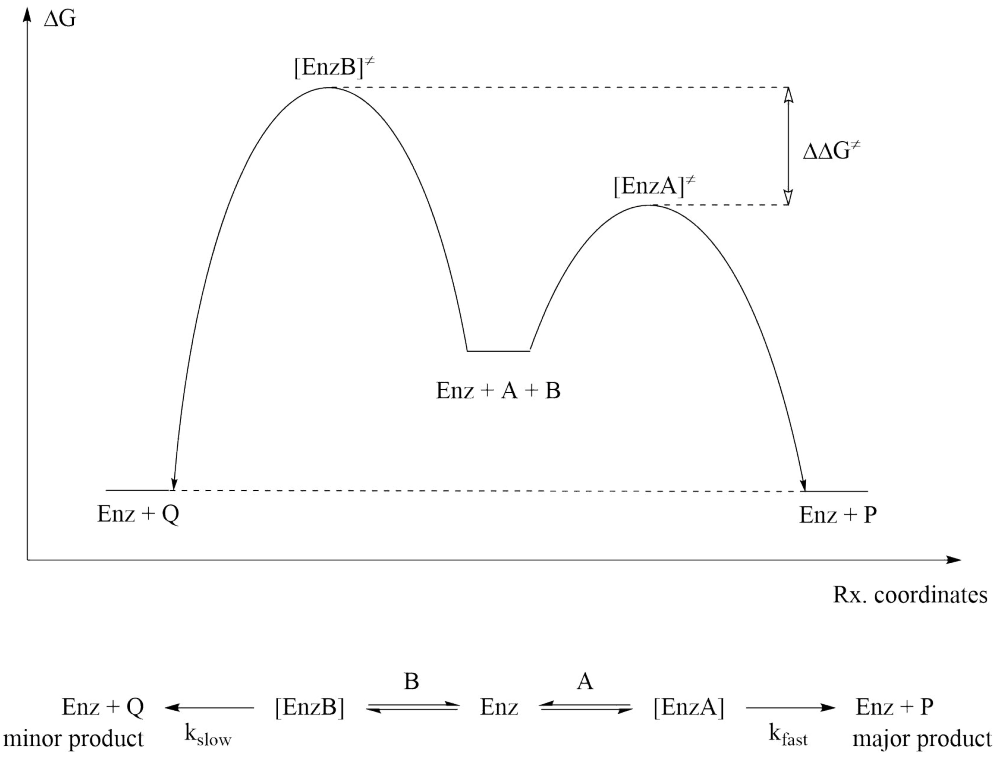

Figure 1.3: The enantioselectivity of an enzyme depends on the difference in free energy (ΔG) of the complexes formed between the substrate transition state and the enzyme ($[EnzA]^{\neq}$, $[EnzB]^{\neq}$) [43]. This causes a difference in acitvation energy ($\Delta\Delta G^{\neq}$) and thus reaction rates (k_{fast}, k_{slow}). Enz = enzyme, A & B = enantiomeric substrates, P & Q = enantiomeric products, [EnzA] & [EnzB] = enzyme-substrate complexes, $\neq$ denotes transition state.

Enantiomeric excess (*ee*)

Though the ideal kinetic resolution would effect complete chiral separation, this is rarely the case. Enantiomeric excess, a measure of enantiomeric purity, is needed to determine the

success of the resolution. The enantiomeric excess (ee) denotes how much there is of one enantiomer over the other, see Equation (1.2).

$$ee = \frac{P - Q}{P + Q} \cdot 100\% \tag{1.2}$$

In this equation, P is the amount of the enantiomer in excess and Q of the one in dearth. Commonly, these amounts are determined by chiral HPLC or -GC, see Section 1.9.

Substrate conversion (c)

The progression of a kinetic resolution reaction can be tracked by calculation of substrate conversion, see Equation (1.3). Enantiomeric excess is often plotted as a function of conversion to illustrate the course of the reaction.

$$c = \frac{ee_S}{ee_S + ee_P} \tag{1.3}$$

Enantiomeric ratio (E)

The enantioselectivity of an enzyme is commonly evaluated by its enantiomeric ratio (E), which describes the enzyme's ability to differentiate between the two enantiomers. The ratio can be expressed by the enantiomeric excess of both product (ee_P) and substrate (ee_S), see Equation (1.4).

$$E = \frac{\ln \frac{ee_P(1-ee_S)}{ee_P+ee_S}}{\ln \frac{ee_P(1+ee_S)}{ee_P+ee_S}} \tag{1.4}$$

This equation is a good model for ping-pong bi-bi mechanisms [49], like those of lipase catalyzed transesterification reactions, see Section 1.7.3. As fluctuations in the enantiomeric

ratio has been observed in kinetic resolution reactions [50], computational software tools such as *E & K Calculator* can be used for calculation of enantiomeric ratio across conversion.

1.7.2 Enzyme classifications

Enzymes are primarily classified as one of six categories, depending on the type of reaction they generally catalyze, see Table 1.1 [43]. Of these categories, it is the oxireductases and hydrolases that are most practically applicable. As enzymes often are used in their cellular form, however, it is not always easy to determine which enzyme is catalyzing the observable reaction.

Table 1.1: Enzyme classifications by the reaction they naturally catalyse [43].

Enzyme class	*Reaction type*
1. Oxireductases	Oxidation-reduction reactions
2. Transferases	Transfer of aldehyde-, ketone-, acyl groups etc.
3. Hydrolases	Formation of esters, amides, lactones etc. by hydrolysis
4. Lyases	Addition-elimination of small molecules on double bonds
5. Isomerases	Isomerizations like racemization, epimerization etc.
6. Ligases	Formation-cleavage of carbon-carbon or carbon-heteroatom bonds

Hydrolases are often favored for organic reactions due to their independence of cofactors and generally relaxed substrate specificity [43]. The most common subclasses of hydrolases are proteases, esterases, and lipases.

1.7.3 Lipases

Lipases (EC 3.1.1.3) are a category of hydrolases that in humans catalyze the hydrolysis of stored triacylglycerols, which releases fatty acids used as fuel [51]. In organic synthesis, lipases catalyze the hydrolysis of esters or esterification of alcohols. Commercially they are used in laundry detergent, baking and the pulp- and paper industry, as well as for chemically industrial purposes such as chiral resolution [42].

The most accurate description of lipase catalyzed reactions is the ping-pong bi-bi mechanism, regardless of which reaction type is performed, see Figure 1.4 [52]. First, there is complex formation ([EnzS_1]) between the enzyme (Enz) and the first substrate (S_1). From this, the first product (P_1) is cleaved and an acylated enzyme complex remains (Enz*). The second substrate (S_2) enters the active site and forms a complex ([Enz*S]) with the acylated enzyme. After transformation, the second product (P_2) is cleaved and the enzyme reverts to its original state.

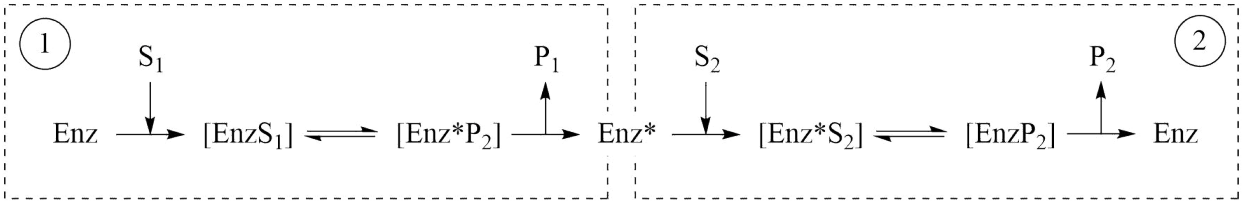

Figure 1.4: The ping-pong bi-bi mechanism occurs in two steps [52].
Enz = Enzyme, Enz* = Acylenzyme, S = Substrate, P = Product.

1.7.4 Inhibition of lipases

Enzyme activity is heavily impacted by the presence of certain inhibitors. Inhibition can be both reversible and irreversible, depending on the manner in which the inhibitor interacts with the active site. Partial inhibition, where the enzyme retains some activity, is also common. Many lipase inhibitors have been reported, though sensitivity varies between species.

Lipases from the *Bacillus* species are competitively inhibited by metal cations such as Na^+, Cu^{2+} and Co^{2+} [53]. Inhibition of *Bacillus* lipases by chelating agent ethylenediaminetetraacetic acid (EDTA) and anionic surfactant Sodium dodecyl sulfate (SDS) has also been reported. This suggests that the lipases require the presence of some metal cations that are chelated out with EDTA, but are inhibited by others. Inhibition of lipases from *Chromohalobacter japoricus* by metal cations has been reported, explicitly by Ni^{2+}, Zn^{2+} and K^+ [54]. However, increased activity as well as stability was observed in the presence of Ca^{2+}.

Lipase B from *Candida antarctica* displays inhibited activity in the presence of solvents like 2- and 3-pentanone during transacylation reactions [55]. The solvents competitively bond with the active site of the enzyme. Inhibition of CALB with 1-propanol has also been reported, as has inhibition by substrate alcohols in alcoholysis reactions [56].

1.7.5 *Candida antarctica* Lipase B

Candida antarctica is a species of yeast that produces the two lipases A and B. *Candida antarctica* lipase B (CALB) exhibits high enantioselectivity and catalytic efficiency, and is used for a wide variety of biocatalytic esterification reactions [57]. As a current example, CALB is being used for esterification of ribose in the firs synthesis step of Molnupiravir, a drug currently investigated for its effects against covid-19 [58]. It has also been found as a highly enantioselective catalyst in transesterification reactions of secondary alcohols [1].

CALB consists of 137 amino acids and has a molar mass of about 33 kDa [59]. The catalytic site is made up of serine, histidine and aspartate, and is activated by hydrogen-bonding between them.

Reactions catalyzed by CALB follow a ping-pong bi-bi mechanism known as the serine hydrolase mechanism, see Scheme 1.6 [43, 60]. In this, the acyl donor Substrate 1 enters the active site of the enzyme and forms Tetrahedal Intermediate 1 - so named for the conformation of the carbonyl carbon - by bonding with serine. The alcohol Product 1, which in this setting is regarded as waste, is protonated and released from the site. Remaining is an acyl-enzyme, which reacts further with the racemic alcohol Substrate 2 to form Tetrahedal Intermediate 2. When the carbonyl reforms, serine is protonated and the ester Product 2 is released from the site. This regenerates the enzyme for a new catalytic cycle.

The reaction is catalyzed by stabilization of the oxanion formed in both the first and second tetrahedal intermediates [60]. Stabilization occurs through electrostatic interactions with the oxanion hole (Thr, Gln). Complex molecular modeling of these catalytic mechanisms suggests shorter hydrogen bonds between one CALB-enantiomeric complex than the other,

resulting in increased stability in the formation of one ester-enantiomer [61]. It has also been suggested that the rate-determining step in transesterification reactions of secondary alcohols is the deacylation step in which Product 2 is formed [62].

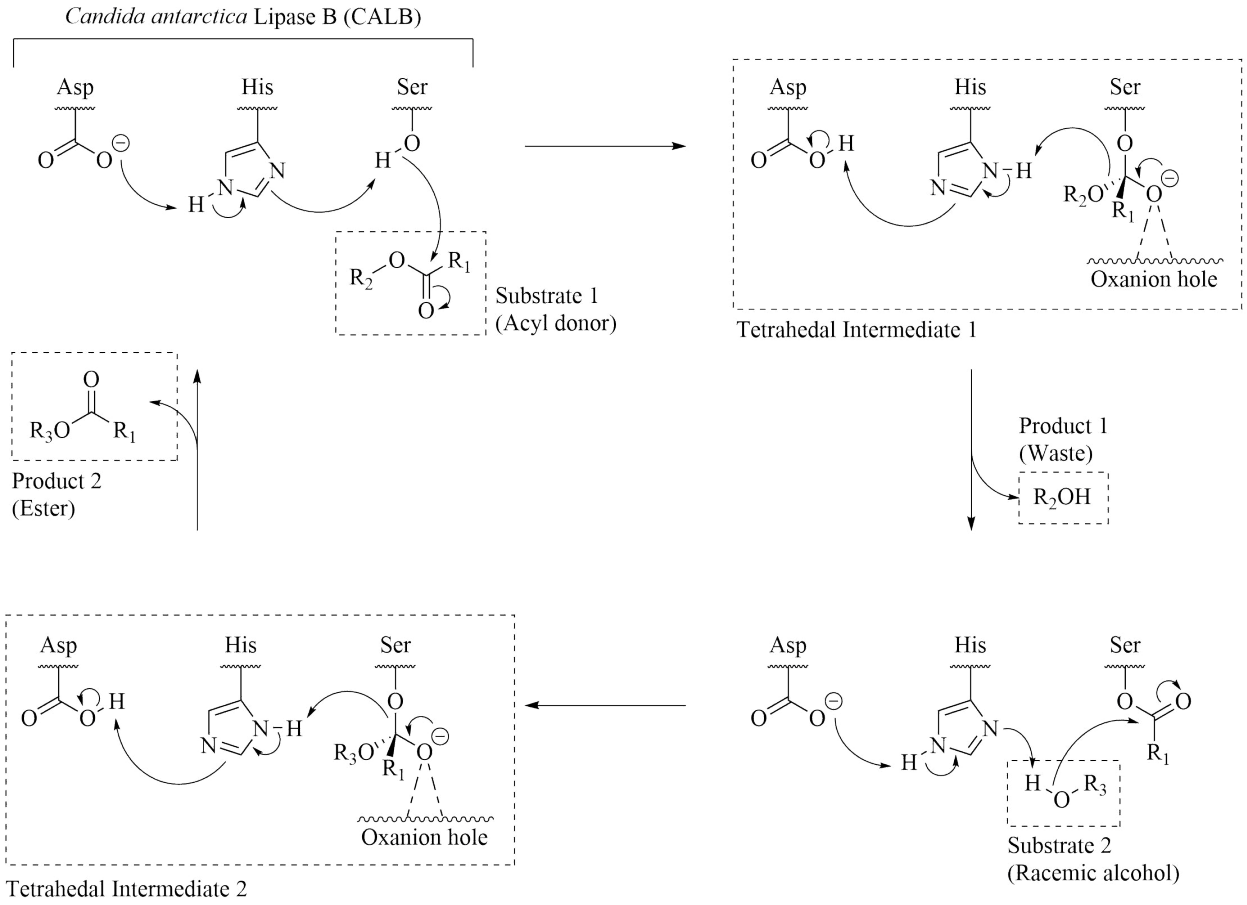

Scheme 1.6: Serine hydrolase mechanism [43, 60].

1.7.6 Effect of substrate stereochemistry on enantioselectivity

The ability an enzyme has to recognize its intended substrate depends heavily on substrate stereochemistry. A general model explaining lipase stereoselectivity for secondary alcohols was developed by Kazlauskas *et al.* [63], see Figure 1.5. They noted that an increase in stereoselectivity was observed with an increase in size difference between the substituents. From this it was gathered that lipases generally exhibit an increased reaction rate for transformation of (*S*)-alcohols when the small substrate group (S) is of higher priority than the large

one (L). The selectivity is naturally reversed when the priority of the groups are reversed. Similar effects were reported by Jacobsen *et al.* [64], who observed an increase in enantioselectivity during transesterification of secondary alcohols for substrates substituted with small hydrocarbon chains. Anthonsen and Hoff [65] reported increased enantioselectivity for substrates with fluoride substituents than with chloride substituents.

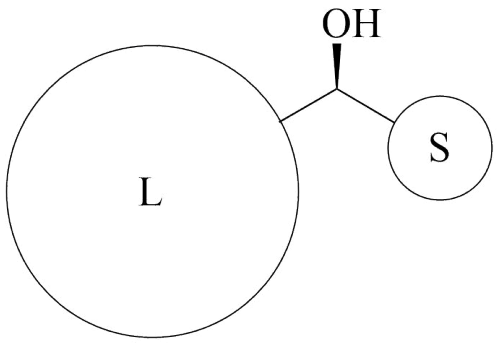

Figure 1.5: The stereoselectivity of lipase catalyzed transformations of secondary alcohols depends on the difference in size between the small (S) and the large (L) substituents [63].

1.7.7 Effect of reaction media on enantioselectivity

The natural environment of an enzyme is in water [43]. This generally poses a problem in organic chemistry, where most substrates show poor solubility in water. The high boiling point can also make work-up of a reaction quite tedious. For these and many other reasons, enzyme reactions, when applied in organic chemistry, are often performed in organic solvents or biphasic solutions [43]. Another very important advantage of using organic solvents in enzyme reactions is a shift in the thermodynamic equilibrium that favors synthesis over hydrolysis. This will allow the enantioselective synthesis of esters by lipase enzymes.

Many methods of measuring the compatibility of an organic solvent with enzyme activity have been developed, but the logarithm of the partition coefficient (log P) of a solvent between 1-octanol and water has provided the most reliable results [66]. Polar solvents have $\log P < 2$, moderately polar solvents $2 < \log P < 4$ and apolar solvents $\log P > 4$. Generally, solvents with higher log P are more suited for biocatalysis than those of low log P [67]. This

is for the simple reason that solvents with high water affinity may strip the enzyme of its structural water and prevent catalysis. The log P of acetonitrile has been reported as −0.3 [68], and only highly sturdy enzymes like CALB are compatible with such low values [43].

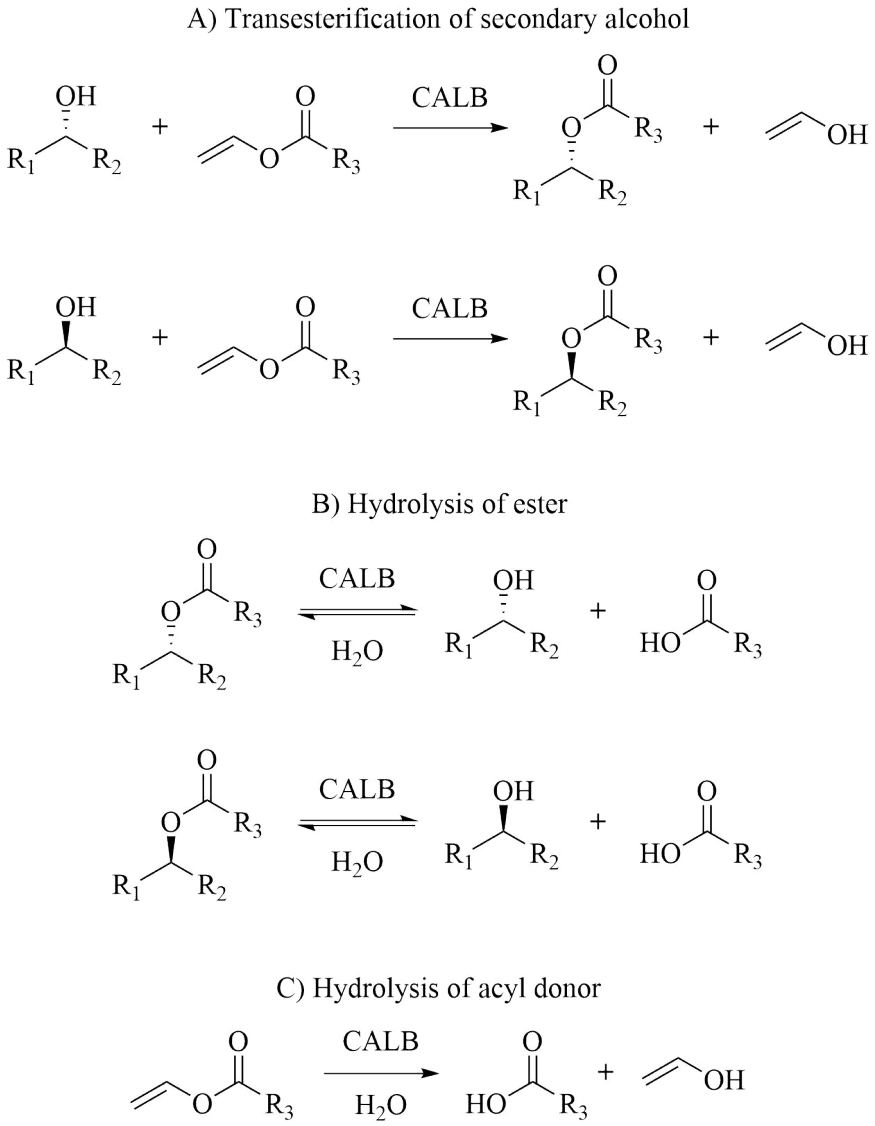

Scheme 1.7: The five equilibrium that must be considered during transesterification reactions of secondary alcohols with vinyl butanoate as acyl donor and CALB as catalyst [68].

The water activity (a_w) of a given solvent describes the actual content of water present. Most enzymes require a certain a_w to remain active, but lipases have been reported to work well even at water activities as low as 0.0-0.2 [43]. Increased enantioselectivity has been

reported for transesterification reactions of secondary alcohols with CALB in solvents with high water activity [68]. This is likely due to the conformational changes of the active cite of the enzyme caused by increased hydrogen-bonding to water [69]. The water activity of a solvent can be controlled by use of salt hydrates, which will continuously replenish consumed water in the solvent to maintain optimal water activity [70].

Experiments regarding the kinetic resolution of racemic 3-bromo-1-phenoxy-2-propanol catalyzed by CALB in solvents of controlled water activity was performed by Jacobsen and Anthonsen [68]. It was noted that five different equilibrium existed in the presence of water, see Scheme 1.7. Three are irreversible transesterification reactions, and two reversible hydrolysis reactions. The irreversibility of the former are due to the nature of the acyl donor, which is discussed more in the next section. At higher water content, the side reactions will significantly slow down the wanted transesterification reactions. To achieve acceptable reaction rates, low water activity should be considered, though this will come at the cost of increased enantioselectivity.

1.7.8 Effect of acyl donor on reaction rate

During kinetic resolutions, thermodynamic equilibrium should not be entered into as it prevents high yield and selectivity [43]. While hydrolysis reactions are practically irreversible in high excess of water, transesterification reactions are generally reversible. Modified esters are often employed as acyl donors to push the reaction in the wanted direction.

Activated esters are a group of esters substituted with electron-withdrawing groups, like cyanomethyl- and 2-haloethyl esters [71]. As the reaction occurs, the group is released as an alcohol. The alcohol with electron-withdrawing groups will be less nucleophilic than the alcohol substrate, driving the reaction in the right direction and causing quasi-irreversible conditions. Trifluoroethyl esters are very common at small reaction scales as they release the easily volatile trifluoroethanol (b.p. 78 °C). At larger scales, trichloroethyl esters can be used at lower cost, but release involatile trichloroethanol (b.p. 151 °C). Thiol esters [72] and

oxime esters [73] have also been used.

Enol esters such as vinyl- or *iso*-propenyl esters are another available choice of acyl donor. They liberate unstable enols during reaction, which tautomerize to volatile acetaldehyde (b.p. 20 °C) or acetone (b.p. 56 °C), see Scheme 1.8 [74]. This ensures complete irreversibility of the reaction. Lipase catalyzed transesterification reactions using enol esters have been shown to have 10-100 times faster reaction rates than those using activated esters [75]. The downside is that acetaldehyde may react with the ϵ-amino group of lysine to form a Schiff base [76, 77]. This can cause deactivation of the enzyme. Addition of molecular sieves to trap acetaldehyde or stabilization of the enzyme by immobilization has been reported to have some positive effect on the formation of Schiff bases. *Candida antarctica* lipases have shown remarkable stability in this issue [78].

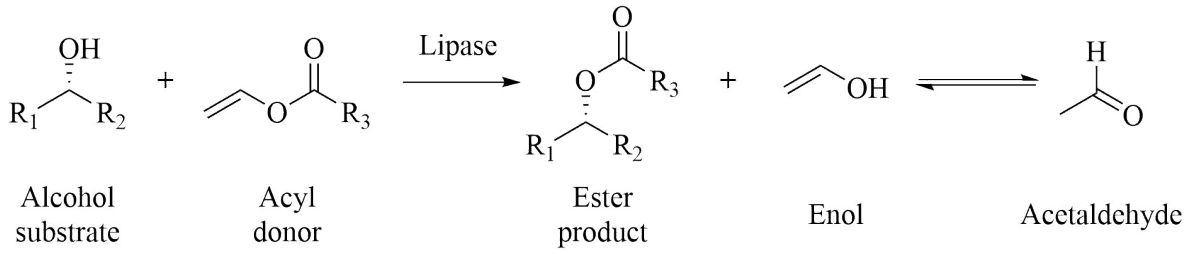

Scheme 1.8: Lipase catalyzed transesterification reaction of a secondary alcohol with a vinyl ester. The reaction forms an ester and an unstable enol, which tautomerizes to acetaldehyde.

1.8 Synthesis of (*S*)-carteolol precursors for kinetic resolution

Synthesis of (*S*)-carteolol by kinetic resolution requires a suitable precursor on which the kinetic resolution can be performed. High enantioselectivity of *Candida antarctica* Lipase B (CALB) has been observed for secondary alcohols. Our research group has successfully resolved chloride-substituted secondary alcohol (chlorohydrin) precursors of β-blockers in previous projects [1]. (*R*)-7-(3-Chloro-2-hydroxypropoxy)-3,4-dihydroquinolin-2(1H)-one is the chlorohydrin precursor of a 7-substituted (*S*)-carteolol derivative, and was obtained by transesterification reaction with vinyl butanoate, see Scheme 1.9. The (*R*)-chlorohydrin was

obtained in 34% yield and 96% *ee*, and (*S*)-1-chloro-3-((2-oxo-1,2,3,4-tetrahydroquinolin-7-yl)oxy)propan-2-yl butanoate in 51% yield and 86% *ee*. The enantiomeric ratio (E) calculated for the reaction was E = 157. Achieved enantiopurity was preserved after conversion to the (*S*)-carteolol derivative.

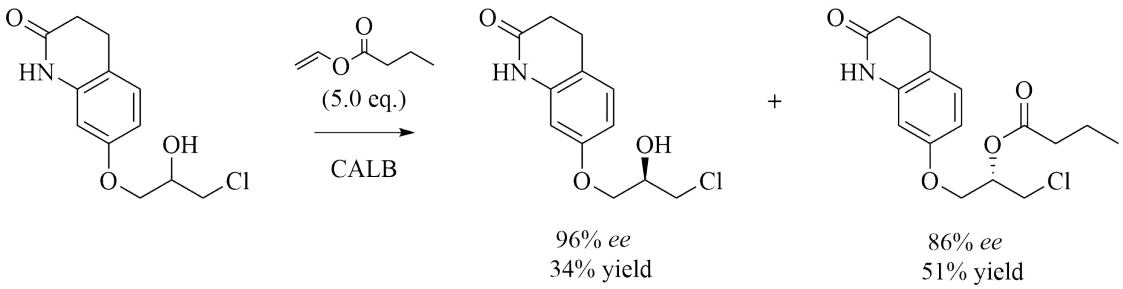

Scheme 1.9: Kinetic resolution of 7-(3-chloro-2-hydroxypropoxy)-3,4-dihydroquinolin-2(1H)-one, the chlorohydrin precursor to an (*S*)-carteolol derivative, by transesterification reaction with vinyl butanoate [1]. The reaction was catalyzed by CALB.

A secondary alcohol can easily be obtained from an epoxide by ring-opening with lithium chloride, as performed by Bajwa and Anderson [79]. They opened the epoxide of 2-(phenoxymethyl)oxirane and obtained 1-chloro-3-phenoxypropan-2-ol in 100% yield. It was noted that use of more reactive lithium halogens permitted shorter reaction times. An alternative approach was developed by Chini *et al.* [80], who used an excess of hydrochloric acid. From this they obtained the same chlorohydrin in 96% yield. It should be noted that use of harsh chemicals may negatively affect sensitive functional groups of the target molecule.

Gundersen [81] used a similar approach for the synthesis of carteolol precursor 5-(3-chloro-2-hydroxypropoxy)-3,4-dihydroquinolin-2(1H)-one from 5-hydroxy-3,4-dihydro-quinolin-2(1H)-one, see Scheme 1.10. His work combined the method developed by Mangishi *et al.* [20] with that of Bajwa and Anderson [79]. After reaction of the alcohol starting material with epichlorohydrin in alkaline conditions, the chlorohydrin precursor and 5-hydroxy-(2,3-epoxypropoxy)-3,4-dihydroquinolin-2(1H)-one were obtained in a 1:4 ratio. The epoxide was then opened with lithium chloride and acetic acid. With this method, the chlorohydrin precursor was obtained in 61% yield across both steps.

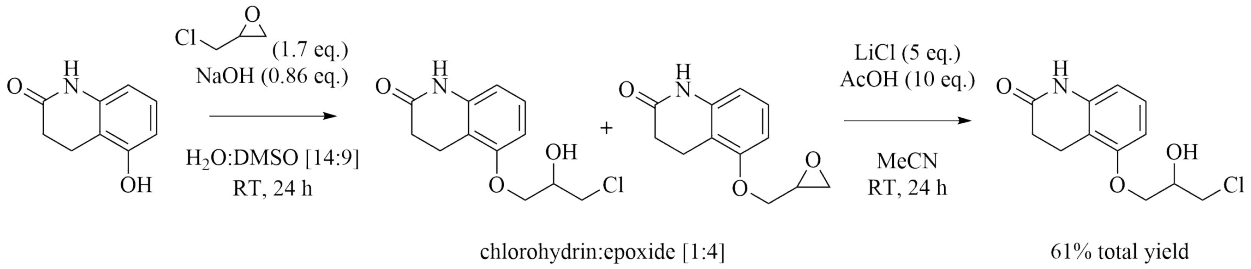

Scheme 1.10: Synthesis of 5-(3-chloro-2-hydroxypropoxy)-3,4-dihydroquinolin-2(1H)-one, a chlorohydrin precursor to carteolol, by alkylation of 5-hydroxy-3,4-dihydroquinolin-2(1H)-one with epichlorohydrin in a basic environment, and ring-opening of 5-hydroxy-(2,3-epoxypropoxy)-3,4-dihydroquinolin-2(1H)-one with lithium chloride in an acidic environment [81].

The fluoride substituted alcohol 5-(3-chloro-2-hydroxypropoxy)-3,4-dihydroquinolin-2(1H)-one (Figure 1.6) can be synthesized as an alternative to chloride substituted alcohols. The electrophilic abilities of fluoride render it a poor leaving group, mostly eliminating the issue of epoxide formation, as shown by Fujinaga *et al.* [82]. They synthesized 1-(1,1-biphenyl)-3-fluoropropan-2-ol from 4-phenylphenol by substitution of epifluorohydrin. From this, they obtained the fluorohydrin in a 75% yield.

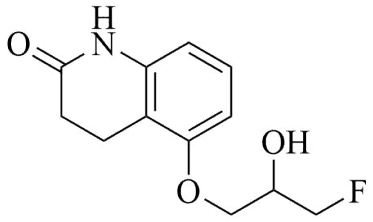

Figure 1.6: The chemical structures of 5-(3-fluoro-2-hydroxypropoxy)-3,4-dihydroquinolin-2(1H)-one, a fluorohydrin precursor to carteolol.

As discussed in Section 1.7.6, CALB has shown higher enantioselectivity for fluoride substituted secondary alcohols than chloride substituted ones. Synthesis of a fluorohydrin precursor also circumvents the use of epichlorohydrin, which is a suspected carcinogen. However, the electrophilicity of fluoride may render it too unreactive for the alkylation of *tert*-butylamine, and thus unsuitable for synthesis of carteolol. Epifluorohydrin is also significantly more expensive than epichlorohydrin.

1.8.1 Epoxide ring-opening with halide ions in acidic environment

Epoxides are vulnerable to nucleophilic attacks due to the high strain of a three-membered ring [83]. Nucleophilic ring-opening can be achieved under both acidic and basic conditions. The product stereochemistry of nucleophilic ring-opening in acidic condition relies on the degree to which the C-O bond is weakened, see Scheme 1.11. A mostly intact C-O bond will facilitate a break at the least substituted epoxide carbon due to the steric hindrance associated with heavily substituted sites. In contrast, a mostly ruptured C-O bond will facilitate a break at the most substituted site, as it can more easily stabilize the generation of positive charge.

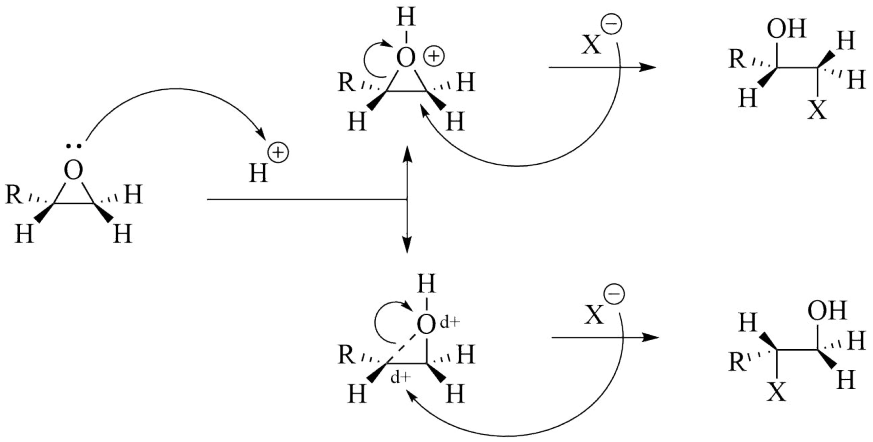

Scheme 1.11: Nucleophilic ring-opening of an epoxide by halide ions in acidic conditions [83].

Multiple factors affect product stereochemistry of nucleophilic ring-opening in acidic environments [83]. Ring-opening with halide ions will often perpetuate attack of the ion at the least substituted site of simple molecules, as will use of oxygen-coordinating Lewis acids. Substitution with groups that further stabilize carbocation intermediates have the opposite effect, and perpetuate attack at the most substituted site.

1.9 Analysis of chiral compounds

Analysis of the enantiomeric excess in both substrate and product is necessary to determine the enantiopurity of the synthesized compounds, as well as the enantioselectivity of the enzyme. As discussed in Section 1.4, the enantiomers of a chiral compound only exhibit different abilities in a chiral environment or in the rotation of polarized light. These difference are the basis of many chiral analytical methods such as chiral gas chromatography (GC) and -high-performance liquid chromatography (HPLC), chiral nuclear magnetic resonance and polarimetry.

1.9.1 Chiral chromatography

Chiral chromatography is the most common method for analytical separation of enantiomers today [22]. The principle of chromatography is the difference in affinity that compounds hold for various stationary- and mobile phases [84]. When the compounds in questions are enantiomers of the same compound, separation can be achieved by using chiral mobile phases or chiral stationary phases (CSP) [85]. Analysis of enantiopurity can also be performed by enantioselective derivatization of the compound prior to achiral HPLC analysis [22]. For chiral chromatography analyses, GC and HPLC are used.

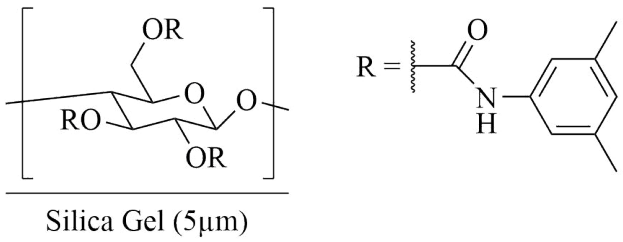

Figure 1.7: The CSP of Chiralcel OD-H columns: cellulose tris(3,5-dimethylphenylcarbamate) coated on silica gel (5μm).

For compounds with high boiling points, which is often the case for larger molecules, HPLC is preferred. For this reason, there has been a large number of CSPs developed for chiral separation by HPLC. The chiral abilities of chiral columns are often caused by synthetic or natural polymers, or immobilized chiral molecules [85]. The optically active material is

often coated onto a supporting material such as silica gel. A common natural polymer is polysaccharides such as cellulose, amylose or chitin [86]. As an example, the material of a Chiralcel OD-H column is shown in Figure 1.7.

Baseline separation, which is when the resolution factor (R_S) is above 1.5, is necessary for accurate calculations of enantiomeric excess. The R_S of chiral HPLC columns can be expressed as a function of the retention times (t_1, t_2) and peak widths at half height ($\frac{1}{2}w_1$, $\frac{1}{2}w_2$), see Equation (1.5) [87]. It is the area of the detected peaks that can be utilized for calculation of enantiomeric excess, see Section 1.7.1.

$$R_S = 1.177 \times \frac{t_2 - t_1}{\frac{1}{2}w_1 + \frac{1}{2}w_2} \tag{1.5}$$

1.9.2 Polarimetry

Each enantiomer of a chiral compounds is optically active, which is an ability they have to rotate plane polarized light [34]. The optical activity of a compound is measured by a polarimeter. In its simplest form, a polarimeter consists of a light source, a polarizer, a sample cell and another polarizer through which the degree of rotation is determined.

When the plane polarized light passes through an enantiopure sample, it will bend the light to a fixed angle [34]. This optical rotation (α) can be used to calculate optical purity. Calculation of the optical purity is performed by comparison of the specific optical rotation of a sample with that of the enantiopure form. This requires knowledge of the enantiopure rotation, which is not always known. In modern times, polarimetry has mostly been replaced by chromatography and spectroscopy, with which the exact enantiomeric excess can be determined [85].

The specific optical rotation ($[\alpha]_\lambda^T$) is measured at a certain temperature (T) and wavelength (λ). The most common wavelength is that emitted by sodium at 589 nm (D). $[\alpha]_\lambda^T$ is often expressed as a function of optical rotation (α), the length of the sample tube (l) and the concentration of the sample concentration (c), see Equation (1.6) [34].

$$[\alpha]_\lambda^T = \frac{100 \times \alpha}{l \times c} \tag{1.6}$$

2 Aim of Thesis

This project aimed to synthesize (*S*)-carteolol ((*S*)-**4**) from 5-hydroxy-3,4-dihydroquinolin-2(1H)-one (**1**) in a method both financially and environmentally sustainable. It was divided into four goals: synthesis of precursor 5-(3-chloro-2-hydroxypropoxy)-3,4-dihydroquinolin-2(1H)-one (**2a**), kinetic resolution thereof, amine alkylation with the resulting single enantiomer and synthesis of the alternative precursor 5-(3-fluoro-2-hydroxypropoxy)-3,4-dihydroquinolin-2-(1H)-one (**2d**), see Scheme 2.1 and 2.2.

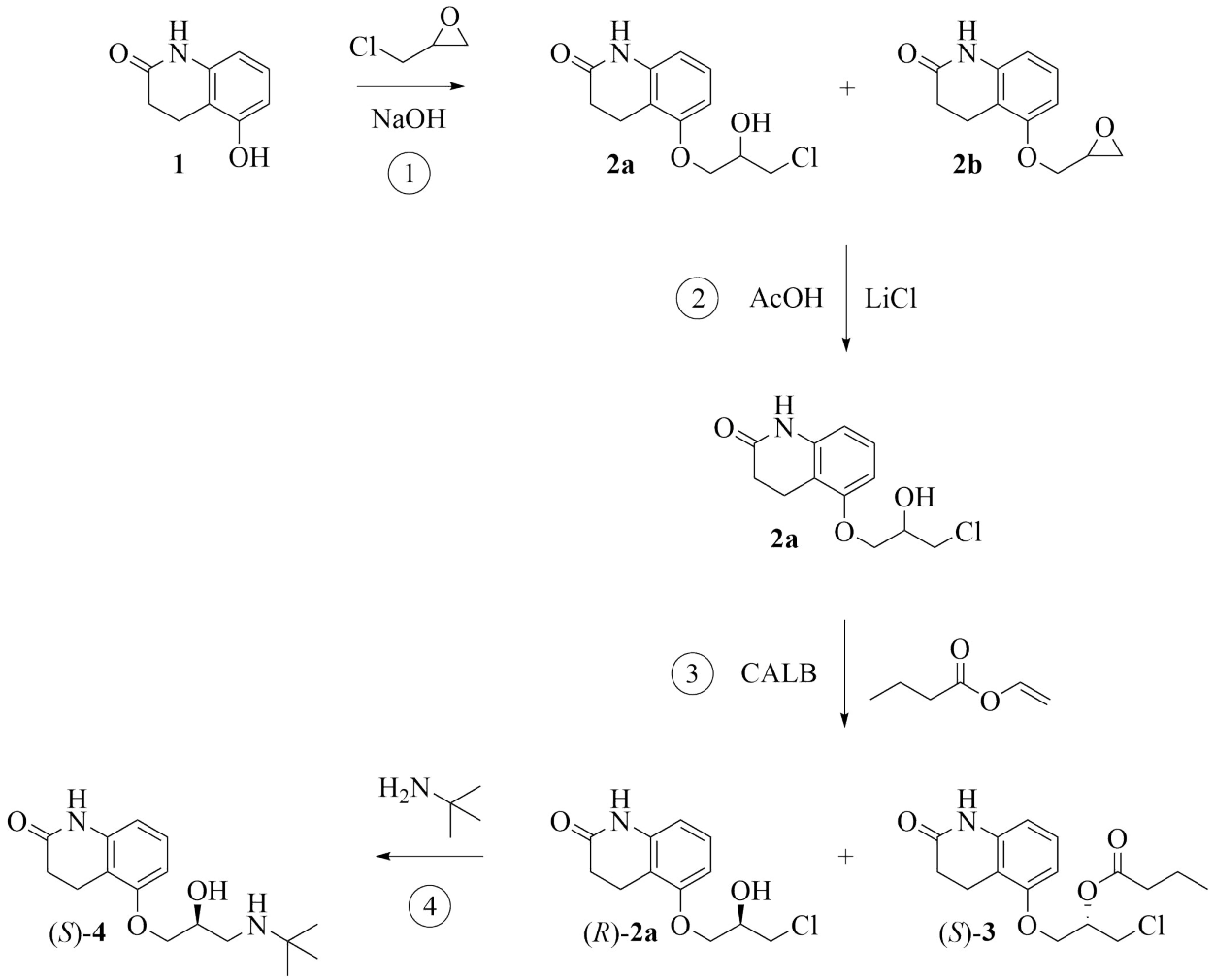

Scheme 2.1: Synthesis pathway of (*S*)-carteolol ((*S*)-**4**) from alcohol **1**.

The synthesis of chlorohydrin **2a** from alcohol **1** was performed as in step 1 and 2. Alcohol **1** was reacted with epichlorohydrin and sodium hydroxide to form chlorohydrin **2a** and 5-hydroxy-(2,3-epoxypropoxy)-3,4-dihydroquinolin-2(1H)-one (**2b**). The epoxide was then converted to chlorohydrin by ring-opening with lithium chloride and acetic acid. Different reaction conditions were examined for their impact on purity, selectivity and yield.

Kinetic resolution of **2a** using *Candida antarctica* Lipase B was then investigated in step 3, as this enzyme has shown excellent selectivity of similarly structured substrates previously [1]. Chlorohydrin **2a** underwent a transesterification reaction to (*S*)-1-chloro-3-((2-oxo-1,2,3,4-tetrahydroquinolin-5-yl)oxy)propan-2-yl butanoate ((*S*)-**3**). The aim of this goal was to obtain (*R*)-**2a** in 96 % enantiomeric excess, as this would satisfy the necessary requirements of active pharmaceutical ingredients.

The synthesis of (*S*)-**4** was performed by alkylation of *tert*-butylamine with (*R*)-**2a** in step 4. Various reaction conditions were examined for their impact on conversion and product purity.

Fluorohydrin **2d** was synthesized from alcohol **1** as an alternative precursor to (*S*)-**4**. Alcohol **1** was reacted with epifluorohydrin and sodium hydroxide to form fluorohydrin **2d**. The aim of this goal was to remove the need for two synthesis steps by using a less reactive halogen that only forms a secondary alcohol.

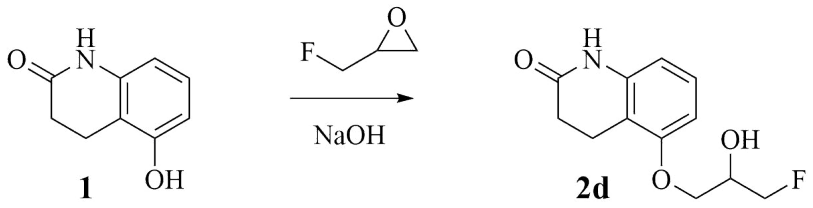

Scheme 2.2: Synthesis pathway of fluoride **2d** from alcohol **1**.

3 Results and Discussion

This project focused on the synthesis of (*S*)-carteolol ((*S*)-**4**) from 5-hydroxy-3,4-dihydroquinolin-2(1H)-one (**1**). The synthesis was performed in four steps, *via* precursor 5-(3-chloro-2-hydroxypropoxy)-3,4-dihydroquinolin-2(1H)-one (**2a**) and 5-hydroxy-(2,3-epoxypropoxy)-3,4-dihydroquinolin-2(1H)-one (**2b**). (*S*)-1-chloro-3-((2-oxo-1,2,3,4-tetrahydroquinolin-5-yl)-oxy)propan-2-yl butanoate ((*S*)-**3**) was formed during kinetic resolution of chlorohydrin **2a**. The byproduct 5,5'-((2-hy-droxypropane-1,3-diyl)bis(oxy))bis(3,4-dihydroquinolin-2(1H)-one) (**2c**) was also observed.

The first two reaction steps are discussed in Section 3.1, the third step in Section 3.3, and the fourth and final step in Section 3.4. Synthesis of 5-(3-fluoro-2-hydroxypropoxy)-3,4-dihydroquinolin-2(1H)-one (**2d**) as an alternative to chlorohydrin **2a** is discussed in Section 3.5.

3.1 Synthesis of chlorohydrin 2a

The first two steps in the synthesis of (*S*)-**4** regard the synthesis of precursor chlorohydrin **2a**. This section also discusses the conversion of intermediate **2b** into **2a**, removal of dimer **2c** and use of catalytic amounts of base. The methods developed are based on the work of previous master's candidate Morten Gundersen [81].

3.1.1 Description of step 1 in the synthesis of (*S*)-4

The first step in synthesis of (*S*)-**4** is conversion of alcohol **1** into chlorohydrin **2a** and epoxide **2b**. A proposed mechanism for this step is presented in Scheme 3.1. First, alcohol **1** is deprotonated by the hydroxide ion supplied from NaOH, forming alkoxide $\mathbf{1_{anion}}$. This intermediate functions as the nucleophile in an S_N2 reaction with epichlorohydrin, which is primarily attacked at two electrophilic sites, see pathway A and B.

Pathway A forms intermediate $\mathbf{2_{anion}}$ through simultaneous attack on the least substituted epoxide carbon and displacement of the oxygen. The intermediate is then protonated by H_2O through pathway C and forms chlorohydrin **2a**. The hydroxide ion is regenerated by this mechanism, opening the possibility of catalytic amounts of base, see Section 3.1.7.

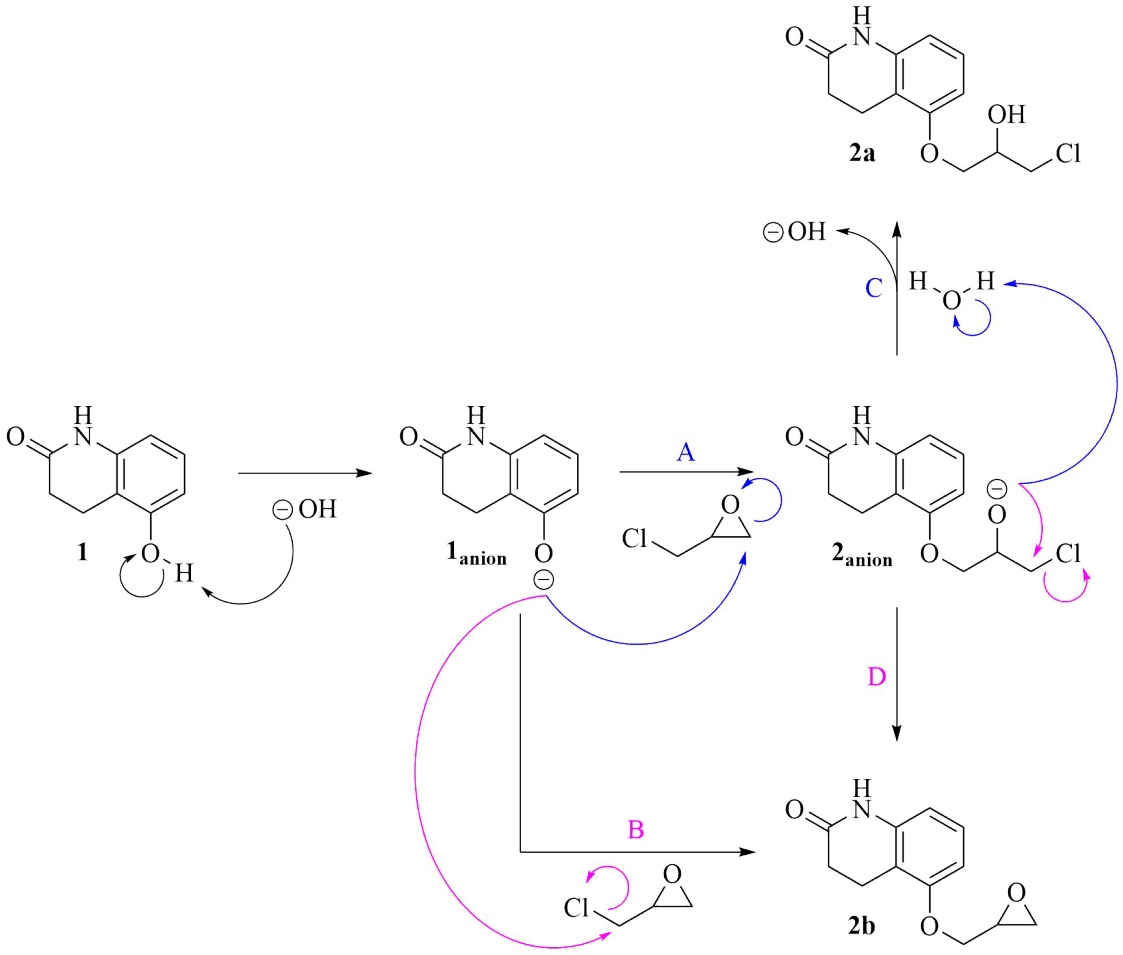

Scheme 3.1: Proposed mechanism for the synthesis of chlorohydrin **2a** and epoxide **2b**. Alcohol **1** is first deprotonated, and then undergoes an S_N2 reaction with epichlorohydrin. Formation of chlorohydrin **2a** regenerates the hydroxide ion, while epoxide **2b** is formed by Williamson ether syntheses.

Epoxide **2b** can be formed by Williamson ether synthesis, primarily through two mechanisms. Intermolecular Williamson ether synthesis can occur by nucleophilic attack of alkoxide $\mathbf{1_{anion}}$ on epichlorohydrin in α-position to chloride, see pathway B. Similarly, intramolecular Williamson ether synthesis may occur, where the alkoxide of intermediate $\mathbf{2_{anion}}$ performs a

nucleophilic attack on the carbon in α-position to chloride, see pathway D. In both mechanisms, chloride is displaced and epoxide **2b** formed.

Synthesis of chlorohydrin **2a** and epoxide **2b** from alcohol **1** was performed with 2 equivalents of epichlorohydrin and 0.3 equivalents of NaOH dissolved in a H_2O:DMSO solution [3:2], see Scheme 3.2. The product was filtered off after 24 hours at room temperature. A **2a**:**2b** product mixture [75:24] (mol. ratio) was obtained in 91% of the expected amount when adjusted for the mixed product composition, and 99% purity. Trace amounts of starting material **1** (0.5%) and byproduct **2c** (0.6%) were detected as impurities.

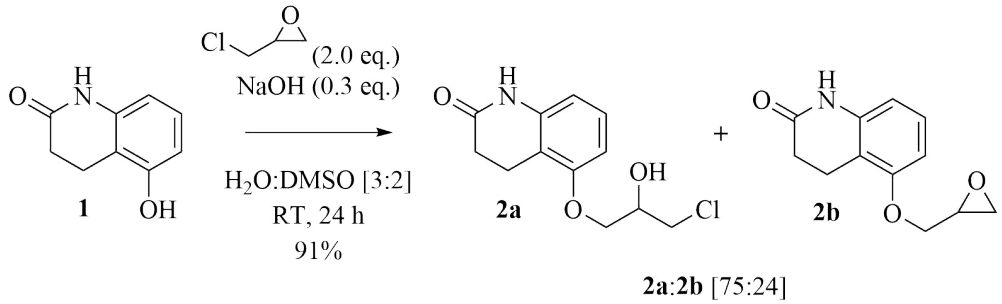

Scheme 3.2: Synthesis of chlorohydrin **2a** and epoxide **2b** from alcohol **1** by use of epichlorohydrin in alkaline conditions.

3.1.2 Description of step 2 in the synthesis of (*S*)-4

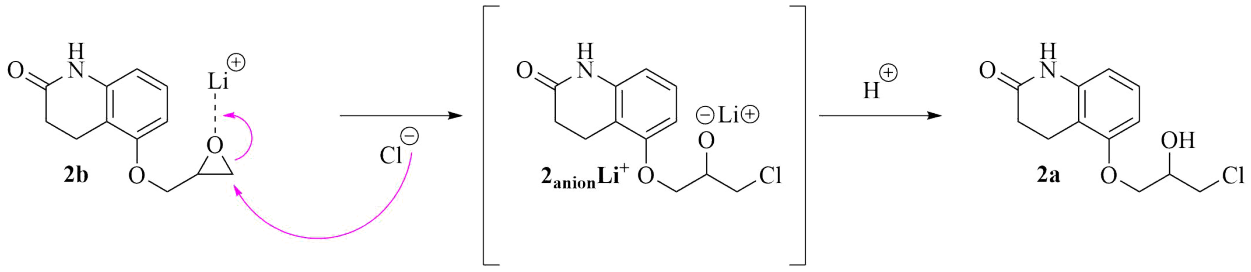

Scheme 3.3: Proposed mechanism for the synthesis of chlorohydrin **2a** from epoxide **2b**. The epoxide undergoes ring-opening with LiCl in an acidic environment.

The second step in synthesis of (*S*)-**4** is the conversion of epoxide **2b** into chlorohydrin **2a**. A proposed mechanism for this step is shown in Scheme 3.3. The mechanism is that of

an acidic lithium halogen epoxide ring-opening, where epoxide **2b** undergoes simultaneous coordination of the oxygen with a lithium cation and nucleophilic attack by chloride at the least substituted epoxide carbon. After ring-opening, the lithium coordinated alkoxide $\mathbf{2_{anion}Li^+}$ is protonated by the acidic environment and forms chlorohydrin **2a**.

Synthesis of chlorohydrin **2a** from epoxide **2b** was performed with 2 equivalents of LiCl and 2 equivalents of acetic acid dissolved in acetonitrile, see Scheme 3.4. The product was filtered off after 24 hours at room temperature. Chlorohydrin **2a** was obtained in 83% of expected amount when adjusted for the mixed composition of starting material, and 98% purity. A total yield of 76% **2a** was achieved across both steps. The remaining impurity was determined to be epoxide **2b** (1.6%).

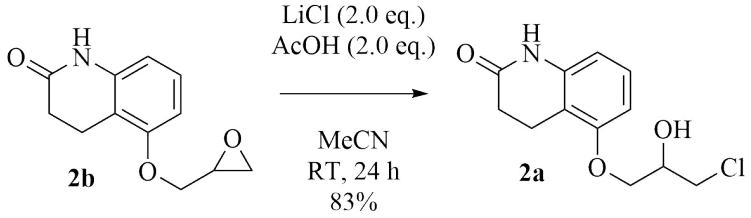

Scheme 3.4: Synthesis of chlorohydrin **2a** from epoxide **2b** by use of lithium chloride in acidic conditions.

3.1.3 Characterization of chlorohydrin 2a

Full characterization of chlorohydrin **2a** was achieved by ^{1}H NMR, ^{13}C NMR, COSY, HSQC and HMBC experiments in $DMSO_{d6}$, see Figure 3.1 and Table 3.1. Analysis by MS detected an exact mass of $[M+H]^+ = 256.1$ m/z. This is concurrent with the theoretically calculated molecular weight of chlorohydrin **2a** (255.7 g/mol). All related spectra are presented in Appendix B.

All carbon positions were assigned chemical shifts as fit with HSQC and HMBC, see Figure 3.1 and Table 3.1. Carbons without protons were as such assigned shifts by two-, three- or four-bond relations.

Table 3.1: Acquired NMR data for chlorohydrin **2a**. Listed proton- and carbon positions are presented in Figure 3.1. All related NMR spectra are found in Appendix B.

Pos.	*^{1}H (int., mult., J [Hz]) [ppm]*	*^{13}C [ppm]*	*COSY*	*HMBC*
1	-	170.5	-	2, 3 (10)
2	2.42-2.38 (2H, t, 7.7)	30.3	3	3, 10
3	2.84-2.80 (2H, t, 7.7)	18.7	2	2 (6, 8)
4	-	111.7	-	2, 3, 6, 8, 10 (7)
5	-	155.9	-	3, 6, 7, 8, 11 (10)
6	6.61-6.59 (1H, d, 8.1)	106.3	7	8 (3, 7)
7	7.09-7.05 (1H, t, 8.1)	128.1	6, 8	(3)
8	6.50-6.48 (1H, d, 7.9)	108.8	7	6 (7, 10)
9	-	139.8	-	3, 7 (6, 8, 10)
10	10.02 (1H, s)	-	-	-
11	3.97-3.96 (2H, m)	69.6	12	12, 13, 14
12	4.06-4.01 (1H, m)	69.1	11, 13, 14	11, 13, 14
13	3.79-3.75 (1H, dd, 11.1, 4.6)	47.3	12	11, 14
	3.70-3.66 (1H, dd, 11.1, 5.5)			
14	5.55-5.54 (1H, d, 5.3)	-	12	-

The chemical shift observed at 10.02 ppm (10) was assigned to the amide-proton due to the shielded nature of such groups. The shifts at 7.09-7.05 (7), 6.61-6.59 (6) and 6.50-6.48 ppm (8) fell within the range characteristic for conjugated systems, and were assigned to the aromatic protons. Shifts observed at 2.84-2.80 ppm (3) and 2.42-2.38 ppm (2) were assigned to the non-aromatic ring. These positions were compatible with the low shifts and observed carbon couplings (1, 5).

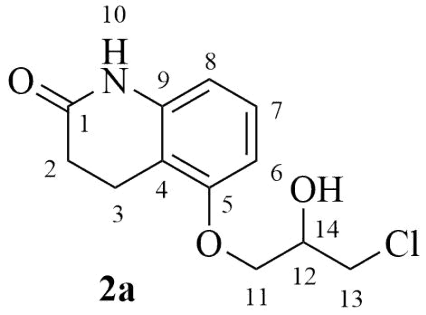

Figure 3.1: Proton- and carbon positions of chlorohydrin **2a** as described in Table 3.1. All related NMR spectra are found in Appendix B.

A shift of split multiplicity was observed at 5.55-5.54 ppm (14) and was assigned to the moderately shielded alcohol-proton. Shifts observed at 4.06-4.01 ppm (12) were assigned the proton located at the chiral center, due to the characteristic multiplicity of chiral centers. The chemical shifts at 3.97-3.96 ppm (11) were assigned to the ether methylene bridge, a position consistent with coupling to the carbon in position 5. Similarly, the shifts at 3.79-3.75 and 3.70-3.66 ppm (13) were assigned the chloride methylene bridge.

3.1.4 Characterization of epoxide 2b

Full characterization of epoxide **2b** was achieved by ^{1}H NMR, ^{13}C NMR, COSY, HSQC and HMBC experiments in $DMSO_{d6}$, see Figure 3.2 and Table 3.2. Analysis by LC-MS detected an exact mass of $[M+H]^{+} = 220.1\ m/z$. This is concurrent with the theoretically calculated molecular weight of epoxide **2b** (219.2 g/mol). All spectra are presented in Appendix C.

All carbon positions were assigned chemical shifts as fit with HSQC and HMBC, see Figure 3.2 and Table 3.2. Carbons without protons were as such assigned shifts by two-, three- or four-bond relations. Chemical shifts observed at 10.04 (10), 7.09-7.05 (7), 6.62-6.60 (6), 6.51-6.49 (8), 2.85-2.80 (3), 2.43-2.39 (2) were assigned to the quinoline group, as they were consisted with previously characterized compounds, see Section 3.1.3.

Table 3.2: Acquired NMR data for epoxide **2b**. Listed proton- and carbon positions refer to those given in Figure 3.2. Complete NMR spectra are found in Appendix C.

Pos.	^{1}H *(int., mult., J [Hz]) [ppm]*	^{13}C *[ppm]*	*COSY*	*HMBC*
1	-	170.5	-	2, 3 (10)
2	2.43-2.39 (2H, t, 7.7)	30.3	3	3, 10
3	2.85-2.80 (2H, m)	18.8	2	2 (6)
4	-	111.7	-	2, 3, 6, 8, 10 (7)
5	-	155.8	-	3, 6, 7, 8, 11
6	6.62-6.60 (1H, d, 8.2)	106.5	7	8 (3, 7)
7	7.09-7.05 (1H, t, 8.1)	128.1	6, 8	(3)
8	6.51-6.49 (1H, d, 7.9)	108.9	7	6 (3, 7, 10)
9	-	139.8	-	3, 7 (6, 8, 10)
10	10.04 (1H, s)	-	-	-
11	4.33-4.29 (1H, dd, 11.4, 2.5)	69.5	12	13
	3.87-3.83 (1H, dd, 11.4, 6.3)			
12	3.35-3.33 (1H, m)	50.2	11, 13	11, 13
13	2.85-2.80 (1H, m)	44.2	12	11
	2.73-2.71 (1H, dd, 5.1, 2.6)			

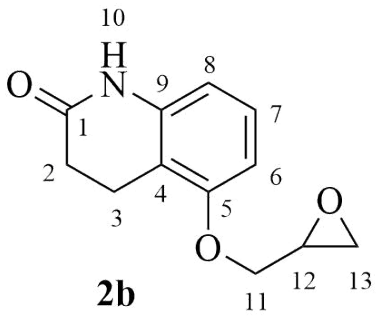

Figure 3.2: Proton- and carbon positions of epoxide **2b** as described in Table 3.2. All related NMR spectra are found in Appendix C.

Shifts observed at 4.33-4.29 and 3.87-3.83 ppm (11) were assigned to the ether methylene bridge, after coupling with the carbon in position 5 was observed. The proton in chiral position was observed at 3.35-3.33 ppm (12), but was interfered with by the water peak and could not be directly integrated. The observed range of chemical shifts was verified by coupling observed on COSY, HSQC and HMBC spectra. The shifts at 2.85-2.80 ppm (3, 13) corresponded to three protons, one of which was assigned the epoxide methylene bridge (13) together with shifts at 2.73-2.71 ppm (13) by process of elimination.

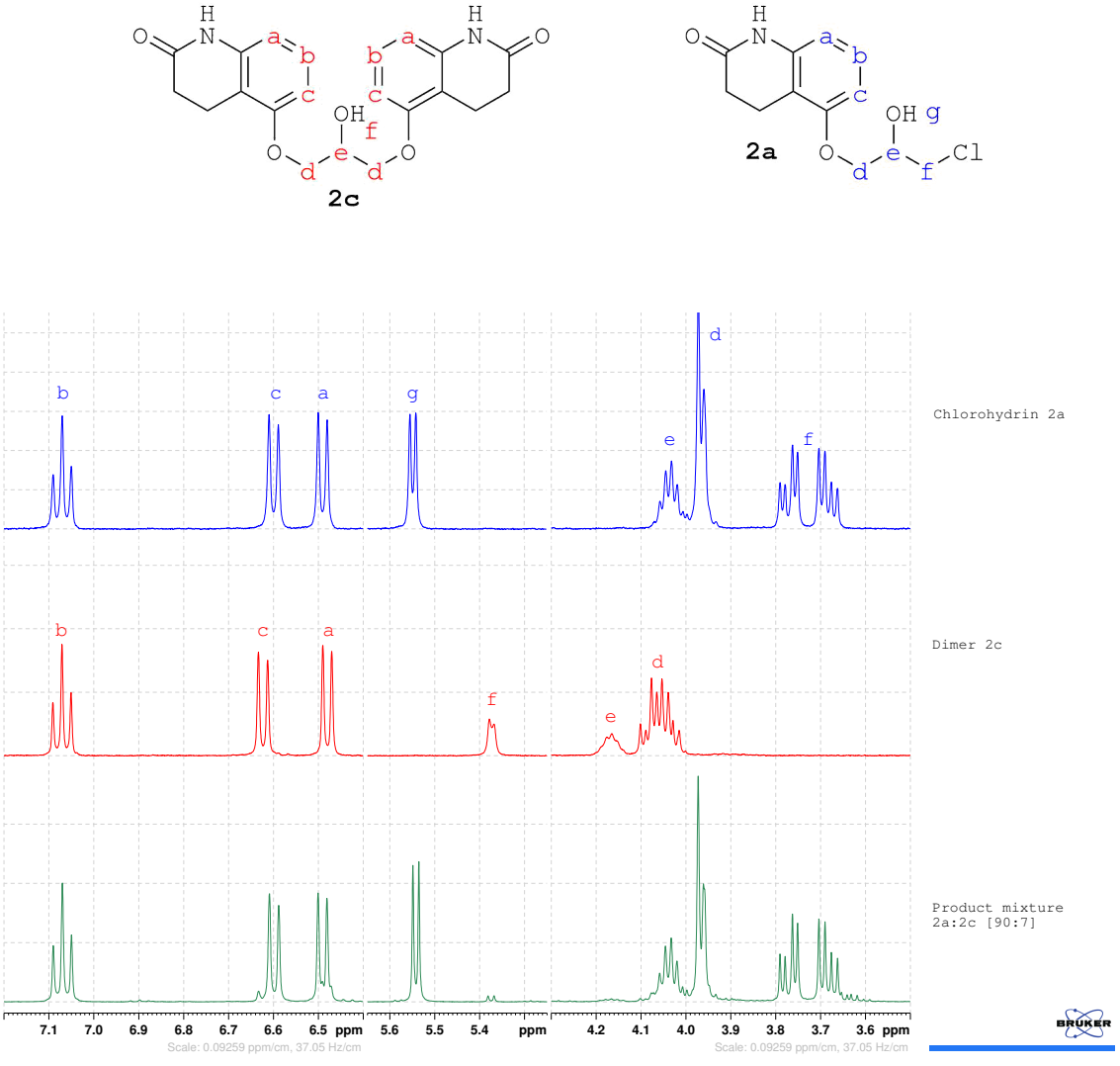

Figure 3.3: Comparison of ^{1}H NMR spectra for a product mixture of chlorohydrin **2a** and dimer **2c** with isolated samples of **2a** and **2c**.

3.1.5 Formation of dimer 2c and other impurities

Some impurities were observed during the synthesis of chlorohydrin **2a**, most notably dimer **2c**, see Figure 3.3. Formation of the dimer occurs during the first synthesis step. A proposed mechanism for dimer formation is shown in Scheme 3.5. The intermediate alkoxide $\mathbf{1_{anion}}$ formed after deprotonation of starting material **1**, see Scheme 3.1, functions as a nucleophile in three possible S_N2 mechanisms. Pathway A and pathway B are both Williamson ether syntheses, in which intermediate $\mathbf{1_{anion}}$ attacks the carbon in α-position to chloride on chlorohydrin **2a** and intermediate $\mathbf{2_{anion}}$ respectively. Similarly, in pathway C the alkoxide $\mathbf{1_{anion}}$ attacks the least substituted epoxide carbon. Pathway B and C both require protonation before complete formation of dimer **2c**.

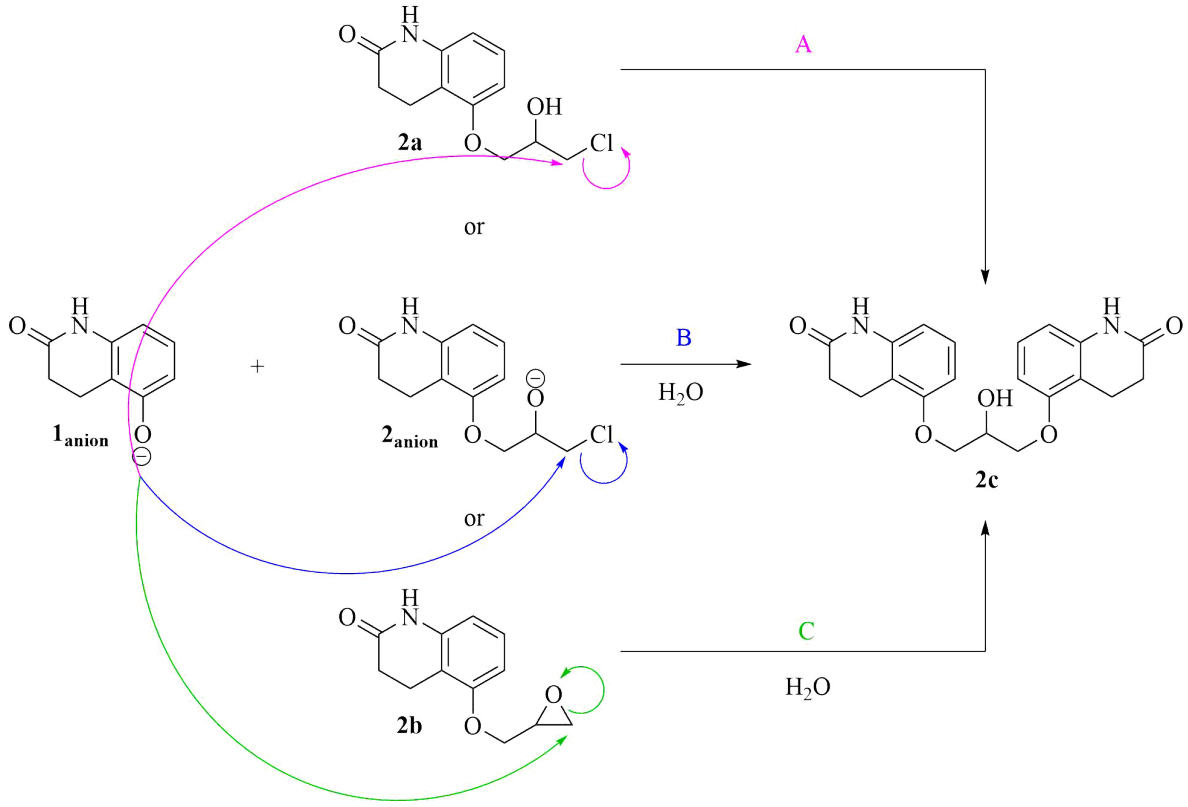

Scheme 3.5: Proposed mechanism for formation of dimer **2c** during synthesis of chlorohydrin **2a** and epoxide **2b** from alcohol **1**. The deprotonated alcohol $\mathbf{1_{anion}}$ attacks the already substituted products (**2a**, **2b**) and intermediates ($\mathbf{2_{anion}}$), forming dimer **2c**.

The removal of byproduct **2c** from wanted products **2a** posed a significant problem further discussed in Section 3.1.9.

Other impurities were also observed after the first synthesis step, but could not be fully characterized. Such impurities may be caused by alternative dimer formations, opening of the amide or alternative substitutions of epichlorohydrin to form chlorohydrin **X1**. A potential mechanism for a side reaction in which the alkoxide $\mathbf{1_{anion}}$ attacks at the most substituted carbon of the epoxide in epichlorohydrin to form chlorohydrin **X1**, is shown in Scheme 3.6. The byproduct was not formed in any substantial amount, and was prevented by use of a DMSO:H_2O solvent system, as suggested by Mangishi *et al.* [20], and not the MeOH:H_2O solvent system suggested by Nakagawa *et al.* [18]. For this reason, the impurity was not isolated or characterized.

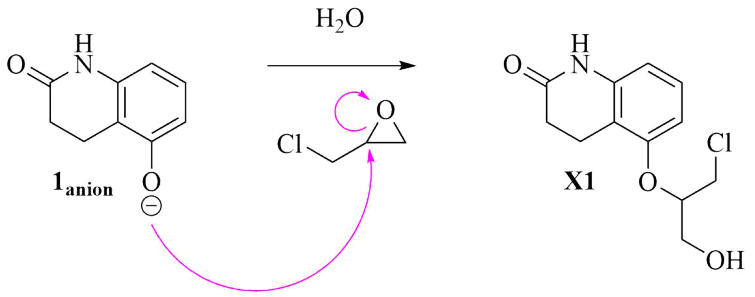

Scheme 3.6: Proposed mechanism for formation of chlorohydrin **X1** during synthesis of chlorohydrin **2a** and epoxide **2b** from alcohol **1**. The deprotonated alcohol $\mathbf{1_{anion}}$ attacks epichlorohydrin at the most substituted site, forming an alternative chlorohydrin.

Another impurity (**X2**) was observed during the second synthesis step, after the reaction was quenched with sodium carbonate. As the pK_a of acetic acid is 4.76 [88], acetate is formed at the addition of base. The observed impurity may have been caused by nucleophilic attack of acetate at the carbon in α-position to chloride on chlorohydrin **2a**, see Scheme 3.7. No isolation of ester **X2** was performed, as formation of the byproduct was easily circumvented by neutralizing the acid with water rather than base.

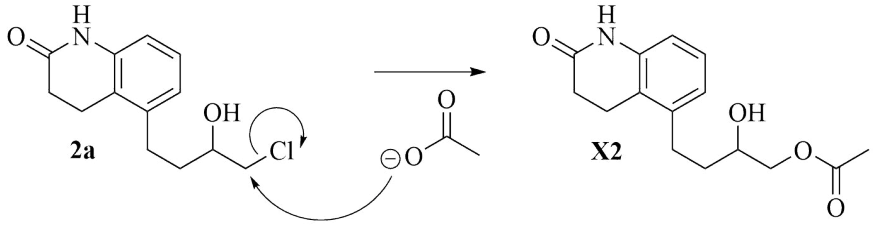

Scheme 3.7: Proposed mechanism for formation of byproduct **X2** during the synthesis of chlorohydrin **2a** from epoxide **2b**. Acetate attacks chlorohydrin **2a** at the carbon in α-position to chloride, forming an ester.

3.1.6 Characterization of dimer 2c

Full characterization of dimer **2c** was achieved by ^{1}H NMR, ^{13}C NMR, COSY, HSQC and HMBC experiments in $DMSO_{d6}$, see Figure 3.4 and Table 3.3. Analysis by LC-MS detected an exact mass of $[M+H]^+ = 383.2$ m/z. This is concurrent with the theoretically calculated molecular weight of dimer **2c** (382.4 g/mol). All spectra are presented in Appendix D.

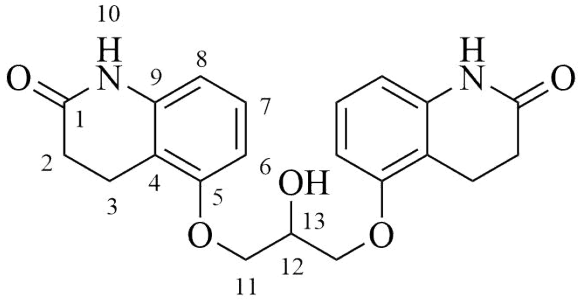

2c

Figure 3.4: Proton- and carbon positions of dimer **2c** as described in Table 3.3. All related NMR spectra are found in Appendix D.

All carbon positions were assigned chemical shifts as fit with HSQC and HMBC, see Figure 3.4 and Table 3.3. Carbons without protons were as such assigned shifts by two-, three- or four-bond relations. The chemical shifts at 10.01 (10), 7.09-7.05 (7), 6.63-6.61 (6), 6.49-6.47 (8), 2.81-2.77 (3) and 2.38-2.34 ppm (2) were assigned to the quinoline group, as they were consistent with previously characterized compounds, see Section 3.1.3.

Table 3.3: Acquired NMR data for dimer **2c**. Listed proton- and carbon positions refer to those presented in Figure 3.4. All related NMR spectra are found in Appendix D.

Pos.	^{1}H *(int., mult., J [Hz]) [ppm]*	^{13}C *[ppm]*	*COSY*	*HMBC*
1	-	170.5	-	2, 3
2	2.38-2.34 (4H, t, 7.7)	30.3	3	3, 10
3	2.81-2.77 (4H, t, 7.7)	18.7	2	2
4	-	111.7	-	2, 3, 6, 8, 10
5	-	156.1	-	3, 7 (6, 8, 11, 12)
6	6.63-6.61 (2H, d, 8.2)	106.3	7	6
7	7.09-7.05 (2H, t, 8.1)	128.1	6, 8	-
8	6.49-6.47 (2H, d, 7.9)	108.7	7	8 (10)
9	-	139.8	-	7, 3 (10)
10	10.01 (2H, s)	-	-	-
11	4.10-4.01 (4H, m)	69.9	12	(11, 12)
12	4.18-4.17 (1H, m)	68.0	11	-
13	5.38-5.37 (1H, d, 4.1)	-	-	-

The shift with split multiplicity at 5.38-5.37 ppm (13) was assigned to the alcohol proton, as the signals are compatible and the integrated value equaled a singular proton. Chemical shifts observed at 4.18-4.17 ppm (12) were similarly assigned to the proton in chiral position due to its characteristic multiplicity. Shifts at 4.10-4.01 ppm (11) were assigned to the ether methylene bridge due to observed coupling with the carbon in position 5.

3.1.7 Effect of catalytic amounts of base on byproduct formation and product distribution

The mechanism proposed for the first synthesis step suggests a partially base catalyzed reaction, see Section 3.1.1. Previously in this project, several reactions were performed with catalytic amounts of base (0.3 - 1.0 eq.) in order to investigate the impact of reduced base equivalents on conversion of starting material **1** and distribution of products formed.

Table 3.4: Comparison of molar product composition [m%] after the first step in synthesis of chlorohydrin **2a** from alcohol **1** with intermediate product **2b** and byproduct **2c**. Molar product composition was determined by ^{1}H NMR.

	Product composition [m%]			
NaOH [eq.]	**1**	**2a**	**2b**	**2c**
1.0	0.1	4.0	93.6	2.2
0.8	0.2	15.9	81.9	2.0
0.7	1.5	50.0	46.6	1.9
0.5	1.7	55.9	41.3	1.1
0.3	2.1	72.5	24.7	0.7

It is clear from the acquired data that catalytic amounts of NaOH only margin-ally affects the conversion of alcohol **1** to products **2a** and **2b**. This confirms the regeneration of hydroxide through product formation in the first synthesis step. For even fewer equivalents of base, extended reaction times may be necessary as the concentration of the nucleophile sinks.

As seen in the mechanism of dimer **2c**, see Section 3.1.5, fewer equivalents of base provide lower concentrations of the deprotonated alcohol **1** and thus less formation of dimer **2c**. Though catalytic amounts of base had a significant impact on dimer formation, it did not negate its formation completely, see Table 3.4. See Section 3.1.9 for a discussion of purification methods that remove this byproduct.

Another interesting observation was the effect of catalytic base equivalents on the **2a**:**2b** product ratio, see Figure 3.5. Whereas stochiometric equivalents of NaOH predominantly formed epoxide **2b**, methods with less base increased formation of chlorohydrin **2a**. This suggests that the low concentration of hydroxide pushes the reaction in favor of hydroxide regeneration and formation of **2a**.

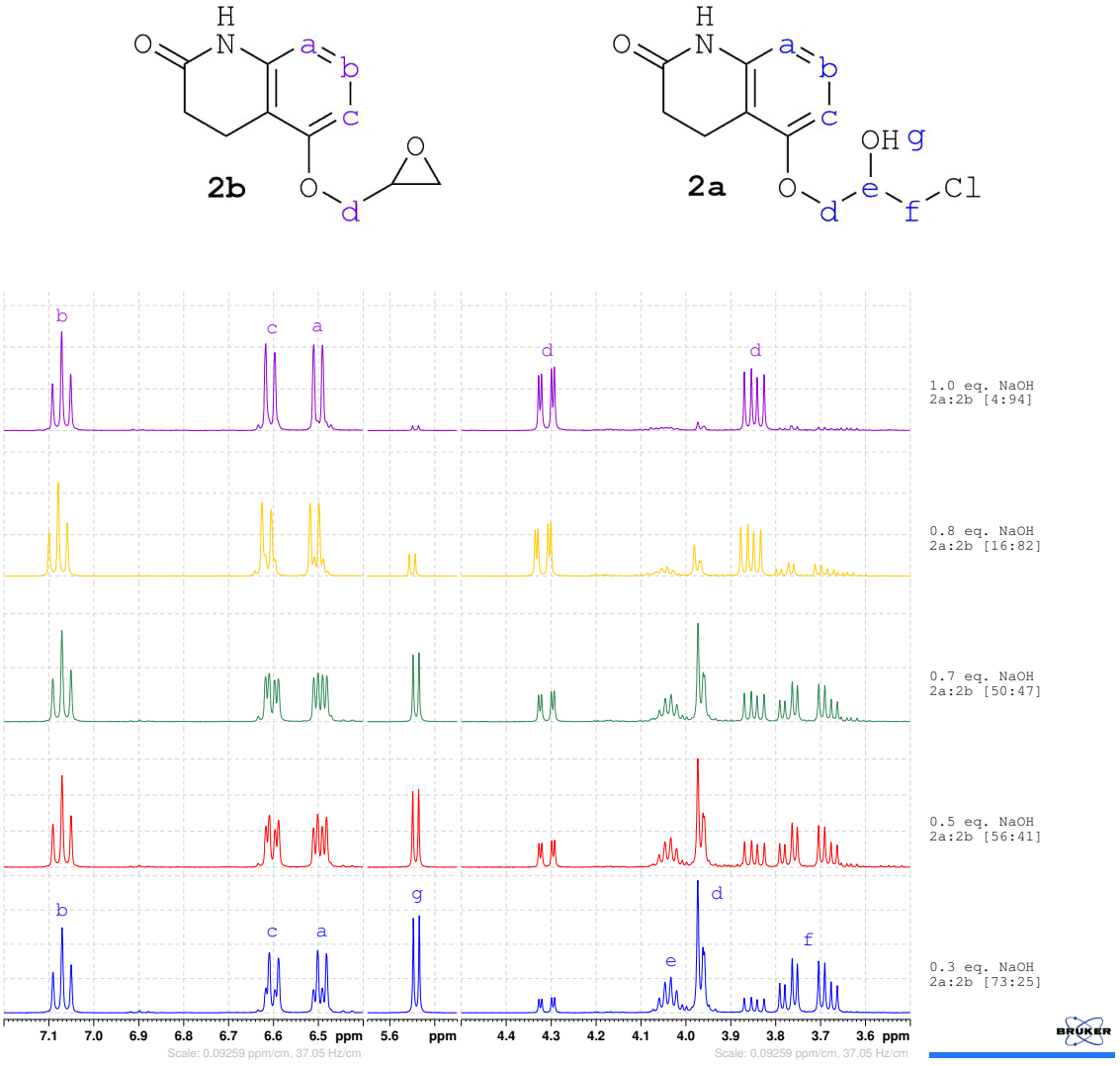

Figure 3.5: Comparison of ^{1}H NMR spectra for chlorohydrin **2a** and epoxide **2b** synthesized with 0.3 to 1.0 equivalents of NaOH, see Table 3.4. With catalytic amounts of base, the ratio of **2a** to **2b** increased.

3.1.8 Examination of kinetic- and thermodynamic product stability in the first synthesis step

Examination of product composition as a function of time revealed a decrease in amount of chlorohydrin **2a** with increasing conversion, see Figure 3.6. The experiment was performed with 1.0 equivalent of NaOH and reached 99% conversion after 8 hours. This suggests that chlorohydrin **2a** is formed first as the kinetically stable product, but is then later converted to the more thermodynamically stable epoxide **2b**, which supports the mechanism proposed in Section 3.1.1. The mechanism shows cyclization of chlorohydrin **2a** by intramolecular Williamson ether synthesis to epoxide **2b**. Heat during the reaction should therefore be avoided, as should excessive reaction time beyond what is needed for full conversion. For the method described in Section 3.1.1, 0.3 equivalents of NaOH were used and conversions of 99% observed after 24 hours. This length of reaction time was considered acceptable.

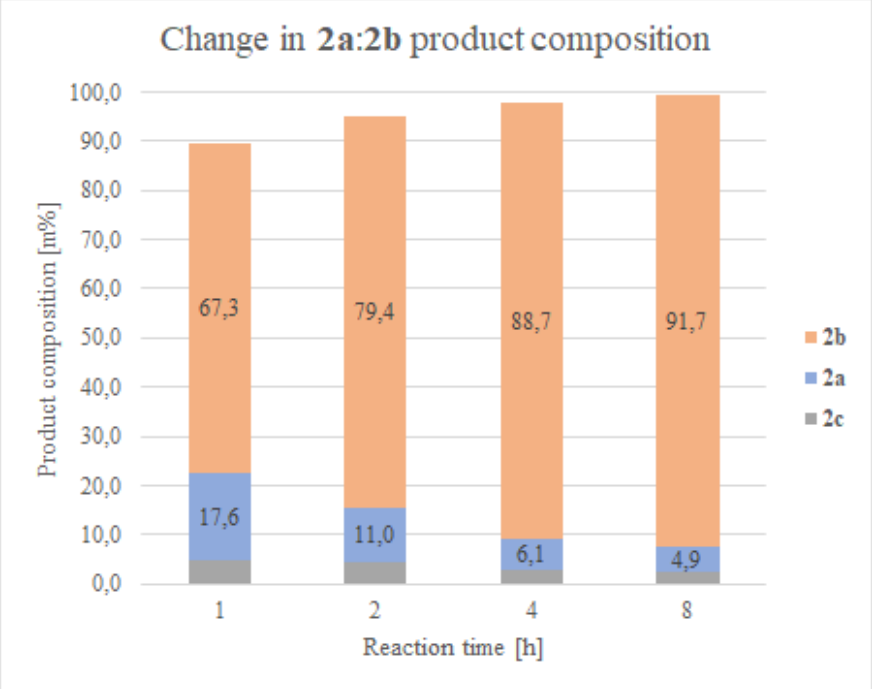

Figure 3.6: Change in molar product composition [m%] as a function of reaction time [h]. A clear decrease of chlorohydrin **2a** was observed at increased reaction conversion.

3.1.9 Removal of dimer 2c and other impurities

As discussed in Section 3.1.5, the formation of dimer **2c** posed a significant issue in the synthesis of chlorohydrin **2a**. Due to the thermal instability of chlorohydrin **2a**, the difficulty of its dissolution and the relative simplicity of the second synthesis step, it was decided that the removal of dimer **2c** should be performed after the first synthesis step.

Previously in this project, the first synthesis step was performed with 1.0 equivalents of NaOH and 2.0 equivalents of epichlorohydrin in a MeOH:H_2O solvent system for 24 hours. This did not provide full conversion, and **1**:**2a**:**2b**:**2c** was obtained in a molar product composition of 3:20:71:6. The same reaction conditions in a DMSO:H_2O solvent system provided **2a**:**2b**:**2c** in a molar product composition of 4:94:2. The higher share of epoxide **2b** and lower share of dimer **2c** is attributed to the aprotic polar nature of DMSO, which is known for supporting S_N2 mechanisms.

Recrystallization of epoxide **2b** was performed as suggested by literature [1], from which **2a**:**2b**:**2c** was obtained in a molar product composition of 4:94:2. Analysis of the filtrate also showed significant amounts of product **2a** and **2b**, indicating too high solubility of the products in ethanol. Due to the wasteful nature and insufficient purification of this method, other techniques were explored. It should however be mentioned that recrystallization from less polar solvents may prove beneficial.

Purification of the product mixture described above was achieved by flash chromatography with ethyl acetate. The eluent was determined by TLC ($R_{f(\mathbf{1},\mathbf{2a},\mathbf{2b})} = 0.46$, $R_{f(\mathbf{2c})} = 0.16$). After separation, **2a**:**2b** was obtained in a molar product composition of 5:95, indicating sufficient separation.

As discussed in Section 3.1.7, use of 0.3 equivalents of NaOH in the first synthesis step resulted in higher yield of **2a** and lower yield of **2b** and **2c** without significant sacrifice in conversion of alcohol **1**. However, due to the issues of dissolution encountered with chlorohydrin **2a**, the developed method of flash chromatography could no longer be utilized.

The methods previously described in this section were all worked up by extraction with dichloromethane and washing of the organic phase with brine. Mangishi *et al.* [20] suggested filtration of product. This was performed with small amounts of H_2O to remove reagents, and produced **1**:**2a**:**2b**:**2c** in a molar product composition of 0.8:74.5:24.3:0.4.

After this, the second reaction step was initiated, where the product was again washed with water to remove reagents and chloroform to remove dimer **2c**. This was only performed after the second synthesis step, as epoxide **2b** also can be dissolved in chloroform. From this method, **2a**:**2b** was achieved in a molar product composition of 98:2. As carteolol (**4**) can by synthesized from both chlorohydrin **2a** and epoxide **2b**, this was considered sufficient purity and the described method was further used throughout the project. It should be noted that the traces of epoxide **2b** may negatively affect the enantiomeric purity of (*S*)-**4**, see Section 3.4.

3.2 Separation of chlorohydrin 2a, ester 3 and carteolol (4) by chiral HPLC

Analysis of enantiomeric excess is necessary both to monitor the reaction and determine the enantioselectivity *Candida antarctica* Lipase B (CALB) expresses towards substrate **2a**. As chlorohydrin **2a**, ester **3** and carteolol (**4**) are large molecules and estimated to have high boiling points, separation was performed by chiral high-pressure liquid chromatography (HPLC). All related chromatograms are presented in Appendix B, F and G.

Chiral separation of chlorohydrin **2a** was attempted with a Chiralcel OD-H column (cellulose tris-(3,5-dimethylphenylcarbamate) coated on silica) and a Chiralpak AD-H column (amylose tris-(3,5-dimethylphenylcarbamate) coated on silica). Baseline separation with superior retention times was observed with the Chiralcel OD-H column. For simplicity, all other compounds were separated with the same column.

Effects of solvent composition, modifiers and flow rates were examined to further optimize the separation of chlorohydrin **2a** enantiomers. Shorter retention times and increased separation was observed when ethanol was used as the alcohol constituent instead of *iso*-propanol. Improved peak shape and separation was also observed with use of modifiers like diethylamine (DEA) and trifluoroacetic acid (TFA). Diethylamine generally improves separation of basic compounds, and trifluoroacetic acid of acidic ones. Slow flow rates (0.4 mL/min) also improved separation when compared to faster flow rates (1.0 mL/min). Complete separation ($R_S = 1.62$) of chlorohydrin **2a** was achieved with a Hex:EtOH:TFA [90:10:0.1] mobile phase composition at a flow rate of 0.4 mL/min, see Table 3.5. This resulted in long retention times ($t_1 = 63.43$ min, $t_2 = 68.68$ min) unsuitable for industrial purposes. For higher efficiency in future experiments, other columns should be explored. As these were the columns available for this project, the results were considered acceptable.

Table 3.5: Description of methods used for chiral HPLC of chlorohydrin **2a**, ester **3** and carteolol (**4**). Flow rate at 0.4 mL/min. Related chromatograms are found in Appendix B, F and G.

	Mobile phase composition						
	Hex [%]	*Alc. ([%])*	*Mod. ([%])*	R_S	α	t_1 *[min]*	t_2 *[min]*
2a	90	EtOH (10)	TFA (0.1)	1.62	1.08	63.43	68.68
3	95	iPrOH (5)	DEA (0.4)	1.53	1.07	108.79	116.21
4	80	iPrOH (20)	DEA (0.4)	7.52	1.78	19.60	34.88

Significantly higher separation of ester **3** was observed with *iso*-propanol as the alcohol constituent than with ethanol. Complete separation ($R_S = 1.53$) was achieved with a Hex:iPrOH:DEA [95:5:0.4] mobile phase composition at a flow rate of 0.4 mL/min, see Table 3.5. As observed solute retention times ($t_1 = 108.79$ min, $t_2 = 116.21$ min) exceeded 60 minutes, this method is highly impractical for industrial purposes. However, for this project it was acceptable. It should be noted that separation was achieved with enantioenriched reaction mixture from the third reaction step. A racemic sample was later analyzed to confirm separation of enantiomers, but full separation was not achieved. This was attributed to the

high concentrations of the sample, as well as a change in solvent. Baseline separation was achieved for all sample analyses included in this project.

The method for separation of **4** on Chiralcel OD-H columns was adapted from previously developed methods [89]. Complete separation ($R_S = 7.52$) was achieved with a Hex:iPrOH:DEA [80:20:0.4] mobile phase composition at a flow rate of 0.4 mL/min, see Table 3.5. It was observed that chlorohydrin **2a** eluted simultaneously as (*S*)-**4** (t_2 = 34.88 min). It should be noted that for samples containing **2a**, this may cause issues for correct calculation of enantiomeric excess, see Section 3.4

3.3 Kinetic resolution of chlorohydrin 2a

The third step in synthesis of (*S*)-carteolol ((*S*)-**4**) was the kinetic resolution of chlorohydrin **2a** by transesterification reaction with CALB. The ping-pong bi-bi mechanism of serine hydrolases is detailed in Section 1.7.5. The transesterification reaction was catalyzed by CALB and performed with 5 equivalents of vinyl butanoate in dry acetonitrile, see Scheme 3.8. This method was based on the previous work of our research group [1]. Molecular sieves (4Å) were added to ensure dry conditions. After 74 hours of reaction at 37 °C and 200 rpm, the sieves and enzymes were filtered off. Ester (*S*)-**3** and chlorohydrin (*R*)-**2a** were separated by flash chromatography (ethyl acetate:*n*-hexane [7:3]).

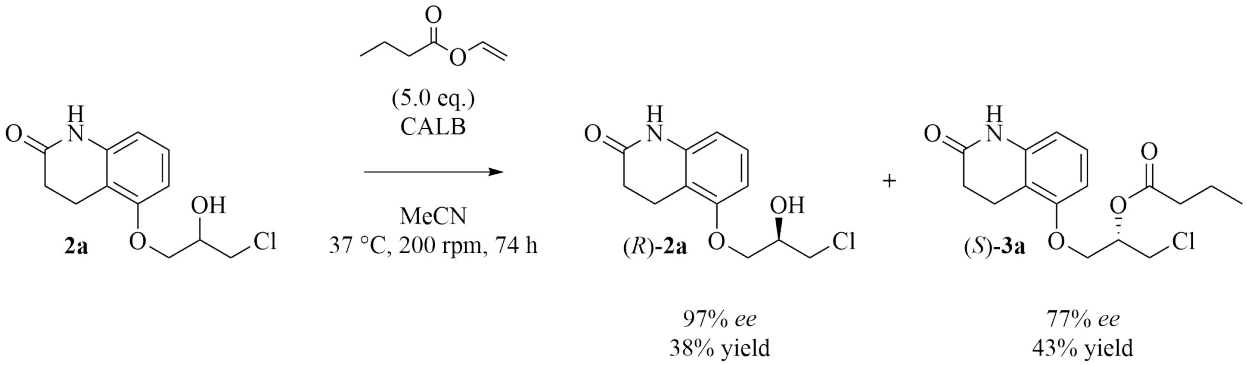

Scheme 3.8: Kinetic resolution of chlorohydrin **2a** by transesterification reaction with CALB and acyl donor vinyl butanoate. This forms chlorohydrin (*R*)-**2a** and ester (*S*)-**3**.

From this method, (*R*)-**2a** was obtained in a 38% yield, with 97% *ee* and 94% purity, see Figure 3.7. The specific optical rotation of chlorohydrin (*R*)-**2a** was determined to be $[\alpha]_D^{20} = -9.9$ ($c = 1.0$, DMSO). No values for the optical rotation of chlorohydrin (*R*)-**2a** have been reported. Traces of epoxide **2b** (2.8%) and ester **3** (2.9%) were detected by ^{1}H NMR. While the epoxide is racemic and optically inactive, the presence of enantioenriched ester (*S*)-**3** may have negatively impacted the observed optical rotation. For future experiments, flash chromatography methods with increased separation should be developed to prevent this issue, see Section 3.3.3.

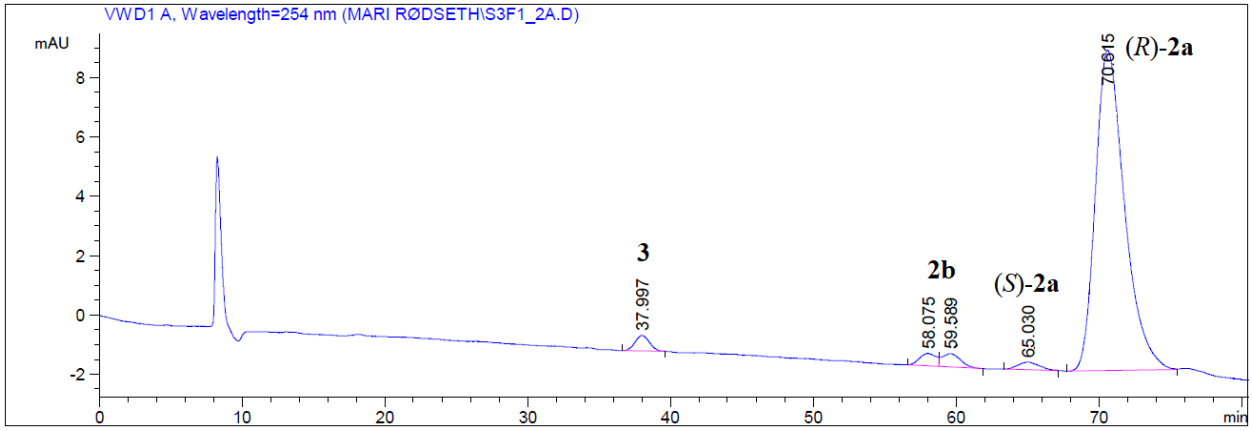

Figure 3.7: Chiral HPLC (Chiralcel OD-H, *n*-hexane:ethanol:trifluoroacetic acid [90:10:0.1], 0.4 mL/min) chromatogram from which the enantiomeric excess of chlorohydrin **2a** (97% *ee*) was calculated after transesterification reaction. Traces of ester **3** and epoxide **2b** were observed.

Ester (*S*)-**3** was obtained in a 43% yield, with 77% *ee* and 93% purity, see Figure 3.8. The specific optical rotation of ester (*S*)-**3** was determined to be $[\alpha]_D^{20} = +9.9$ ($c = 1.0$, DMSO). No values for the optical rotation of ester (*S*)-**3** have been reported. Some butanoic acid was observed (6.5%) in the product, see Section 3.3.4. As butanoic acid is an achiral compound, the effects on observed optical rotation should be negligible.

Replications of the reaction were attempted, but unsuccessful due to enzyme-inhibition, see Section 3.3.5. For this reason, as well as low product quantities preventing experimentation with further purification methods, higher product purity could not be achieved.

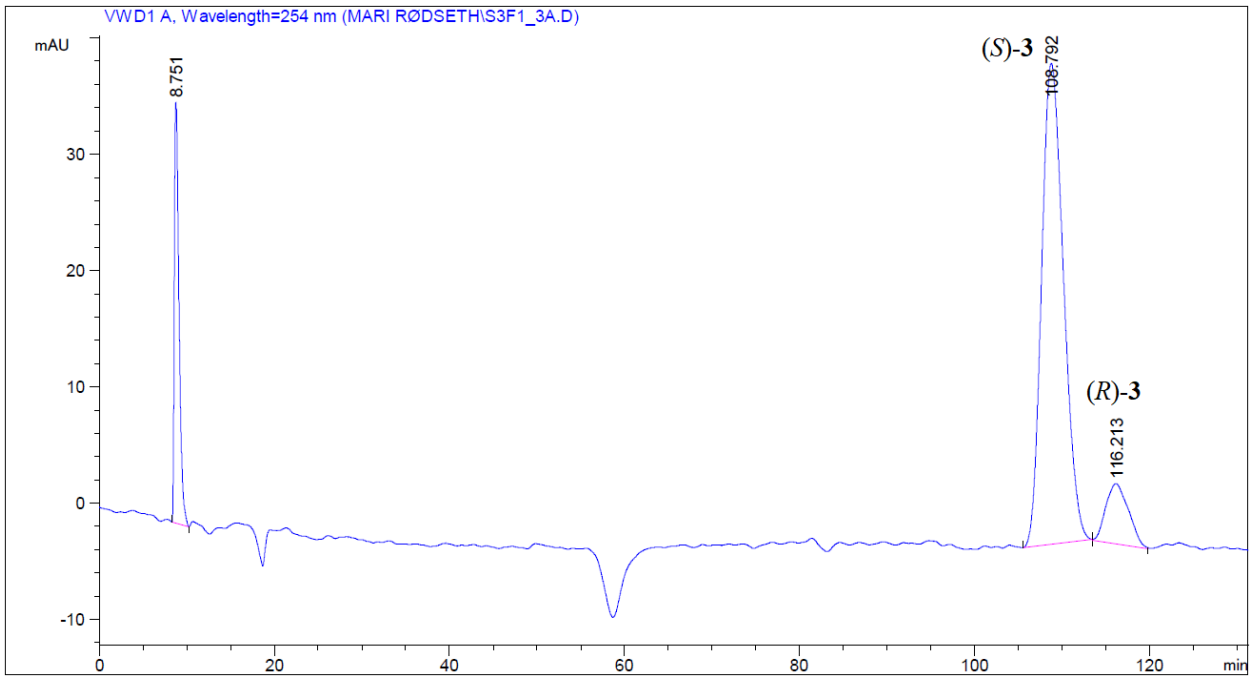

Figure 3.8: Chiral HPLC (Chiralcel OD-H, *n*-hexane:*iso*-propanol:diethylamine [95:5:0.4], 0.4 mL/min) chromatogram from which the enantiomeric excess of ester **3** (77% *ee*) was calculated after transesterification reaction.

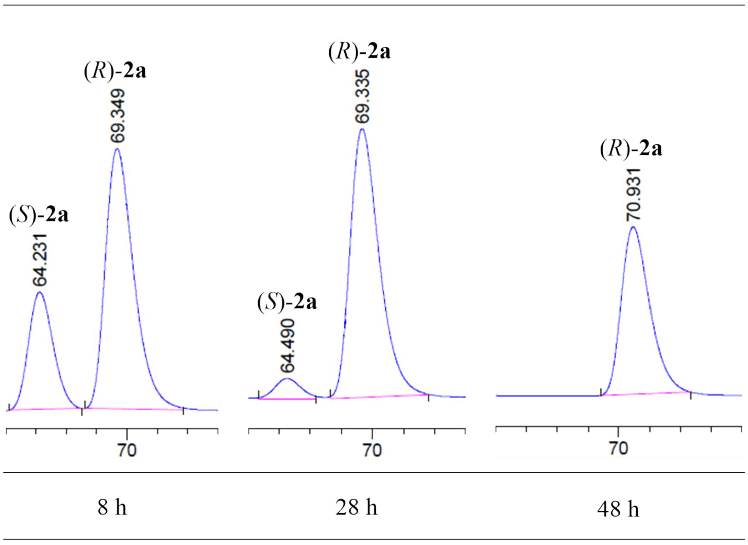

Figure 3.9: Separation of chlorohydrin **2a** by chiral HPLC (Chiralcel OD-H, *n*-hexane:ethanol:trifluoroacetic acid [90:10:0.1], 0.4 mL/min) after 8 (44% *ee*), 28 (88% *ee*) and 48 hours (99% *ee*) of transesterification reaction. The area of each peak relates to the amount of enantiomer it represents.

3.3.1 Enantioselectivity of CALB towards chlorohydrin 2a

Transesterification reaction of chlorohydrin **2a** was also performed at a smaller scale (0.1 mmol **2a**) to map the enantioselectivity of CALB towards **2a**. Regular samples were extracted from the reaction mixture and its progression was monitored by HPLC, as discussed in Section 3.2. Chromatograms analyzed after 8, 28 and 48 hours show the clear decline of (*S*)-**2a** in comparison to (*R*)-**2a**, see Figure 3.9. With the depicted HPLC method, elution of the enantiomers occurs at $t_1 \approx 64$ min (*S*) and $t_2 \approx 70$ min (*R*).

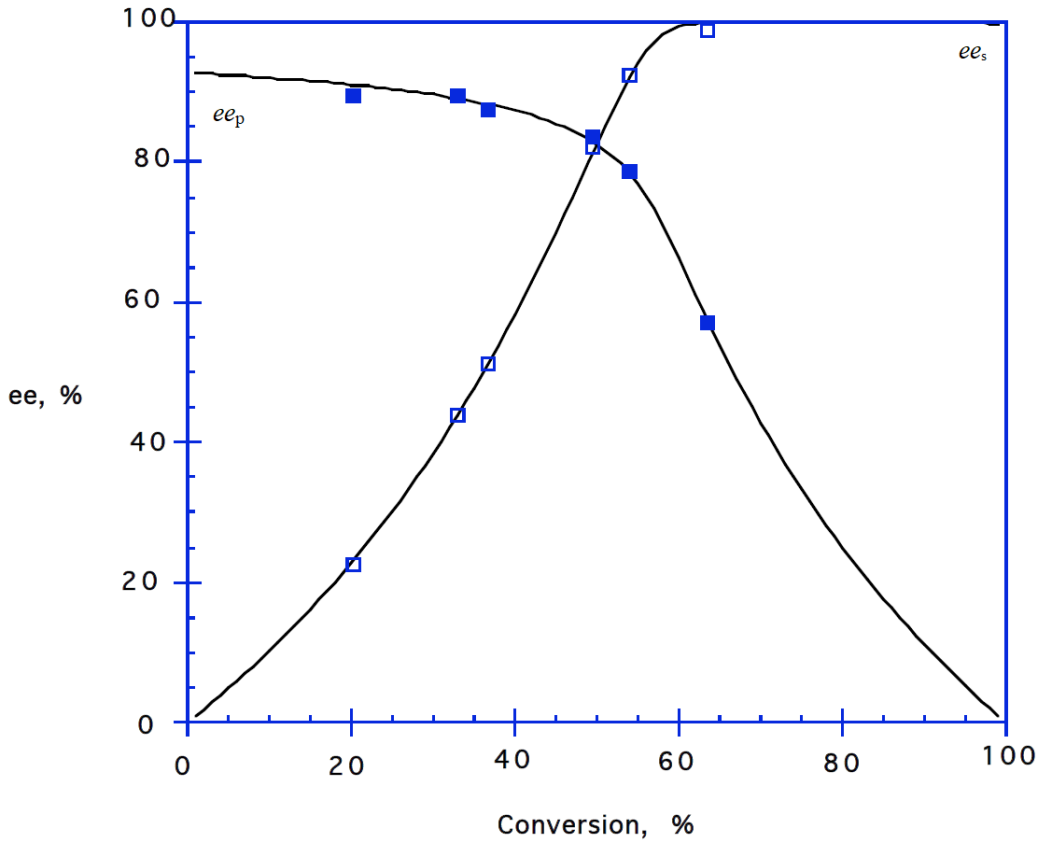

Figure 3.10: Kinetic resolution of substrate **2a** by transesterification reaction with vinyl butanoate and CALB (E = 27, calc. by *E&K Calculator 2.1b0 PPC*). The enantiomeric excess of chlorohydrin (*R*)-**2a** (ee_S, empty squares) and ester (*S*)-**3** (ee_P, filled squares) are plotted as functions of reaction conversion.

Calculation of the enantiomeric ratio (E) of a ping-pong bi-bi mechanism required known ee_S and ee_P at multiple points of conversion (c). From this data, a kaleidograph plot of ee_S and ee_P as a function of reaction conversion was made with E = 27, see Figure 3.10. This was significantly lower than the E-value achieved by our research group for the kinetic resolution of a 7-substituted derivative of chlorohydrin **2a** (E = 157) under the same reaction conditions [1]. The main difference between the two substrates was the steric hindrance of **2a**, which may have impaired the enantioselectivity of CALB. E-values at 50-200 are considered excellent, but even enzymes of lower enantioselectivity (e.g. E = 20) may produce acceptably enantioenriched compounds [69, 90]. This is especially the case when the desired product is the remaining alcohol and not the transformed ester.

3.3.2 Characterization of ester (*S*)-3

Full characterization of ester (*S*)-**3** was achieved by ^{1}H NMR, ^{13}C NMR, COSY, HSQC and HMBC experiments in $DMSO_{d6}$, see Figure 3.11 and Table 3.6. Analysis by MS detected an exact mass of $[M+H]^+ = 326.1$ m/z. This is concurrent with the theoretically calculated molecular weight of ester **3** (325.8 g/mol). All related spectra are presented in Appendix F.

All carbon positions were assigned chemical shifts as fit with HSQC and HMBC, see Figure 3.11 and Table 3.6. Carbons without protons were as such assigned shifts by two-, three- or four-bond relations. Chemical shifts observed at 10.04 (10), 7.10-7.06 (7), 6.62-6.60 (6), 6.51-6.49 (8), 2.79-2.75 (3), 2.41-2.38 (2) were assigned to the quinoline group, as they were consisted with previously characterized compounds, see Section 3.1.3.

Shifts observed at 5.38-5.33 ppm (12) were assigned to the chiral proton due to the characteristic multiplicity of chiral centers. The chemical shifts at 4.21-4.17 and 4.15-4.11 ppm (11) were coupled to the carbon at position 5, and assigned to the ether methylene bridge. Similarly, the shifts at 3.98-3.94 and 3.91-3.86 ppm (13) were assigned to the chloride methylene bridge.

Table 3.6: Acquired NMR data for ester (*S*)-**3**. Listed proton- and carbon positions refer to those given in Figure 3.11. All related NMR spectra are found in Appendix F.

Pos.	^{1}H *(int., mult., J [Hz]) [ppm]*	^{13}C *[ppm]*	*COZY*	*HMBC*
1	–	170.6	–	2, 3
2	2.41-2.38 (2H, t, 7.7)	30.2	3	3, 10
3	2.79-2.75 (2H, t, 7.7)	18.6	2	2
4	–	111.8	–	2, 3, 6, 8, 10
5	–	155.5	–	7, 3 (11, 6)
6	6.62-6.60 (1H, d, 8.0)	106.3	7 (8)	8
7	7.10-7.06 (1H, t, 8.1)	128.2	6, 8	–
8	6.51-6.49 (1H, d, 7.8)	109.1	7 (6)	6
9	–	139.9	–	7, 3
10	10.04 (1H, s)	–	–	–
11	4.21-4.17 (1H, dd, 10.6, 4.1)	67.4	12	13
	4.15-4.11 (1H, dd, 10.6, 6.2)			
12	5.38-5.33 (1H, m)	71.1	11, 13	11, 13
13	3.98-3.94 (1H, dd, 11.8, 4.2)	43.8	12	11
	3.91-3.86 (1H, dd, 11.8, 6.5)			
14	–	172.6	–	15, 16
15	2.35-2.31 (2H, m)	35.8	16	16, 17
16	1.61-1.46 (2H, m)	18.4	15, 17	15, 17
17	0.90-0.85 (3H, m)	13.8	16	15, 16

The shifts at 2.35-2.31 (15), 1.61-1.46 (16) and 0.90-0.85 ppm(17) were assigned to the butanoate-group. They were differentiated by carbon couplings and and compatible proton-values.

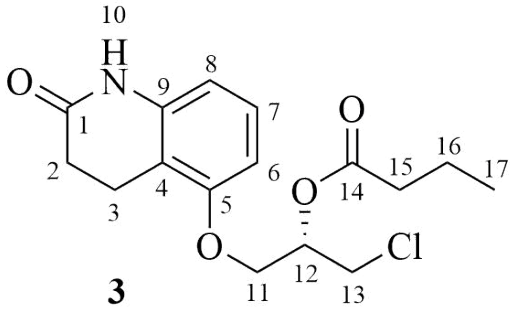

3

Figure 3.11: Proton- and carbon positions of ester (*S*)-**3** as described in Table 3.6. All related NMR spectra are found in Appendix F.

3.3.3 Separation of chlorohydrin (*R*)-2a and ester (*S*)-3 by flash chromatography

Separation of chlorohydrin (*R*)-**2a** and ester (*S*)-**3** was achieved by flash chromatography an ethyl acetate:*n*-hexane [7:3] solvent system. The eluent was optimized by TLC, see Table 3.7. Ethyl acetate was first tested without a co-solvent, as this has performed well for similar compounds, see Section 3.1.9. However, the high retention factors ($R_{f(\mathbf{3})} = 0.51$, $R_{f(\mathbf{2a})} = 0.35$) would likely cause low retention times and poor separation. Instead, *n*-hexane was added in a 7:3 ratio, from which lower rentention factors ($R_{f(\mathbf{3})} = 0.34$, $R_{f(\mathbf{2a})} = 0.16$) and sufficient separation was achieved ($R_{\Delta\ f(\mathbf{2a},\mathbf{3})} = 0.18$).

As discussed in Section 3.1.9, dissolution of chlorohydrin **2a** posed an issue for flash chromatography. This issue was circumvented by performed flash chromatography with the reaction mixture as a concentrated solution in acetonitrile rather than as a dry solid.

It should be mentioned that full separation of chlorohydrin (*R*)-**2a** and ester (*S*)-**3** was not achieved by flash chromatography with this solvent system, and that some of the ester remained as an impurity in chlorohydrin (*R*)-**2a**. This was likely caused by either tailing or dissolution of the compounds in acetonitrile. For future experiments, evaluation of other solvent systems should be performed for optimal product purity. Alternatively, the product mixture may be separated twice by use of the method described.

Table 3.7: Overview over solvent compositions tested as the mobile phase for separation of chlorohydrin (*R*)-**2a** and ester (*S*)-**3** by flash chromatography. Different compositions of ethyl acetate (EtOAc) and *n*-hexane (Hex) were tested.

Mobile Phase [%]

EtOAc	*Hex*	R_f(**3**)	R_f(**2a**)	ΔR_f(**2a**,**3**)
10	0	0.51	0.35	0.16
8	2	0.39	0.21	0.18
7	3	0.34	0.16	0.18
6	4	0.26	0.10	0.16

3.3.4 Formation of butanoic acid in the presence of water

Shifts incompatible with ester (*S*)-**3** were observed by ^{1}H NMR of the ester product, see Figure 3.12. As CALB can catalyze hydrolysis reactions of the ester and vinyl butanoate in the presence of water, butanoic acid may be formed. This byproduct is congruent with the observed impurity. The characteristic odor of butanoic acid was also detected. Formation of the acid could not be confirmed by quantitative tests. While the reaction was performed in dry acetonitrile and with molecular sieves (4Å), it is possible that chlorohydrin **2a** retained some water from previous synthesis steps. It should also be noted that by laboratory standards, the molecular sieves were dried at 1000 °C for 24 hours. Temperatures above 500 °C have been reported to cause irreversible collapse of 4Å molecular sieve structures [91]. This may have contributed to higher water content and an increase in butanoic acid formation. For future experiments, a solution to this issue could be activation of the molecular sieves at lower temperatures (250 °C) or extensive drying of the starting material.

During separation of chlorohydrin (*R*)-**2a** and ester (*S*)-**3**, butanoic acid was eluted with the ester fraction as a constituent of 6.5%. The boiling point of butanoic acid (164 °C) is too high for removal by standard work-up procedures, but can likely be distilled off under reduced pressure. The estimated boiling point of ester **3** (556 °C) is sufficiently high. However, as the ester was not the desired product of this reaction and butanoic acid is optically inactive,

distillation of ester (*S*)-**3** was not performed. No butanoic acid was observed in the fraction of chlorohydrin (*R*)-**2a**.

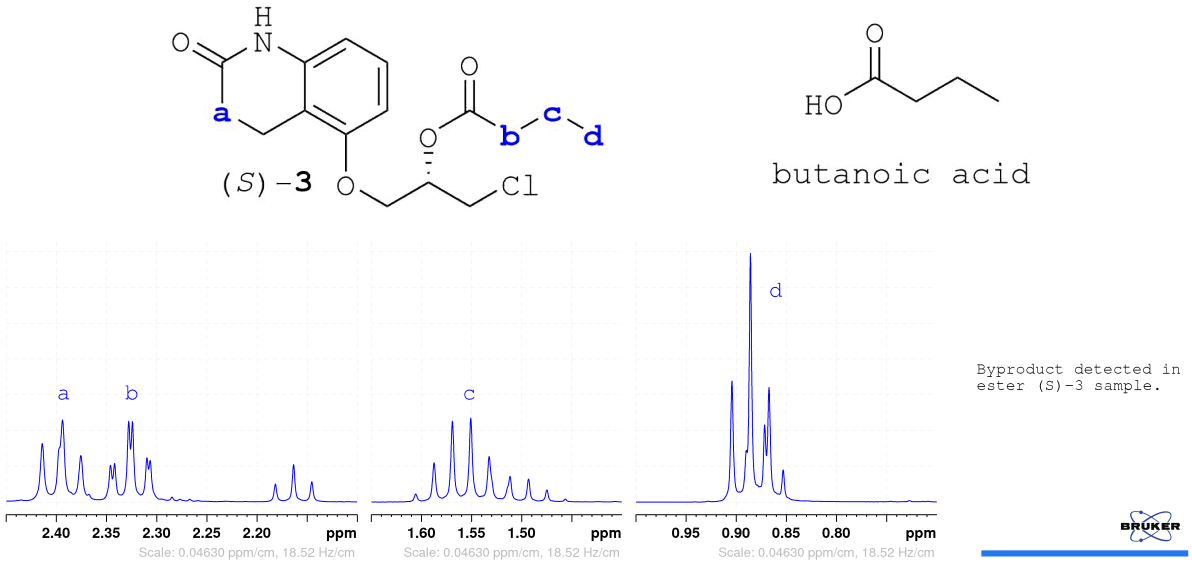

Figure 3.12: ^{1}H NMR spectra of ester (*S*)-**3** synthesized by kinetic resolution of chlorohydrin **2a** with vinyl butanoate. The proton shifts that are incompatible with the ester are congruent with the stereochemistry of butanoic acid.

3.3.5 Inhibition of CALB by heavy metal cations

Clear signs of enzyme inhibition was observed during the transesterification reaction of chlorohydrin **2a**, see Figure 3.13. Multiple parallels were performed with the same reaction conditions and substrate synthesized by the same method, but in different batches. Inhibition was observed for multiple of them.

Compounds like EDTA, SDS and N-hydroxyhydantoin carbamates are known to inhibit lipases, but have not been used in any capacity in this project and are not common contaminations. Acetaldehyde, which is a byproduct of transesterification reactions with vinyl esters, has been found to inhibit some lipases, but not CALB.

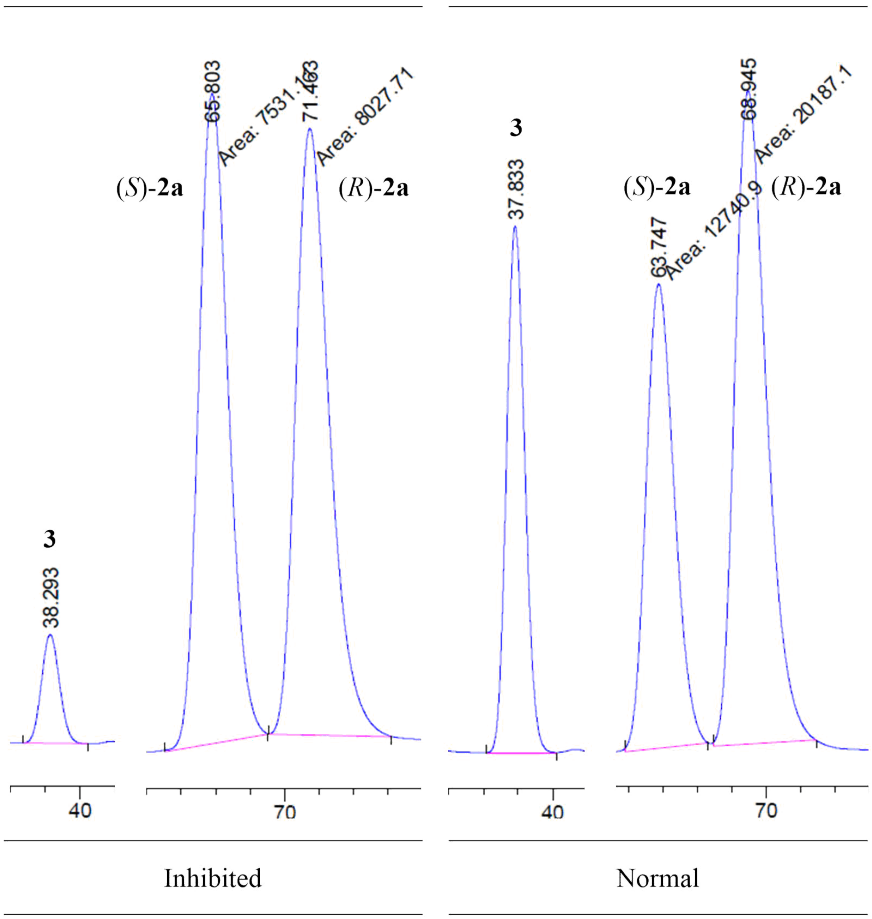

Figure 3.13: Chromatograms (Chiralcel OD-H, *n*-hexane:ethanol:trifluoroacetic acid [90:10:0.1], 0.4 mL/min) of reaction mixtures from transesterification reactions of chlorohydrin **2a** after 4 hours. The reactions were performed with vinyl butanoate and catalyzed by CALB. The chromatogram of the inhibited reaction (left, 3% *ee*) has progressed significantly less than the normal reaction (right, 23% *ee*).

The presence of some metal cations has been reported to inhibit lipases. Lithium chloride was used during the synthesis of **2a**, and some Li^+ may remain after product work-up. As early reaction parallels worked well, however, it is more likely that the observed inhibition was caused by environmental contamination of product. Of possible environmental exposures, iron cations (Fe^{2+}, Fe^{3+}) from rust as well as cations found in tap water (Ca^{2+}, Mg^{2+}, Na^+, K^+ [92]) are the most likely sources. As inhibition was consistent regardless of measures taken to prevent environmental exposures, it is likely that starting materials, solvents or reagents

used were contaminated during the project. Analysis by ICP-MS should be performed on substrate-batches known to inhibit CALB in order to determine the presence of metal cations. Controlled exposure of the enzyme to the suspected cations should also be performed to determine the specific metal cation inhibitors of CALB. Due to time constraints, as well as long-term issues with the ICP-MS instrument, this was not performed.

3.4 Synthesis of (*S*)-carteolol ((*S*)-4)

The fourth and final step in the synthesis of (*S*)-carteolol ((*S*)-**4**) was alkylation of *tert*-butylamine with chlorohydrin (*R*)-**2a**. The proposed mechanism for the reaction is shown in Scheme 3.9. *tert*-Butylamine functions as a nucleophile that attacks the carbon in α-position to chloride. The chloride ion is displaced and cation (*S*)-$\mathbf{4_{cation}}$ formed. Deprotonation of the cation by unreacted *tert*-butylamine forms (*S*)-**4**. The chloride ion may coordinate with the protonated *tert*-butylamine and form a hydrochloride salt, which will be further addressed in Section 3.4.3. Synthesis of both racemic- and (*S*)-**4** was based on the work of Nakagawa *et al* [18].

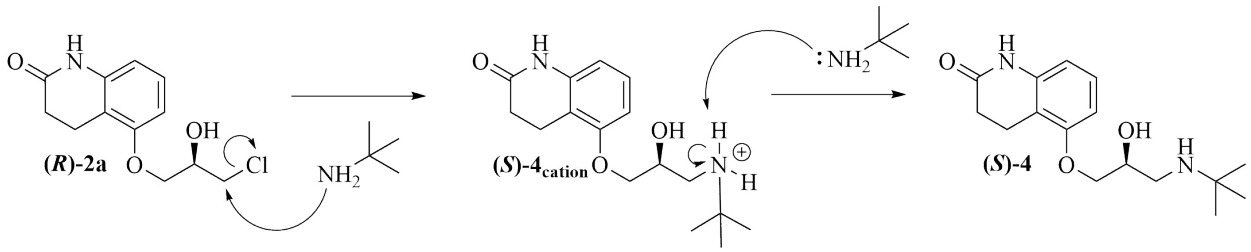

Scheme 3.9: The proposed mechanism for the final step in synthesis of (*S*)-carteolol ((*S*)-**4**) by alkylation of *tert*-butylamine with chlorohydrin (*R*)-**2a**.

Enantioenriched (*S*)-**4** was synthesized with 20 equivalents of *tert*-butylamine dissolved methanol. After 22 hours at 50 °C, the remaining reagents and solvent were evaporated off *in vacuo*. The resulting residue was dissolved in dichloromethane and washed with water. Purification was performed by flash chromatography (iPrOH:Hex:DEA [80:20:3]). (*S*)-carteolol ((*S*)-**4**) was obtained in 25% yield and with 88% *ee*, see Scheme 3.10 and Figure 3.14. Due to unknown impurities originating from diethylamine, purity could not be determined.

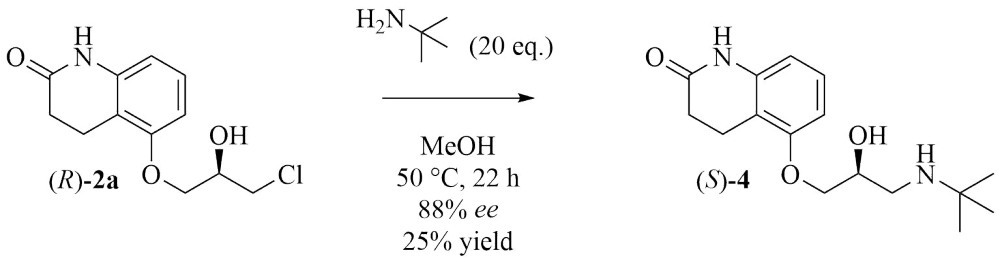

Scheme 3.10: Synthesis of (*S*)-carteolol ((*S*)-**4**) from chlorohydrin (*R*)-**2a** by alkylation of *tert*-butylamine.

No stable optical rotation could be observed, and the low quantities of product prevented further testing of this issue. It is possible that low concentrations or presence of impurities negatively impacted the measurements. The specific optical rotation of (*S*)-**4** hydrochloride has been reported as $[\alpha]_D^{20}$ = -11.0 (c = 2.0, H_2O) [93].

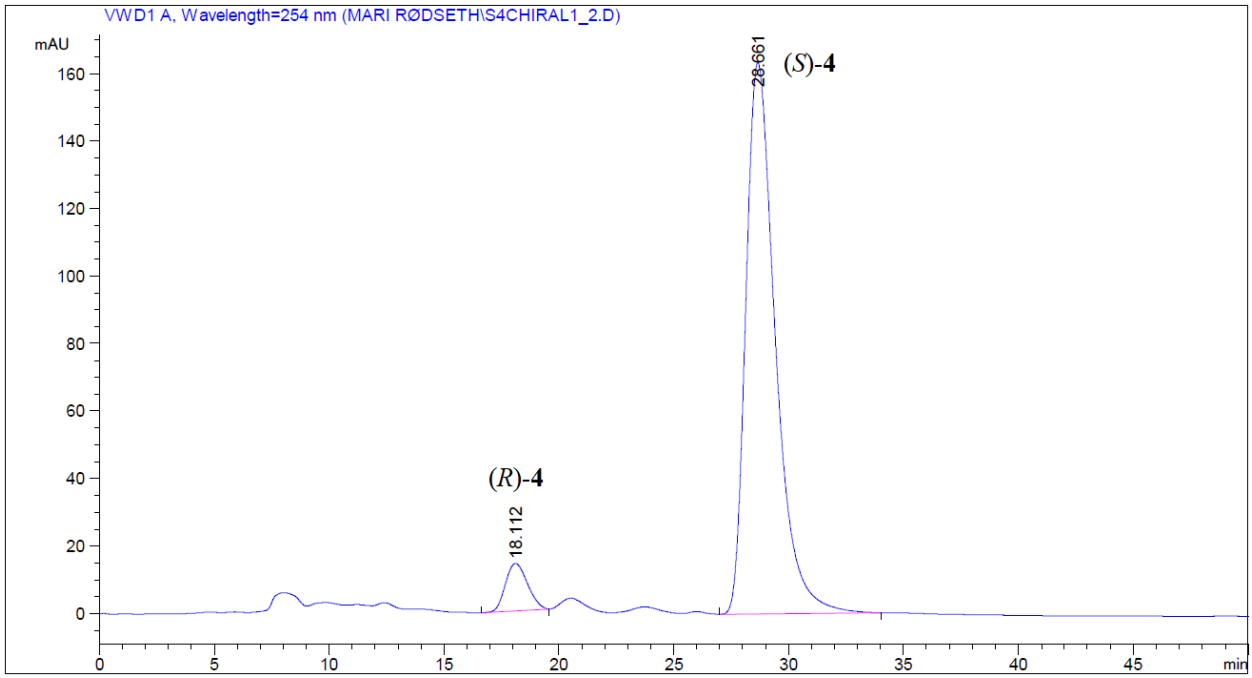

Figure 3.14: Chiral HPLC (Chiralcel OD-H, *n*-hexane:ethanol:trifluoroacetic acid [90:10:0.1], 0.4 mL/min) chromatogram from which the enantiomeric excess of (*S*)-**4** (88% *ee*) was calculated.

Lower enantiomeric excess was calculated for (*S*)-**4** (88% *ee*, Figure 3.14) than for (*R*)-chlorohydrin **2a** (97% *ee*). Similar chlorohydrins have been reported to retain stereochem-

istry during alkylation of *tert*-butylamine [1]. Some decrease in enantiopurity was expected, as the racemic epoxide **2b** was also converted to **4** during reaction. Estimated enantiopurity of (*S*)-**4** when including conversion of epoxide **2b** was 93% *ee*. It is also possible that aminolysis of ester (*S*)-**3** with *tert*-butylamine occurred during the reaction. The resulting alcohol would then be (*S*)-**2a** (77% *ee*), and conversion would mostly form (*R*)-**4**. Estimated enantiopurity when including conversion of both epoxide **2b** and ester (*S*)-**3** to **4** is 90% *ee*. This highlights the importance of purifying starting material (*R*)-**2a** before conversion to (*S*)-**4**.

The impurities from diethylamine appeared bright orange, which suggests strongly conjugated systems. Clear interference of the detected impurities was evident in the chromatogram of (*S*)-**4**, see Figure 3.14. This may also have contributed to the low enantiomeric excess observed.

Racemic **4** was synthesized under the same reaction conditions as (*S*)-**4**. After removal of reagents and solvents *in vacuo*, the resulting residue was dissolved in dichloromethane and washed with water. Racemic carteolol (**4**) was obtained in 77% yield and 95% purity, see Scheme 3.11. The remaining impurity was determined to be unreacted chlorohydrin **2a** (4%).

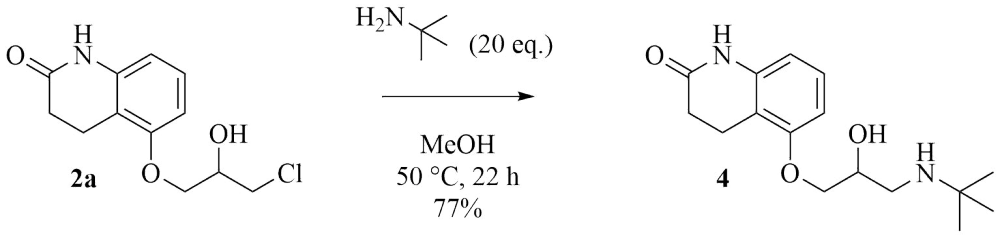

Scheme 3.11: Synthesis of racemic carteolol (**4**) from chlorohydrin **2a** by alkylation of *tert*-butylamine.

3.4.1 Characterization of 4

Full characterization of racemic carteolol (**4**) was achieved by ^{1}H NMR, ^{13}C NMR, COSY, HSQC and HMBC experiments in DMSO$_{d6}$, see Figure 3.15 and Table 3.8. Analysis by MS detected an exact mass of $[M+H]^{+} = 293.2$ m/z. This is concurrent with the theoretically

calculated molecular weight of **4** (292.4 g/mol). All spectra are presented in Appendix G.

Table 3.8: Acquired NMR data for carteolol (**4**). Listed proton- and carbon positions refer to those presented in Figure 3.15. All related NMR spectra are found in Appendix G.

Pos.	^{1}H *(int., mult., J [Hz]) [ppm]*	^{13}C *[ppm]*	*COSY*	*HMBC*
1	–	170.5	–	2, 3
2	2.42-2.39 (2H, t, 7.7)	30.3	3	(3, 10)
3	2.84-2.81 (2H, m)	18.7	2	2
4	–	111.6	–	2, 3, 6, 8 (10)
5	–	156.3	–	7 (3, 6)
6	6.60-6.59 (1H, d, 8.0)	106.3	7	8
7	7.08-70.5(1H, t, 8.1)	128.1	6, 8	–
8	6.48-6.47 (1H, d, 7.8)	108.5	7	6
9	–	139.7	–	7 (3)
10	10.01 (1H, s)	–	–	
11	3.97-3.94 (1H, dd, 9.7, 4.9)	71.4	12	
	3.90-3.87 (1H, dd, 9.7, 5.7)			
12	3.81-3.76 (1H, m)	69.5	11, 13	(11, 13)
13	2.66-2.63 (1H, dd, 11.3, 5.0)	45.6	12	(11, 16)
	2.58-2.55 (1H, dd, 11.3, 6.6)			
14	4.91 (1H, s)	–	–	
15	–	50.1	–	16
16	1.02 (9H, s)	29.3	16	16

All carbon positions were assigned chemical shifts as fit with HSQC- and HMBC spectra, see Figure 3.1 and Table 3.1. Carbons without protons were as such assigned shifts by two-, three- or four-bond relations. Chemical shifts observed at 10.01 (10), 7.08-7.05 (7), 6.60-6.59 (6), 6.48-6.47 (8), 2.84-2.81 (3), 2.42-2.39 ppm (2) were assigned to the quinoline group, as they were consistent with previously characterized compounds, see Section 3.1.3.

The single shift observed at 4.91 ppm (14) was concurrent with the proton of the alcohol group. Chemical shifts at 3.97-3.94 and 3.90-3.87 ppm (11) were assigned to the ether methylene bridge, a position consistent with coupling to the carbon in position 5. Shifts observed at 3.81-3.76 ppm (12) were assigned to the chiral proton due to the characteristic multiplicity of chiral centers. The chemical shifts at 2.66-2.63 and 2.58-2.55 ppm (13) were assigned to the amine methylene bridge due to the slight coupling with protons at position 16. Finally, the shifts observed at 1.02 ppm (16) were assigned to the attached *tert*-butylamine group, as they integrated to the equivalent of 9 protons.

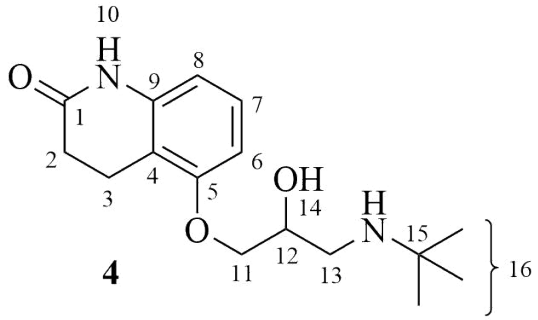

Figure 3.15: Proton- and carbon positions of carteolol (**4**) as described in Table 3.8. All related NMR spectra are found in Appendix G.

No distinct shift for the amine proton was detected, though a very broad shift was observed between 1 and 2 ppm. This is the characteristic area for shifts caused by aliphatic amines. As the shift was too broad for proper integration, this could not be confirmed.

3.4.2 Achieving full conversion of chlorohydrin 2a into 4

Achieving full conversion in alkylation of sterically hindered primary amines can be challenging. Conversion of chlorohydrin **2a** to carteolol (**4**) was first attempted with 5 equivalents of *tert*-butylamine and at room temperature. After 18 hour of reaction, a **2a**:**4** molar ratio of 15:85 was observed. Another 10 equivalents were added, and the reaction was stirred for an additional 20 hours. After this, a **2a**:**4** molar ratio of 44:56 was observed. The reaction was then heated to 50 °C for 16 hours. A **2a**:**4** molar ratio of 87:13 was then observed. It was concluded that both high temperatures and excess of *tert*-butylamine was needed to reach

full conversion.

Chlorohydrin **2a** was reacted with 20 equivalents of *tert*-butylamine at 50 °C for 22 hours, after which a **2a**:**4** molar product ratio of 6:94 was observed. For future experiments, higher excess of *tert*-butylamine will likely result in higher conversion. Longer reaction times or higher temperatures may also be utilized, though it should be noted that a slightly yellowing of the product mixture was observed with an increase in reaction time, suggesting formation of byproducts. Due to time constraints and limited reserves of starting material **2a**, no further experimentation on conversion was performed.

3.4.3 Removal of *tert*-butylamine hydrochloride

In addition to the proton shifts observed for carteolol (**4**), a shift characteristic for *tert*-butyl groups was observed by ^{1}H NMR. This shift was incompatible with shifts observed for unreacted *tert*-butylamine. The mechanism proposed for this reaction step points to deprotonation of $\mathbf{4_{cation}}$ with unreacted *tert*-butylamine, see Scheme 3.9. Coordination between the protonated amine and the displaced chloride ion forms *tert*-butylamine hydrochloride, as proposed in Scheme 3.12. Three different strategies were employed in attempt to remove the salt.

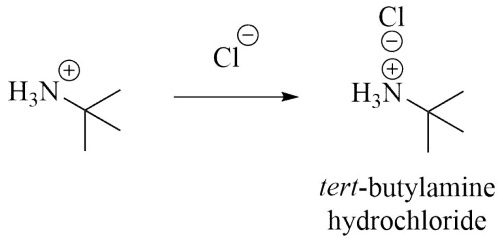

Scheme 3.12: Formation of *tert*-butylamine hydrochloride during synthesis of carteolol (**4**) from chlorohydrin **2a**.

Separate recrystallization from acetone, acetonitrile and ethanol was first performed. No dissolution of **4** was achieved with acetone or acetonitrile. Dissolution of impurities and product appeared simultaneous in ethanol, and no crystals formed upon cooling. Filtration after signs of early dissolution in ethanol was also attempted, but with no improvement. It

was determined that recrystallization was not a good method for removal of *tert*-butylamine hydrochloride from product **4**, and other methods were explored instead.

In an attempt to form an alternative salt that may be more easily removed, stochiometric amounts of triethylamine added in one reaction method [94]. The sterically hindered base would in theory deprotonate $\mathbf{4_{cation}}$ and form triethylamine hydrochloride. However, the previously detected salt was still observed by ^{1}H NMR, as well as new impurities from impure triethylamine, and this method was abandoned.

Removal of the *tert*-butylamine salt from product **4** was finally achieved by extraction. After reaction, solvents and reactants were removed *in vacuo*. The obtained residue was dissolved in dichloromethane and washed with water. After analysis of the product by ^{1}H NMR, no salt was observed.

3.4.4 Purification of (*S*)-4 by flash chromatography

Full conversion was not achieved during synthesis of (*S*)-carteolol ((*S*)-**4**) from chlorohydrin (*R*)-**2a**. As issues with dissolution had been observed during recrystallization, flash chromatography was explored. Amines interact strongly with the acidic silanol groups of silica, and require modification of the mobile phase for easy elution. Diethylamine and triethylamine are common modifiers that bind competitively with the silanol groups. A mobile phase of *iso*-propanol:*n*-hexane:diethylamine [80:20:3] was optimized by TLC ($R_{f(\mathbf{2a})} = 0.66$, $R_{f(\mathbf{4})} = 0.29$).

Two issues were encountered with this method. The first issue was that after concentration of the product fraction, a bright orange oil was obtained. Racemic **4** was observed as a white solid. ^{1}H NMR analyses of both product and diethylamine confirmed that the impurities originated from impure diethylamine, which appeared slightly yellow. As the impurity is unknown, product purity could not be calculated. This issue can be countered by using another modifier or fresh diethylamine of higher purity.

The second issue was overlap of the fraction containing starting material (*R*)-**2a** and that containing product (*S*)-**4**, which resulted in low yield. The retention time of **4** was observed as highly dependent on the amount of diethylamine present in the mobile phase, and this can easily be countered in future experiments by adjusting the added amount of modifier.

No chlorohydrin (*R*)-**2a** was observed in the obtained (*S*)-**4**, and it was determined that this method will work after the noted adjustments. Due to time constraints and limited starting material (*R*)-**2a**, these adjustments could not be made.

3.5 Synthesis of fluorohydrin 2d

Fluorohydrin **2d** was explored as an alternative to chlorohydrin **2a**. The proposed mechanism of this reaction is the same as that for chlorohydrin **2a**, see Scheme 3.1. Alcohol **1** is deprotonated with NaOH and attacks the epoxide of epifluorohydrin, displacing the fluoride ion. Synthesis of fluorohydrin **2d** from alcohol **1** was performed with 2 equivalents of epifluorohydrin and 0.3 equivalents of NaOH dissolved in H_2O:DMSO [3:2], see Scheme 3.13. The product was filtered off after 24 hours at room temperature. Fluorohydrin **2d** was obtained in a 75% yield and 99% purity.

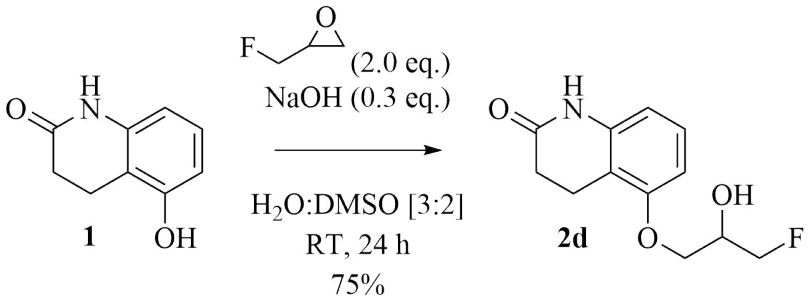

Scheme 3.13: Synthesis of fluorohydrin **2d** from alcohol **1** by use of epifluorohydrin in alkaline conditions.

No epoxide **2b** or dimer **2c** was observed during the synthesis of fluorohydrin **2d**, which supports the claim that the electrophilicity of fluoride prevents intramolecular cyclization and dimerization. Unlike the synthesis of chlorohydrin **2a**, this removes the need for a second

step where the epoxide is opened. Synthesis of carteolol (**4**) from fluorohydrin **2d** was not performed due to time restraints. It should be noted that the fluorohydrin will likely be too unreactive for alkylation of *tert*-butylamine, making it a poor precursor for synthesis of **4**.

3.5.1 Characterization of fluorohydrin 2d

Characterization of fluorohydrin **2d** was achieved by ^{1}H NMR, ^{13}C NMR, COSY, HSQC and HMBC experiments in $DMSO_{d6}$, see Figure 3.4 and Table 3.3. Analysis by MS detected an exact mass of $[M+H]^+ = 240.1$ m/z. This is concurrent with the theoretically calculated molecular weight of fluorohydrin **2d** (239.2 g/mol). All related spectra are presented in Appendix E.

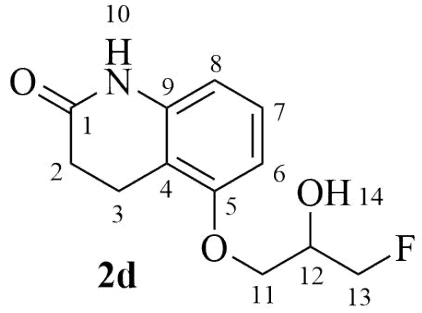

Figure 3.16: Positions of fluorohydrin **2d** as described in Table 3.9. All related NMR spectra are found in Appendix E.

All carbon positions were assigned chemical shifts as fit with HSQC- and HMBC spectra, see Figure 3.1 and Table 3.1. Carbons without protons were as such assigned shifts by two-, three- or four-bond relations. Chemical shifts observed at 10.02 (10), 7.09-7.05 (7), 6.61-6.59 (6), 6.50-6.48 (8), 2.84-2.80 (3), 2.42-2.38 (2) were assigned to the quionoline group, as they were consistent with previously characterized compounds, see Section 3.1.3.

Table 3.9: Acquired NMR data for fluorohydrin **2d**. Listed proton- and carbon positions refer to those presented in Figure 3.16. All related NMR spectra are found in Appendix E.

Pos.	^{1}H *(int., mult., J [Hz]) [ppm]*	^{13}C *(J) [ppm]*	*COSY*	*HMBC*
1	–	170.5	–	2, 3
2	2.42-2.38 (2H, t, 7.7)	30.3	3	3 (10)
3	2.84-2.80 (2H, t, 7.7)	18.7	2	2
4	–	111.7	–	2, 3, 6, 8 (7, 10)
5	–	155.9	–	3, 6, 7, 11 (8)
6	6.61-6.59 (1H, d, 8.0)	106.2	8	8 (7)
7	7.09-7.05 (1H, t, 8.1)	128.1	6, 8	–
8	6.50-6.48 (1H, d, 7.8)	108.7	6	6
9	–	139.8	–	3, 7 (10)
10	10.02 (1H, s)	–	–	–
11	3.95-3.94 (2H, m)	68.8-68.7 (7.9)	12	(13)
12	4.09-4.00 (1H, m, 20.8)	68.2-68.0 (19.1)	11, 13	11 (13)
13	4.60-4.45 (1H, m, 47.5, 9.5, 3.8) 4.55-4.39 (1H, m, 47.6, 9.6, 5.2)	85.7-84.1 (168.1)	12	11
14	5.43 (1H, s)	–	–	–

The shift observed at 5.43 ppm (14) was assigned to the alcohol proton, as such groups are shielded and produce high shifts. Shifts at 4.60-4.45 and 4.55-4.39 ppm (13) were assigned to the fluoride methylene bridge due to the characteristically high hydrogen-fluoride coupling observed. Further, the chemical shifts at 3.95-3.94 ppm (11) were assigned to the methylene bridge, a position consistent with coupling to the carbon at position 5. Finally, the shifts at 4.09-4.00 ppm (12) were assigned to the chiral proton due to the characteristic multiplicity of chiral centers.

4 Conclusion

Synthesis of chlorohydrin **2a** from alcohol **1** was performed over two steps, with a total yield of 76%. Alcohol **1** was first reacted with epichlorohydrin (2 eq.) and sodium hydroxide (0.3 eq.), dissolved in a water and dimethyl sulfoxide. A **2a**:**2b** product mixture of 75:24 (mol. ratio, determined by ^{1}H NMR) was obtained in 91% of expected amounts (0.9138 g, 99% purity) when adjusted for product composition. Epoxide **2b** was then opened with lithium chloride (2.0 eq.) and acetic acid (2.0 eq.), dissolved in acetonitrile. Chlorohydrin **2a** was obtained in 83% of expected amounts (0.7751 g, 3.03 mmol, 98% purity) when adjusted for composition of starting material. Formation of **2a**, **2b** and **2c** was verified by NMR and MS.

Kinetic resolution of **2a** was performed by transesterification reaction with vinyl butanoate (2.0 eq.) catalyzed by CALB in dry acetonitrile. Chlorohydrin (*R*)-**2a** was obtained in 38% yield (0.0652 g, 0.25 mmol, 94% purity) and 97% *ee*. The specific optical rotation of (*R*)-**2a** was determined as $[\alpha]_D^{20} = -9.9$. Ester (*S*)-**3** was obtained in 43% yield (0.0947, 0.29 mmol, 93% purity) and 77% *ee*. The specific rotation on (*S*)-**3** was determined as $[\alpha]_D^{20} = +9.9$. An enantiomeric ratio of 27 was calculated. Formation of **3** was verified by NMR and MS.

Synthesis of racemic- and enantioenriched (*S*)-**4** was performed by alkylation of *tert*-butylamine (20 eq.) with racemic- and enantioenriched chlorohydrin (*R*)-**2a**, dissolved in methanol at 50°C. Racemic carteolol (**4**) was obtained in 77% yield (0.1142, 0.39 mmol, 95% purity). (*S*)-carteolol ((*S*)-**4**) was obtained in 25% yield (0.0117 g, 0.04 mmol) in 88% *ee*. The enantiopure sample was contaminated with unknown impurities during purification by flash chromatography. For this reason, purity and optical rotation were not determined. Formation of **4** was verified by NMR and MS.

Synthesis of fluorohydrin **2d** from alcohol **1** was performed in one step. Alcohol **1** was reacted with epifluorohydrin (2.0 eq.) and sodium hydroxide (0.3 eq.), dissolved in a water- and dimethyl sulfoxide solution. Fluorohydrin **2d** was obtained in 75% yield (0.1839 g, 0.77 mmol, 99% purity). Formation of **2d** was verified by NMR and MS.

5 Further Work

Synthesis of chlorohydrin **2a** may be improved by further reducing the amount of sodium hydroxide used (< 0.3 equivalents) in the first step, as discussed in Section 3.1.7. The goal should be to completely eliminate formation of dimer **2c**. Optimization with another base may also be of interest. Adjusting the amount of epichlorohydrin used can further decrease the environmental impact of this reaction step, see Section 1.6. It should be noted that decreasing the amount of reagent may cause lower reaction rates, see Section 1.3.2.

While high conversion (98%) was achieved in the second step, some epoxide **2b** remained as an impurity after work-up, see Section 3.1.9. This affected the enantiomeric excess observed after conversion to (*S*)-carteolol ((*S*)-**4**), see Section 3.4. Basic strategies like increasing reaction temperature or increasing amounts of acetic acid and lithium chloride may improve conversion to **2a**. If full conversion cannot be achieved, separation of **2a** and **2b** by flash chromatography should be further explored.

Separation of chlorohydrin **2a** and ester **3** enantiomers was achieved by high-performance liquid chromatography with a Chiralcel OD-H column, but with impractically high analysis times, see Section 3.2. Alternative columns should be selected for their ability to separate secondary alcohols with halogen substituents and large quinoline group. Due to the high calculated boiling points of these compounds, chiral separation by gas chromatography is not an option, see Section 1.9.1. If no suitable chiral stationary phases are commercially available, separation by chiral mobile phases may be a viable alternative.

Major issues of enzyme inhibition were encountered during the kinetic resolution of chlorohydrin **2a**, see Section 3.3.5. Transesterification reaction was performed with **2a** and vinyl butanoate, catalyzed by *Candida antarctica* Lipase B. Inductively coupled plasma mass spectrometry analyses should be performed to detect possible traces of metal cations in the sample batches where inhibition was observed, see Section 3.3.5.

Achieved enantiomeric excess of (*R*)-**2a** was 97% *ee*. Higher enantiomeric excess can be achieved by repeated transesterification- and hydrolysis reactions of enantioenriched (*R*)-**2a**, though this will reduce the obtained yield. More rigorous drying of starting material **2a** may improve conversion rate of the reaction and reduce the formation of butanoic acid, see Section 1.7.7. Some overlap was observed during resolution of chlorohydrin (*R*)-**2a** and ester (*S*)-**3** by flash chromatography, see Section 3.3.3. Higher yield and increased product purity can be achieved by further improving the utilized mobile phase. The butanoic acid was observed in the ester (*S*)-**3** fraction, and may likely be removed by distillation under reduced pressure due to the high difference in boiling points, see Section 3.3.4. The enantioselectivity of CALB for **2a** (E = 27) may be improved by selecting a different reaction medium, as discussed in Section 1.7.7.

Improved conversion rates of **2a** during alkylation of *tert*-butylamine may be achieved with higher excess of the amine or increased reaction temperatures, as discussed in Section 3.4.2. It should be noted that this also may contribute to increased formation of byproducts. Some overlap was observed during separation of starting material (*R*)-**2a** and product (*S*)-**4** by flash chromatography, as noted in Section 3.4.4. Higher yield may be obtained by decreasing the amount of modifier (diethylamine) used in the mobile phase to achieve better separation. Issues of impurities in diethylamine transferring to product (*S*)-**4** were encountered, and use of pure solvent should be ensured in future methods. Use of alternative modifiers like triethylamine may also be explored. Achieved enantiomeric excess of (*S*)-**4** was 88% *ee*. The low enantiomeric excess was likely caused by conversion of epoxide **2b** and ester **3** to product **4**, as discussed in Section 3.4, and may be avoided by increased purification of (*R*)-**2a**.

In Section 3.5 it was observed that synthesis of fluorohydrin **2d** could be achieved with only one step, whereas chlorohydrin **2a** is synthesized in two. It is also likely that CALB will express higher enantioselectivity for **2b** than **2a**, as discussed in section 1.7.6. This should be further examined. However, the low reactivity of fluoride and expense of epifluorohydrin noted in Section 1.8 will likely make fluorohydrin **2b** an unsuitable precursor to **4**.

6 Experimental

6.1 Materials and methods

All syntheses and analyses were performed at the Department of Chemistry, Faculty of Sciences and Technology, Norwegian University of Science and Technology, Trondheim, Norway.

6.1.1 Substrates, reagents and solvents

All substrates, reagents and solvents utilized in the subsequent syntheses are commercially available, of analytical grade and were purchased from Sigma-Aldrich Norway (Oslo, Norway) or vwr Norway (Oslo, Norway). Solvents used for HPLC analyses were of HPLC grade.

Dry solvents

Dry solvents were obtained from a solvent purifier, MBraun MD-SPS800 (München, Germany). New solvent was acquired for each use and stored shortly in a flask with molecular sieves (4Å).

Enzymes

Candida antarctica Lipase B (CALB) (activity $\geq$ 10000 PLU/g, LOT#20170315) immobilized to highly hydrophobic macroporous resin, produced in fermentation with genetically modified *Pichia pastoris*. Gifted from SyncoZymes Co., Ltd. (Shanghai, China).

Molecular sieves

Molecular sieves (1/8 pellet, pore diameter 4Å) was activated by drying the sieves at 1000 °C in a porcelain bowl for 24 hours. The sieves were then stored in a desiccator.

6.1.2 Chromatographic analyses

Chiral High performance liquid chromatography (HPLC)

All chiral HPLC analyses were performed on an Agilent HPLC 1100 (Santa Clara, California, USA) instrument with a manual injector (Rheodyne 77245i/Agilent 10 μL loop). All samples were run on a Chiralcel OD-H column (250 $\times$ 4.6 mm ID, 5 μm; Daicel, Chiral Technologies Europe, Gonthier d'Andernach, Illkirch, France). The program used for analysis of chlorohydrin **2a** was isocratic *n*-hexane:EtOH:TFA acid (90:10:0.1), 10 μL, 0.4 mL/min, UV 254 nm. The program used for analysis of ester **3** was isocratic *n*-hexane:iPrOH:DEA (95:5:0.4), 10 μL, 0.4 mL/min, UV 254 nm. The program used for analysis of **4** was isocratic *n*-hexane:iPrOH:DEA (80:20:0.4), 10 μL, 1.0 mL/min, UV 254 nm.

Thin layer chromatography (TLC)

All TLC analyses were performed on Merck silica 60 F_{254} (0.2 mm) from Sigma-Aldrich Norway (Oslo, Norway), with UV detection at $\lambda = 254$ nm.

Flash column chromatography

All flash column chromatography separations were performed using silica gel from Sigma-Aldrich Norway (Oslo, Norway) with pore size 60 Å, 230-400 mesh particle size and 40-63 μm particle size.

6.1.3 Spectroscopic analyses

Nuclear magnetic resonance spectroscopy (NMR)

All NMR analyses were performed on a Bruker 400 MHz Avance III HD instrument equipped with a 5 mm SmartProbe Z-gradient probe (Bruker, Fällanden, Switzerland) or on a Bruker 600 MHz Avance III HD instrument equipped with a 5 mm cryogenic CP-TCI Z-gradient probe (Bruker, Fällanden, Switzerland).

Liquid chromatography mass spectroscopy (LC-MS)

Non-target analyses were performed on an Acquity UPLC system (IClass Waters™, Milford, USA)) coupled to a Synapt G2-S (Waters™, Milford, USA)) electrospray Q-TOF instrument in positive mode. Analytical columns, BEH C18 (100 mm × 2.1 mm, 1.7 μm) were used for chromatographic separation at 30 °C. The mobile phase consisted of water v/v 0.1% formic acid and acetonitrile v/v 0.1% formic acid introduced at a flow rate of 400 μL/min. The mobile phase was isocratic [75:25] for 15 minutes.

Mass spectroscopy (MS)

Accurate mass determination in positive and negative mode was performed on a "Synapt G2-S" Q-TOF instrument from Waters™ (Milford, USA)). Samples were ionized by the use of ASAP probe (APCI) or ESI probe. No chromatographic separation was used previous to the mass analysis. Calculated exact mass and spectra processing was done by Waters™ Software Masslynx V4.1 SCN871.

6.1.4 Other equipment

Optical rotation

All optical rotations were measured on an Anton Paar (MCP 5100) polarimeter with a 2.5 cm long cell (Dipl. Ing. Houm AS, Oslo, Norway). The analyses were performed at 20 °C and the samples were dissolved in DMSO (c = 1.0 g / 100 mL). The wavelength used was 589 nm (D).

Orbital shaker

The orbital shakers used for enzymatic reactions was a New Brunswick G24 Environmental Incubator Shaker (New Brunswick Co. Inc., Edison, New Jersey, USA).

6.2 Step 1: Synthesis of chlorohydrin 2a, epoxide 2b, dimer 2c and fluorohydrin 2d from alcohol 1

The primary method (A) was developed for the first step of (*S*)-**4** synthesis, for which the primary products were chlorohydrin **2a** and epoxide **2b**. In an earlier method (B), epoxide **2b** and dimer **2c** were isolated and characterized. Finally, a method for synthesis of fluorohydrin **2d** was developed (C). Product composition and purity was determined by ^{1}H NMR.

6.2.1 Method A: Synthesis of chlorohydrin 2a and epoxide 2b

Alcohol **1** (0.6525, 4.0 mmol) was dissolved in H_2O (2.4 mL) and DMSO (1.6 mL), after which epichlorohydrin (0.627 mL, 8.0 mmol) was added to the solution. NaOH solution (3.0 M, 0.400 mL, 1.2 mmol) and H_2O (0.932 mL) were mixed separately and added drop-wise into the mixture. The reaction was continuously stirred at room temperature for 24 hours before TLC (Hexane:iPrOH [4:1], $R_{f(\mathbf{1})} = 0.26$, $R_{f(\mathbf{2a},\mathbf{2b})} = 0.20$, $R_{f(\mathbf{2c})} = 0.06$) showed full conversion. The product mixture was then filtered off, washed with H_2O (0 °C, ca. 2 mL) and dried *in vacuo*. From this, a **2a**:**2b** [75:24] (mol. ratio) product mixture was obtained in 91% of expected amount (0.9138 g, 99% purity). Starting material **1** (0.5%) and byproduct **2c** (0.6%) were also detected.

6.2.2 Method B: Synthesis of epoxide 2b and isolation of dimer 2c

Alcohol **1** (0.1641 g, 1.0 mmol) was dissolved in MeOH (3 mL), and NaOH solution (0.3 M, 3.3 mL, 1.0 mmol) was added to the reaction mixture. Epichlorohydrin (0.392 mL, 5.0 mmol) was then added drop-wise. The reaction mixture was stirred at room temperature for 25 hours, after which TLC (Hexane:iPrOH [4:1]) showed full conversion. The mixture was extracted with CH_2Cl_2 (3 × 30 mL), washed with brine (2 × 10 mL) and dried over $MgSO_4$. After filtration, solvents were removed *in vacuo* and a white solid (0.2569 g) was obtained and recrystallized from EtOH. Epoxide **2b** was obtained in 25% yield (0.0556 g, 0.25 mmol, 92% purity). Some of chlorohydrin **2a** (4.0%) and dimer **2c** (4.0%) was also detected. **2b**: ^{1}H-NMR (400 MHz, $DMSO_{d6}$) δ: 10.04 (s, 1H, NH), 7.09-7.05 (t, 1H, $^3J_{HH}$

= 8.1 Hz, Ar-H), 6.62-6.60 (d, 1H, $^3J_{HH}$ = 8.2 Hz, Ar-H), 6.51-6.49 (d, 1H, $^3J_{HH}$ = 7.9 Hz, Ar-H), 4.33-4.29 (dd, 1H, $^2J_{HH}$ = 11.4 Hz, $^3J_{HH}$ = 2.5 Hz, O-CH_2), 3.87-3.83 (dd, 1H, $^2J_{HH}$ = 11.4 Hz, $^3J_{HH}$ = 6.3 Hz, O-CH_2), 3.35-3.33 (m, 1H, CH), 2.85-2.80 (m, 3H, CH_2, CH_2-O), 2.73-2.71 (dd, 1H, $^2J_{HH}$ = 5.1 Hz, $^3J_{HH}$ = 2.6 Hz, CH_2-O), 2.43-2.39 (t, 2H, $^3J_{HH}$ = 7.7 Hz, CH_2); ^{13}C-NMR (400 MHz, $DMSO_{d6}$) δ: 170.5, 155.8, 139.8, 128.1, 111.7, 108.9, 106.5, 69.5, 50.2, 44.2, 30.3, 18.8; LC-HRMS (TOF-ASAP$^+$): $[M+H]^+$ = 220.0974 m/z (calc. mass: 219,2400, $C_{12}H_{13}NO_3$).

The EtOH solvent was removed from the filtrate *in vacuo*, and dimer **2c** was isolated by flash chromatography (EtOAc, $R_{f(\mathbf{1,2a,2b})}$ = 0.46, $R_{f(\mathbf{2c}}$ = 0.16). **2c**: ^{1}H-NMR (400 MHz, $DMSO_{d6}$) δ: 10.01 (s, 2H, NH), 7.09-7.05 (t, 2H, $^3J_{HH}$ = 8.1 Hz, Ar-H), 6.63-6.61 (d, 2H, $^3J_{HH}$ = 8.2 Hz, Ar-H), 6.49-6.47 (d, 2H, $^3J_{HH}$ = 7.9 Hz, Ar-H), 5.38-5.37 (d, 1H, $^3J_{HH}$ = 4.1 Hz, OH), 4.18-4.17 (m, 1H, CH), 4.10-4.01 (m, 4H, O-CH_2), 2.81-2.77 (t, 4H, $^3J_{HH}$ = 7.7 Hz, CH_2), 2.38-2.34 (t, 4H, $^3J_{HH}$ = 7.7 Hz, CH_2); ^{13}C-NMR (400 MHz, $DMSO_{d6}$) δ: 170.5, 156.1, 139.8, 128.1, 111.7, 108.7, 106.3, 69.9, 68.0, 30.3, 18.7; LC-HRMS (TOF-ASAP$^+$): $[M+H]^+$ = 383.1609 m/z (calc. mass: 382,4160, $C_{21}H_{22}N_2O_5$).

6.2.3 Method C: Synthesis of fluorohydrin 2d

Alcohol **1** (0.1668, 1.0 mmol) was dissolved in H_2O (0.6 mL) and DMSO (0.4 mL), after which epifluorohydrin (0.139 mL, 2.0 mmol) was added to the solution. NaOH solution (3.0 M, 0.100 mL, 0.3 mmol) and H_2O (0.233 mL) were mixed separately and added dropwise into the mixture. The reaction was continuously stirred at room temperature for 24 hours before TLC (Hexane:iPrOH [4:1], $R_{f(\mathbf{2d})}$ = 0.22) showed full conversion. The product mixture was then filtered off, washed with H_2O (0 °C, ca. 1 mL) and dried *in vacuo*. From this, fluorohydrin **2d** was obtained as a white solid in 75% yield (0.1839 g, 0.77 mmol, 99% purity). **2d**: ^{1}H-NMR (400 MHz, $DMSO_{d6}$) δ: 10.02 (s, 1H, NH), 7.09-7.05 (t, 1H, $^3J_{HH}$ = 8.1 Hz, Ar-H), 6.61-6.59 (d, 1H, $^3J_{HH}$ = 8.0 Hz, Ar-H), 6.50-6.48 (d, 1H, $^3J_{HH}$ = 7.8 Hz, Ar-H), 5.43 (s, 1H, OH), 4.60-4.45 (m, 1H, $^2J_{HH}$ = 9.5 Hz, $^2J_{HF}$ = 47.5 Hz, $^3J_{HH}$ = 3.8 Hz, CH_2-F), 4.55-4.39 (m, 1H, $^2J_{HH}$ = 9.6 Hz, $^2J_{HF}$ = 47.6 Hz, $^3J_{HH}$ = 5.2 Hz, CH_2-F),

4.09-4.00 (m, 1H, $^{3}J_{\mathrm{HF}}$ = 20.8 Hz, CH), 3.95-3.94 (m, 2H, O-CH_2), 2.84-2.80 (t, 2H, $^{3}J_{\mathrm{HH}}$ = 7.7 Hz, CH_2), 2.42-2.38 (t, 2H, $^{3}J_{\mathrm{HH}}$ = 7.7 Hz, CH_2); ^{13}C-NMR (400 MHz, $DMSO_{d6}$) δ: 170.5, 155.9, 139.8, 128.1, 111.7, 108.7, 106.2, 85.7-84.1 ($^{1}J_{\mathrm{CF}}$ = 168.1 Hz), 68.8-68.7 ($^{3}J_{\mathrm{CF}}$ = 7.9 Hz), 68.2-68.0 ($^{2}J_{\mathrm{CF}}$ = 19.1 Hz); HRMS (TOF-ASAP^{+}): $[M+H]^{+}$ = 240.1040 m/z (calc. mass: 239.2460, $C_{12}H_{14}NO_3F$).

6.2.4 Effect of catalytic amounts of base on conversion and product distribution

Alcohol **1** (0.1641-0.1677 g, 1.0 mmol) was dissolved in H_2O (0.6 mL) and DMSO (0.4 mL), after which epichlorohydrin (0.157 mL, 2.0 mmol) was added to the solution. NaOH solution (3.0 M, 0.100-0.333 mL, 0.3-1.0 mmol) was added drop-wise to the mixture, which was then continuously stirred at room temperature for 24 hours. The mixture was extracted with CH_2Cl_2 (3 × 20 mL), washed with brine (2 × 10 mL) and dried over $MgSO_4$. After filtration, solvents were removed *in vacuo* to yield white solids (0.2241-0.2766 g). Obtained product composition was determined by ^{1}H NMR.

6.2.5 Examination of kinetic- and thermodynamic product stability

Alcohol **1** (0.3320 g, 2.0 mmol) was dissolved in H_2O (0.6 mL) and DMSO (0.4 mL), after which epichlorohydrin (0.314 mL, 4.0 mmol) was added to the solution. NaOH solution (3.0 M, 0.666 mL, 2.0 mmol) was added drop-wise to the mixture, which was then continuously stirred at room temperature. Samples (0.250 mL) were extracted with CH_2Cl_2 (2 × 0.50 mL), washed with brine (2 × 0.25 mL) and flushed with nitrogen every hour for the first 8 hours of reaction. Obtained product composition was determined by ^{1}H NMR.

6.3 Step 2: Synthesis of chlorohydrin 2a by ring-opening of epoxide 2b

This method was developed for the second step in synthesis of (*S*)-**4**, where the primary product was chlorohydrin **2a**. The method described is a direct continuation of method A from the first step.

A mixture of **2a**:**2b** (75:24 mol. ratio, 0.9138 g, < 4.0 mmol) was obtained from Step 1 (A) and dissolved in CH_3CN (1 mL), after which AcOH (0.458 mL, 8.0 mmol) and LiCl (0.3392 g, 8.0 mmol) were added to the solution. The reaction was continuously stirred at room temperature for 24 hours before TLC ($CHCl_3$:Acetone [4:1], $R_{f(\mathbf{2a})}$ = 0.15, $R_{f(\mathbf{2b})}$ = 0.29, $R_{f(\mathbf{2c})}$ = 0.03) showed full conversion. The product mixture was then filtered off, washed with H_2O (0 °C, ca. 4 mL) and $CHCl_3$ (0 °C, ca. 3 mL), and dried *in vacuo*. From this, chlorohydrin **2a** was obtained as a white solid in 83% of expected amount (0.7751 g, 3.03 mmol, 98% purity), and 76% yield across both steps. Epoxide **2b** (1.6%) was also detected. **2a**: ^{1}H-NMR (400 MHz, $DMSO_{d6}$) δ: 10.02 (s, 1H, NH), 7.09-7.05 (t, 1H, $^3J_{HH}$ = 8.1 Hz, Ar-H), 6.61-6.59 (d, 1H, $^3J_{HH}$ = 8.1 Hz, Ar-H), 6.50-6.48 (d, 1H, $^3J_{HH}$ = 7.9 Hz, Ar-H), 5.55-5.54 (d, 1H, $^3J_{HH}$ = 5.3 Hz, OH), 4.06-3.01 (m, 1H, CH), 3.97-3.96 (m, 2H, O-CH_2), 3.79-3.75 (dd, 1H, $^2J_{HH}$ = 11.1 Hz, $^3J_{HH}$ = 4.6 Hz, CH_2-Cl), 3.70-3.66 (dd, 1H, $^2J_{HH}$ = 11.1 Hz, $^3J_{HH}$ = 5.5 Hz, CH_2-Cl), 2.84-2.80 (t, 2H, $^3J_{HH}$ = 7.7 Hz, CH_2), 2.42-2.38 (t, 2H, $^3J_{HH}$ = 7.7 Hz, CH_2); ^{13}C-NMR (400 MHz, $DMSO_{d6}$) δ: 170.5, 155.9, 139.8, 128.1, 111.7, 108.8, 106.3, 69.6, 69.1, 47.3, 30.3, 18.7; HRMS (TOF-ASAP$^+$): $[M+H]^+$ = 256.0745 m/z (calc. mass: 255.7010, $C_{12}H_{14}NO_3Cl$).

6.4 Step 3: Kinetic resolution of chlorohydrin 2a by transesterification reaction with CALB

Derivatization of racemic chlorohydrin **2a** was performed for optimization of chiral HPLC separation of ester **3**. Transesterification reaction of **2a** with CALB was first monitored at scales of 0.1 mmol substrate. Then kinetic resolution of **2a** was performed at scales of 0.7 mmol using the same method.

6.4.1 Derivatization of racemic chlorohydrin 2a

Chlorohydrin **2a** (0.019 g, 0.07 mmol) was dissolved in pyridine (2 drops) and butanoic anhydride (5 drops). The reaction mixture was then heated to 60 °C for 1 hour, diluted and analyzed by HPLC. **2a**: HPLC (Hexane:EtOH:TFA [90:10:0.1], t_1 = 63.43 min (S), t_2 =

68.68 min (*R*), R_S = 1.62). **3**: HPLC (Hexane:iPrOH:DEA [95:5:0.4], t_1 = 108.93 min (*S*), t_2 = 116.61 min (*R*), R_S = 1.16).

6.4.2 Transesterification reaction of chlorohydrin 2a with CALB

Chlorohydrin **2a** (0.0256 g, 0.1 mmol) was dissolved in dry CH_3CN (3.0 mL) and vinyl butanoate (0.063 mL, 0.5 mmol). Molecular sieves (4 Å) were added, and the mixture was placed in an incubator shaker (37 °C, 200 rpm). When dissolved, CALB (0.0521 g) was added to the mixture. After 28 hour of reaction, additional CALB (0.0481 g) was also added. Samples (0.150 mL) were extracted and analyzed by HPLC after 4, 8, 10, 24, 30 and 48 hours. E = 27 (Calculated by *E&K Calculator 2.1b0 PPC*).

6.4.3 Kinetic resolution of chlorohydrin 2a by large-scale transesterification reaction with CALB

Chlorohydrin **2a** (0.1724 g, 0.7 mmol) was dissolved in dry CH_3CN (20 mL) and vinyl butanoate (0.428 mL, 3.4 mmol). Molecular sieves (4Å) were added, and the mixture was placed in an incubator shaker (37 °C, 200 rpm). When dissolved, CALB (0.3377 g) was added to the mixture. Additional CALB (0.3378 g) was added after 28 hours. The reaction was monitored by HPLC analysis of extracted samples (0.100 mL). After 74 hours total, the immobilized enzyme and molecular sieves were filtered off and the organic phase concentrated *in vacuo*. The products were separated by flash chromatography, for which the eluent was optimized by TLC (EtOAc:Hexane [7:3], $R_{f(\mathbf{2a})}$ = 0.16, $R_{f(\mathbf{3})}$ = 0.34). Chlorohydrin (*R*)-**2a** was isolated as a white solid in 38% yield (0.0652 g, 0.25 mmol, 94% purity, *ee* = 97%). Remains of epoxide **2b** (2.8%) and ester **3** (2.9%) were observed. Ester (*S*)-**3** was isolated as a white solid in 43% yield (0.0947 g, 0.29 mmol, 93% purity, *ee* = 77%). Some butanoic acid (6.5%) was observed. **2a**: HPLC (Hexane:EtOH:TFA [90:10:0.1], t_1 = 65.03 min (*S*), t_2 = 70.62 min (*R*), R_S = 1.74); $[\alpha]_D^{20} = -9.9$ (c = 1.0, DMSO). **3**: HPLC (Hexane:iPrOH:DEA [95:5:0.4], t_1 = 108.79 min (*S*), t_2 = 116.21 min (*R*), R_S = 1.53); $[\alpha]_D^{20} = +9.9$ (c = 1.0, DMSO); ^{1}H NMR (400 MHz, $DMSO_{d6}$) δ: 10.04 (s, 1H, NH), 7.10-7.06 (t, 1H, $^3J_{HH}$ = 8.1

Hz, Ar-H), 6.62-6.60 (d, 1H, $^{3}J_{\mathrm{HH}} = 8.0$ Hz, Ar-H), 6.51-6.49 (d, 1H, $^{3}J_{\mathrm{HH}} = 7.8$ Hz, Ar-H), 5.38-5.33 (m, 1H, CH), 4.21-4.17 (dd, 1H, $^{2}J_{\mathrm{HH}} = 10.6$ Hz, $^{3}J_{\mathrm{HH}} = 4.1$ Hz, O-CH_2), 4.15-4.11 (dd, 1H, $^{2}J_{\mathrm{HH}} = 10.6$ Hz, $^{3}J_{\mathrm{HH}} = 6.2$ Hz, O-CH_2), 3.98-3.94 (dd, 1H, $^{2}J_{\mathrm{HH}} = 11.8$ Hz, $^{3}J_{\mathrm{HH}} = 4.2$ Hz, CH_2-Cl), 3.91-3.86 (dd, 1H, $^{2}J_{\mathrm{HH}} = 11.8$ Hz, $^{3}J_{\mathrm{HH}} = 6.5$ Hz, CH_2-Cl), 2.79-2.75 (t, 2H, $^{3}J_{\mathrm{HH}} = 7.7$ Hz, CH_2), 2.41-2.38 (t, 2H, $^{3}J_{\mathrm{HH}} = 7.7$ Hz, CH_2), 2.35-2.31 (m, 2H, CH_2), 1.61-1.46 (m, 2H, CH_2), 0.90-0.85 (m, 3H, CH_3); ^{13}C NMR (400 MHz, $DMSO_{d6}$) δ: 172.6, 170.6, 155.5, 139.9, 128.2, 111.8, 109.1, 106.3, 71.1, 67.4, 43.8, 35.8, 30.2, 18.6, 18.4, 13.8; HRMS (TOF-ASAP^{+}): $[M+H]^{+} = 326.1162$ m/z (calc. mass: 325,7920, $C_{16}H_{20}NO_4Cl$).

6.5 Step 4: Synthesis of (*S*)-4 from chlorohydrin (*R*)-2a

Two methods were developed (A and B) for synthesis of racemic- and (*S*)-**4** respectively.

6.5.1 Method A: Synthesis of racemic 4

Chlorohydrin **2a** (0.1290 g, 0.5 mmol) was dissolved in MeOH (1.8 mL) and *t*-BuNH_2 (1.051 mL, 10.0 mmol). The reaction mixture was then stirred at 50 °C for 22 hours, after which TLC ($CHCl_3$:acetone [3:2], $R_{f(\mathbf{2a})} = 0.57$, $R_{f(\mathbf{4})} = 0.00$)) showed full conversion. Solvent and reagent was then evaporated off *in vacuo*. From this, a yellow residue was obtained and diluted with CH_2Cl_2 (30 mL). The organic phase was washed with water (5 mL), dried over $MgSO_4$, filtered and dried *in vacuo*. **4** was obtained as a white solid in 77% yield (0.1142 g, 0.39 mmol, 95% purity). Remains of chlorohydrin **2a** (5%) was detected. **4**: HPLC (HPLC (Hexane:iPrOH:DEA [80:20:0.4], $t_1 = 19.60$ min (*R*), $t_2 = 34.88$ min (*S*), $R_S = 7.52$); ^{1}H NMR (600 MHz, $DMSO_{d6}$) δ: 10.01 (s, 1H, NH), 7.08-7.05 (t, 1H, $^{3}J_{\mathrm{HH}} = 8.1$ Hz, Ar-H), 6.60-6.59 (d, 1H, $^{3}J_{\mathrm{HH}} = 8.0$ Hz, Ar-H), 6.48-6.47 (d, 1H, $^{3}J_{\mathrm{HH}} = 7.8$ Hz, Ar-H), 4.91 (s, 1H, OH), 3.97-3.94 (dd, 1H, $^{2}J_{\mathrm{HH}} = 9.7$ Hz, $^{3}J_{\mathrm{HH}} = 4.9$ Hz, O-CH_2), 3.90-3.87 (dd, 1H, $^{2}J_{\mathrm{HH}} = 9.7$ Hz, $^{3}J_{\mathrm{HH}} = 5.7$ Hz, O-CH_2), 3.81-3.76 (m, 1H, CH), 2.84-2.81 (m, 2H, CH_2), 2.66-2.63 (dd, 1H, $^{2}J_{\mathrm{HH}} = 11.3$ Hz, $^{3}J_{\mathrm{HH}} = 5.0$ Hz, CH_2-N), 2.58-2.55 (dd, 1H, $^{2}J_{\mathrm{HH}} = 11.3$ Hz, $^{3}J_{\mathrm{HH}} = 6.6$ Hz, CH_2-N), 2.42-2.39 (t, 2H, $^{3}J_{\mathrm{HH}} = 7.7$ Hz, CH_2), 1.02 (s, 9H, CH_3); ^{13}C NMR (600 MHz, $DMSO_{d6}$) δ: 170.5, 156.3, 139.7, 128.1, 111.6, 108.5, 106.3, 71.4, 69.5, 50.1, 45.6,

30.3, 29.3, 18.7; HRMS (TOF-ASAP$^+$): $[M+H]^+$ = 293.1868 m/z (calc. mass: 292.3790, $C_{16}H_{24}N_2O_3$).

6.5.2 Method B: Synthesis of (*S*)-4

Chlorohydrin (*R*)-**2a** (0.0403 g, 0.16 mmol) was dissolved in MeOH (0.550 mL) and *t*-BuNH_2 (0.331 mL, 3.1 mmol). The reaction mixture was then stirred at 50 °C for 22 hours, after which TLC ($CHCl_3$:acetone [3:2]) showed high conversion. Solvent and reagent was then evaporated off *in vacuo*, and the resulting yellow residue was obtained and diluted with CH_2Cl_2 (15 mL). The organic phase was washed with water (2 mL), dried over $MgSO_4$, filtered off and dried *in vacuo*. An opalescent residue (0.0292 g) was obtained and separated by flash chromatography, optimized by TLC (iPrOH:Hexane:DEA [80:20:3], $R_{f(\mathbf{2a})}$ = 0.66, $R_{f(\mathbf{4})}$ = 0.29). (*S*)-**4** was obtained as an orange oil in 25% yield (0.0117 g, 0.04 mmol, *ee* = 88%). Product purity could not be estimated. (*S*)-**4**: HPLC (Hexane:iPrOH:DEA [80:20:0.4], t_1 = 18.11 min (*R*), t_2 = 28.66 min (*S*), R_S = 5.16).

Literature

(1) Gundersen, M. A.; Austli, G. B.; Løvland, S. S.; Hansen, M. B.; Rødseth, M.; Jacobsen, E. E. Lipase catalyzed synthesis of enantiopure precursors and derivatives of β-blockers practolol, pindolol and carteolol. *Catalysts* **2020**, *11*, 503.

(2) Schuster, A. K.; Erb, C.; Hoffmann, E. M.; Dietlein, T.; Pfeiffer, N. The diagnosis and treatment of glaucoma. *Dtsch. Arztebl. Int.* **2020**, *117*, 225–244.

(3) Tham, Y. C.; Li, X.; Wong, T. Y.; Quigley, H. A.; Aung, T.; Cheng, C. Y. Global prevalence of glaucoma and projections of glaucoma burden through 2040: a systematic review and meta-analysis. *Ophthalmology* **2014**, *121*, 2081–2090.

(4) Steinmetz, J. D. et al. Causes of blindness and vision impairment in 2020 and trends over 30 years, and prevalence of avoidable blindness in relation to VISION 2020: the Right to Sight: an analysis for the Global Burden of Disease Study. *Lancet Glob. Health* **2021**, *9*, e144–e160.

(5) Green, K.; Elijah, D.; Lollis, G.; Mayberry, L. Beta adrenergic effects on ciliary epithelial permeability, aqueous humor formation and pseudofacility in the normal and sympathectomized rabbit eye. *Curr. Eye Res.* **1981**, *1*, 419–423.

(6) Stiles, G. L.; Caron, M. G.; Lefkowitz, R. J. β-Adrenergic receptors: biochemical mechanism of physiological regulation. *Physiol. Rev.* **1984**, *64*, 661–743.

(7) Poole-Wilson, P. A.; Swedberg, K.; F., C. J. G.; Di Lenarda, A.; Hanrath, P.; Komajda, M.; Lubsen, J.; Lutiger, B.; Metra, M.; Remme, W. J.; Torp-Pedersen, C.; Scherhag, A.; Skene, A. Comparison of carvedilol and metoprolol on clinical outcomes in patients with chronic heart failure in the Carvedilol Or Metoprolol European Trial (COMET): randomised controlled trial. *Lancet* **2003**, *362*, 7–13.

(8) Baker, J. G. The selectivity of beta-adrenoceptor antagonists at the human beta1, beta2 and beta3 adrenoceptors. *Br. J. Pharmacol.* **2005**, *144*, 317–322.

(9) Cappetta, D.; Urbanek, K.; Berrino, L.; De Angelis, A. In *Brain and Heart Dynamics*, Govoni, S., Politi, P., Vanoli, E., Eds.; Springer International Publishing: Cham, 2020, pp 745–752.

(10) Henness, S.; Harrison, T. S.; Keating, G. Ocular carteolol. *Drugs Aging* **2007**, *24*, 509–528.

(11) Drugs.com. Ocupress. https://www.drugs.com/mtm/ocupress.html, (accessed Apr 04, 2021).

(12) Drugs.com. Carteolol. https://www.drugs.com/uk/carteolol-hydrochloride-1-eye-drops-leaflet.html, (accessed Apr 04, 2021).

(13) Hoyng, P. F. J.; van Beek, L. M. Pharmacological therapy for glaucoma. *Drugs* **2000**, *59*, 411–434.

(14) Coulangeon, L. M.; Sole, M.; Menerath, J. M.; Sole, P. [Aqueous humor flow measured by fluorophotometry. A comparative study of the effect of various beta-blocker eyedrops in patients with ocular hypertension]. *Ophtalmologie* **1990**, *4*, 156–161.

(15) Stewart, W. C.; Dubiner, H. B.; Mundorf, T. K.; Laibovitz, R. A.; Sall, K. N.; Katz, L.; Singh, K.; Shulman, D. G.; Siegel, L. I.; Hudgins, A. C.; Nussbaum, L.; Apostolaros, M. Effects of carteolol and timolol on plasma lipid profiles in older women with ocular hypertension or primary open-angle glaucoma. *Am. J. Ophthalmol.* **1999**, *127*, 142–147.

(16) Netland, P. A.; Weiss, H. S.; Stewart, W. C.; Cohen, J. S.; Nussbaum, L. L.; the Night Study Group Cardiovascular effects of topical carteolol hydrochloride and timolol maleate in patients with ocular hypertension and primary open-angle glaucoma. *Am. J. Ophthalmol.* **1997**, *123*, 465–477.

(17) Watson, P.; Barnett, M. F.; Parker, V.; Haybittle, J. A 7 year prospective comparative study of three topical beta blockers in the management of primary open angle glaucoma. *Br. J. Ophthalmol.* **2001**, *85*, 962–968.

(18) Nakagawa, K.; Murakami, N.; Yoshikazi, S.; Tominaga, M.; Mori, H.; Yabuuchi, Y.; Shintani, S. Derivatives of 3,4-dihydrocarbostyril as β-adrenergic blocking agents. *J. Am. Chem. Soc.* **1974**, *17*, 529–533.

(19) Tamura, Y.; Nakagawa, K.; Yoshizaki, S.; Murakami, N. 3,4-Dihydrocarbostyril derivatives and a process for preparing the same, 3,910,924, 1975.

(20) Mangishi, E.; Perego, B.; Salimbeni, A. A process for the preparation of 5-(3-tert-butylamino-2-hydroxypropoxy)-3,4-dihydrocarbostyryl. EP 0 579 096 A2, 1994.

(21) Bruice, P. Y., *Essential Organic Chemistry*, 3rd ed.; Pearson Education Limited: 2016.

(22) Clayden, J.; Greeves, N.; Warren, S., *Organic Chemistry*, 2012, pp 197–221, 328–359.

(23) Center for Drug Evaluation and Research. Development of New Stereoisomeric Drugs. https://www.fda.gov/regulatory-information/search-fda-guidance-documents/development-new-stereoisomeric-drugs, (accessed May 17, 2021).

(24) Agranat, I.; Caner, H.; Caldwell, J. Putting chirality to work: the strategy of chiral switches. *Nat. Rev. Drug Discov.* **2002**, *1*, 753–768.

(25) McConathy, J.; Owens, M. J. Sthereochemistry in drug action. *Prim. Care Companion J. Clin. Psychiatry* **2003**, *5*, 70–73.

(26) Nguyen, L. A.; He, H.; Pham-Huy, C. Chiral drugs: an overview. *Int. J. Biomed. Sci.* **2006**, *2*, 85–100.

(27) Koike, K.; Horinouchi, T.; Takayanagi, I. Comparison of interactions of R(+)- and S(−)-isomers of β-adrenergic partial agonists, befunolol and carteolol, with high affinity site of β-adrenoceptors in the microsomal fractions from guinea-pig ciliary body, right atria and trachea. *Gen. Pharmacol. Vasc. S.* **1994**, *25*, 1477–1481.

(28) Owens, M. J.; Knight, D. L.; Nemeroff, C. B. Second-generation SSRIs: human monoamine transporter binding profile of escitalopram and (*R*)-fluoxetine. *Biol. Psychiat.* **2001**, *50*, 345–350.

(29) Stoschitzky, K.; Egginger, G.; Zernig, G.; Klein, W.; Lindner, W. Stereoselective features of (*R*)- and (*S*)-atenolol: Clinical pharmacological, pharmacokinetic, and radioligand binding studies. *Chirality* **1993**, *5*, 15–19.

(30) Norsk Legemiddelhåndbok: L8.2.2.1 Atenolol. https://www.legemiddelhandboka.no/L8.2.2.1/Atenolol, (accessed Apr 04, 2021).

(31) Mahanth, P.; Konda, N. S.; Kumar, R. Chiral synthesis: an overview. *Int. J. Pharm. Res. Dev.* **2014**, *6*, 70–78.

(32) Herdeis, C.; Hubmann, H. P.; Lotter, H. Chiral pool synthesis of trans-(2*S*,3*S*)-3-hydroxyproline and castanodiol from (*S*)-pyroglutamic acid. *Tetrahedron: Asymmetry* **1994**, *5*, 119–128.

(33) Sharpless, K. B.; Amberg, W.; Bennani, Y. L.; Crispino, G. A.; Hartung, J.; Jeong, K. S.; Kwong, H. L.; Morikawa, K.; Wang, Z. M. The osmium-catalyzed asymmetric dihydroxylation: a new ligand class and a process imporovement. *J. Org. Chem.* **1992**, *57*, 2768–2771.

(34) Solomons, T. W. G.; Fryhle, C. B., *Organic Chemistry*, 2011, pp 186–229.

(35) Kagan, H. B.; Fiaud, J. C. In *Topics in Stereochemistry*; John Wiley & Sons, Ltd: 2007, pp 249–330.

(36) Wei, S.; Jun, Y.; Jiangling, Z. Synthetic methods of chiral aryloxy propanol amine compounds and salts thereof, CN 101323580A, 2008.

(37) Tsuda, Y.; Yoshimoto, K.; Nishikawa, T. Practical Syntheses of [R]- and [S]-1-Alkylamino-3-aryloxy-2-porpanols from a Single Carbohydrate Precursor. *Chem. Pharm. Bull.* **1981**, *29*, 3593–3600.

(38) Anastas, P.; Eghbali, N. Green Chemistry: Principles and Practice. *Chem. Soc. Rev.* **2010**, *39*.

(39) Poliakoff, M.; Licence, P. Green chemistry. *Nature* **2007**, *450*, 810–812.

(40) Ferreira-Leitão, V. S.; Christe Cammarota, M.; Gonçalves Aguieiras, E. C.; de Sá, L. R. V.; Fernandez-Lafuente, R.; Guimarães Freire, D. M. The protagonism of biocatalysis in green chemistry and its environmental benefits. *Catalysts* **2017**, *7*, 9–42.

(41) Singh, R.; Kumar, M.; Mittal, A.; Mehta, P. K. Microbial enzymes: industrial progress in 21st century. *3 Biotech* **2016**, *6*.

(42) Li, S.; Yang, X.; Yang, S.; Zhu, M.; Wang, X. Technology prospecting on enzymes: application, marketing and engineering. *Comput. Struct. Biotechnol. J.* **2012**, *2*, e201209017.

(43) Faber, K., *Biotransformations in organic chemistry*, 6th ed.; Springer: 2011, pp 1–27, 315–342.

(44) Menger, F. M. Enzyme reactivity from an organic perspective. *Acc. Chem. Res.* **1993**, *26*, 206–212.

(45) Pasteur, L. C. R. *Hebd. Seance. Acad. Sci. Paris* **1858**, *46*, 615–618.

(46) Keith, J. M.; Larrow, J. F.; Jacobsen, E. N. Practical considerations in kinetic resolution reactions. *Adv. Synth. Catal.* **2001**, *343*, 5–26.

(47) Verho, O.; Bäckvall, J.-E. Chemoenzymatic dynamic kinetic resolution: a powerful tool for the preparation of enantiomerically pure alcohols and amines. *J. Am. Chem. Soc.* **2015**, *137*, 3996–4009.

(48) Persson, B. A.; Larsson, A. L. E.; Le Ray, M.; Bäckvall, J.-E. Ruthenium- and enzyme-catalyzed dynamic kinetic resolution of secondary alcohols. *J. Am. Chem. Soc.* **1999**, *121*, 1645–1650.

(49) Rakels, J. L. L.; Straathof, A. J. J.; Heijnen, J. J. A simple method to determine the enantiomeric ratio in enantioselective biocatalysis. *Enzyme Microb. Technol.* **1993**, *15*, 1051–1056.

(50) Jacobsen, E. E.; Hellemond, E.; Moen, A. R.; Prado, L. C. V.; Anthonsen, T. Enhanced selectivity in Novozym 435 catalyzed kinetic resolution of secondary alcohols and butanoates caused by the (*R*)-alcohols. *Tetrahedron Lett.* **2003**, *44*, 8453–8455.

(51) Nelson, D. L.; Cox, M. M., *Lehninger: Principles of Biochemistry*, 7th ed.; Macmillian Higher Education: 2017, pp 361–366.

(52) Paiva, A. L.; Balcão, V. M.; Malcata, F. Kinetics and mechanisms of reactions catalyzed by immobilized lipases. *Enzyme Microb. Technol.* **2000**, *27*, 187–204.

(53) Ghori, I.; Iqbal, M.; Hameed, A. Characterization of a novel lipase from *Bacillus* sp. isolated from tannery wastes. *Braz. J. Microbiol.* **2011**, *42*, 22–9.

(54) Hertadi, R.; Widhyastuti, H. Effect of Ca^{2+} ion to the activity and stability of lipase isolated from chromohalobacter japonicus BK-AB18. *Procedia Chem.* **2015**, *16*, 306–313.

(55) Graber, M.; Irague, R.; Rosenfeld, E.; Lamare, S.; Franson, L.; Hult, K. Solvent as a competitive inhibitor for *Candida antarctica* lipase B. *Biochim. Biophys. Acta, Proteins Proteomics* **2007**, *1774*, 1052–1057.

(56) Bousquet-Dubouch, M.-P.; Graber, M.; Sousa, N.; Lamare, S.; Legoy, M.-D. Alcoholysis catalyzed by *Candida antarctica* Lipase B in a gas/solid system obeys a Ping Pong Bi Bi mechanism with competitive inhibition by the alcohol substrate and water. *Biochim. Biophys. Acta, Protein Struct. Mol. Enzymol.* **2001**, *1550*, 90–99.

(57) Kundys, A.; Białecka-Florjańczyk, E.; Fabiszewska, A.; Małajowicz, J. *Candida antarctica* Lipase B as catalyst for cyclic esters synthesis, their polymerization and degradation of aliphatic polyesters. *J. Polym. Environ.* **2018**, *26*, 396–407.

(58) Benkovics, T. et al. Evolving to an Ideal Synthesis of Molnupiravir, an Investigational Treatment for COVID-19. *ChemRxiv*, *Preprint*.

(59) Strzelczyk, P.; Bujacz, G.; Kiełbasiński, P.; Błaszczyk, J. Crystal and molecular structure of hexagonal form of Lipase B from *Candida antarctica*. *Acta Biochim. Pol.* **2016**, *63*, 103–109.

(60) Ferrario, V.; Ebert, C.; Nitti, P.; Gardossi, L. Modelling and predicting enzyme enantioselectivity: the aid of computational methods for the rational use of Lipase B from *Candida Antarctica*. *Curr. Biotechnol.* **2015**, *4*, 87–99.

(61) Kwon; Hoon, C.; Shin, D. Y.; Lee, J. H. Molecular modeling and its experimental verification for the catalytic mechanism of *Candida antarctica* Lipase B. *J. Microbiol. Biotechn.* **2007**, *17*, 1098–1105.

(62) Schopf, P.; Warshel, A. Validating computer simulations of enantioselective catalysis; reproducing the large steric and entropic contributions in *Candida Antarctica* Lipase B. *Proteins* **2014**, *82*, 1387–1399.

(63) Kazlauskas, R. J.; Weissfloch, A. N. E.; Rappaport, A. T.; Cuccia, L. A. A rule to predict which enantiomer of a secondary alcohol reacts faster in reactions catalyzed by cholesterol esterase, lipase from Pseudomonas cepacia, and lipase from *Candida rugosa*. *J. Org. Chem.* **1991**, *56*, 2656–2665.

(64) Jacobsen, E. E.; Hoff, B. H.; Anthonsen, T. Enantiopure derivatives of 1,2-alkanediols: Substrate requirements of Lipase B from **Candida antarctica**. *Chirality* **2000**, *12*, 654–659.

(65) Anthonsen, T.; Hoff, B. H. Resolution of derivatives of 1,2-propanediol with Lipase B from *Candida antarctica*: Effect of substrate structure, medium, water activity and acyl donor on enantiomeric ratio. *Chem. Phys. Lipids* **1998**, *93*, 199–207.

(66) Laane, C.; Boeren, S.; Vos, K.; Veeger, C. Rules for optimization of biocatalysis in organic solvents. *Biotechnol. Bioeng.* **1987**, *30*, 81–87.

(67) Zaks, A.; Klibanov, A. M. The effect of water on enzyme action in organic media. *J. Biol. Chem.* **1988**, *263*, 8017–8021.

(68) Jacobsen, E. E.; Anthonsen, T. Water content influences the selectivity of CALB-catalyzed kinetic resolution of phenoxymethyl-substituted secondary alcohols. *Can. J. Chem.* **2002**, *80*, 577–581.

(69) Jacobsen, E. E. Synthesis of enantiopure building blocks for biologically active compounds by enzyme catalysis: Optimization of reaction conditions for increased enantioselectivity and activity, Ph.D. Thesis, 2004.

(70) Halling, P. J. Salt hydrates for water activity control with biocatalysts in organic media. *Biotechnol. Tech.* **1992**, *6*, 271–276.

(71) Kirchner, G.; Scollar, M. P.; Klibanov, A. M. Resolution of racemic mixtures via lipase catalysis in organic solvents. *J. Am. Chem. Soc.* **1985**, *107*, 7072–7076.

(72) Orrenius, C.; Öhrner, N.; Rotticci, D.; Mattson, A.; Hult, K.; Norin, T. *Candida antarctica* lipase B catalysed kinetic resolutions: Substrate structure requirements for the preparation of enantiomerically enriched secondary alcanols. *Tetrahedron: Asymmetry* **1995**, *6*, 1217–1220.

(73) Ghogare, A.; Kumar, G. S. Oxime esters as novel irreversible acyl transfer agents for lipase catalysis in organic media. *J. Chem. Soc. Chem. Comm.* **1989**, 1533–1535.

(74) Degueil-Castaing, M.; De Jeso, B.; Drouillard, S.; Maillard, B. Enzymatic reactions in organic synthesis: 2- ester interchange of vinyl esters. *Tetrahedron Lett.* **1987**, *28*, 953–954.

(75) Wang, Y. F.; Lalonde, J. J.; Momongan, M.; Bergbreiter, D. E.; Wong, C. H. Lipase-catalyzed irreversible transesterifications using enol esters as acylating reagents: preparative enantio- and regioselective syntheses of alcohols, glycerol derivatives, sugars and organometallics. *J. Am. Chem. Soc.* **1988**, *110*, 7200–7205.

(76) Donohue, T. M.; Tuma, D. J.; Sorrell, M. F. Acetaldehyde adducts with proteins: Binding of [^{14}C]acetaldehyde to serum albumin. *Arch. Biochem. Biophys.* **1983**, *220*, 239–246.

(77) Moran, L. A.; Horton, R. A.; Scrimgeour, G.; Perry, M., *Principles of Biochemistry*, 5th ed.; Pearson Education Limited: 2014, pp 184–189.

(78) Weber, H.; Stecher, H.; Faber, K. Sensitivity of microbial lipases to acetaldehyde formed by acyl-transfer reactions from vinyl esters. *Biotechnol. Lett.* **1995**, *17*, 803–808.

(79) Bajwa, J. S.; Anderson, R. C. A highly regioselective conversion of epoxides to haloliydrins by lithium halides. *Tetrahedon Lett.* **1991**, *32*, 3021–3024.

(80) Chini, M.; Crotti, P.; Gardelli, C.; Macchia, F. Regio- and stereoselective synthesis of β-halohydrins from 1,2-epoxides with ammonium halides in the presence of metal salts. *Tetrahedon* **1992**, *48*, 3805–3812.

(81) Gundersen, M. A. Synthesis of enantiopure derivative of β-blocker (*S*)-carteolol by lipase catalysis, MA thesis, NTNU, 2020.

(82) Fujinaga, M.; Ohkubo, T.; Yamasaki, T.; Zhang, Y.; Mori, W.; Hanyu, M.; Kumata, K.; Hatori, A.; Xie, L.; Nengaki, N.; Zhang, M.-R. Automated synthesis of (*rac*)-, (*R*)-, and (*S*)-[^{18}F]epifluorohydrin and their application for developing PET radiotracers containing a 3-[^{18}F]fluoro-2-hydroxypropyl moiety. *ChemMedChem* **2018**, *13*, 1723–1731.

(83) Carey, F. A.; Sundberg, R. J., *Advanced Organic Chemistry Part B: Reaction and synthesis*, 5th ed.; Springer Science+Business Media: 2007.

(84) Greibrokk, T.; Lundanes, E.; Rasmussen, K. E., *Kromatografi: Separasjon og Deteksjon*, 3rd ed., 1994, pp 6–24, 173–226.

(85) Okamoto, Y.; Ikai, T. Chiral HPLC for efficient resolution of enantiomers. *Chem. Soc. Rev.* **2008**, *37*, 2593–2608.

(86) Chen, X.; Yamamoto, C.; Okamoto, Y. Polysaccharide derivatives as useful chiral stationary phases in high-performance liquid chromatography. *Pure Appl. Chem.* **2007**, *79*, 1561–1573.

(87) Mayer, S.; Schurig, V. Enantiomer separation by electrochromatography on capillaries coated with Chirasil-Dex. *J. High Resolut. Chromatogr.* **1992**, *15*, 129–131.

(88) Harned, H. S.; Ehlers, R. W. The Dissociation Constant of Acetic Acid from 0 to 60° Centigrade. *J. Am. Chem. Soc.* **1933**, *55*, 652–656.

(89) Schmid, M. G.; Gecse, O.; Szabo, Z.; Kilár, F.; Gübitz, G.; Ali, I.; Aboul-Enein, H. Y. Comparative study of the chiral resolution of β-blockers on cellulose tris (3,5-dimethylphenylcarbamate) phases in normal and reversed phase modes. *J. Liq. Chromatogr. Relat. Technol.* **2001**, *24*, 2493–2504.

(90) Straathof, A.; Jongejan, J. The enantiomeric ratio: origin, determination and prediction. *Enzyme Microb. Technol.* **1997**, *21*, 559–571.

(91) Gabruś, E.; Nastaj, J.; Tabero, P.; Aleksandrzak, T. Experimental studies on 3A and 4A zeolite molecular sieves regeneration in TSA process: Aliphatic alcohols dewatering–water desorption. *Chem. Eng. J.* **2015**, *259*, 232–242.

(92) U.S. Geological Survey. Ground-water quality. https://pubs.usgs.gov/wri/wri024045/htms/report2.htm, (accessed Jun 01 2021).

(93) Yamamoto, K.; Uno, T.; Ishihara, T.; Nakagawa, K. Synthesis of optically active 5-(3-tert-Butylamino-2-hydroxypropoxy)-3,4-dihydrocarbostyril Hydrochloride and their β-adrenergic blocking activities. *Yakugaku Zasshi* **1976**, *96*, 289–292.

(94) Banoth, L.; Banerjee, U. New chemical and chemo-enzymatic synthesis of (*RS*)-, (*R*)-, and (*S*)-esmolol. *Arabian J. Chem.* **2017**, *10*, S3603–S3613.

A ^{1}H NMR of alcohol 1

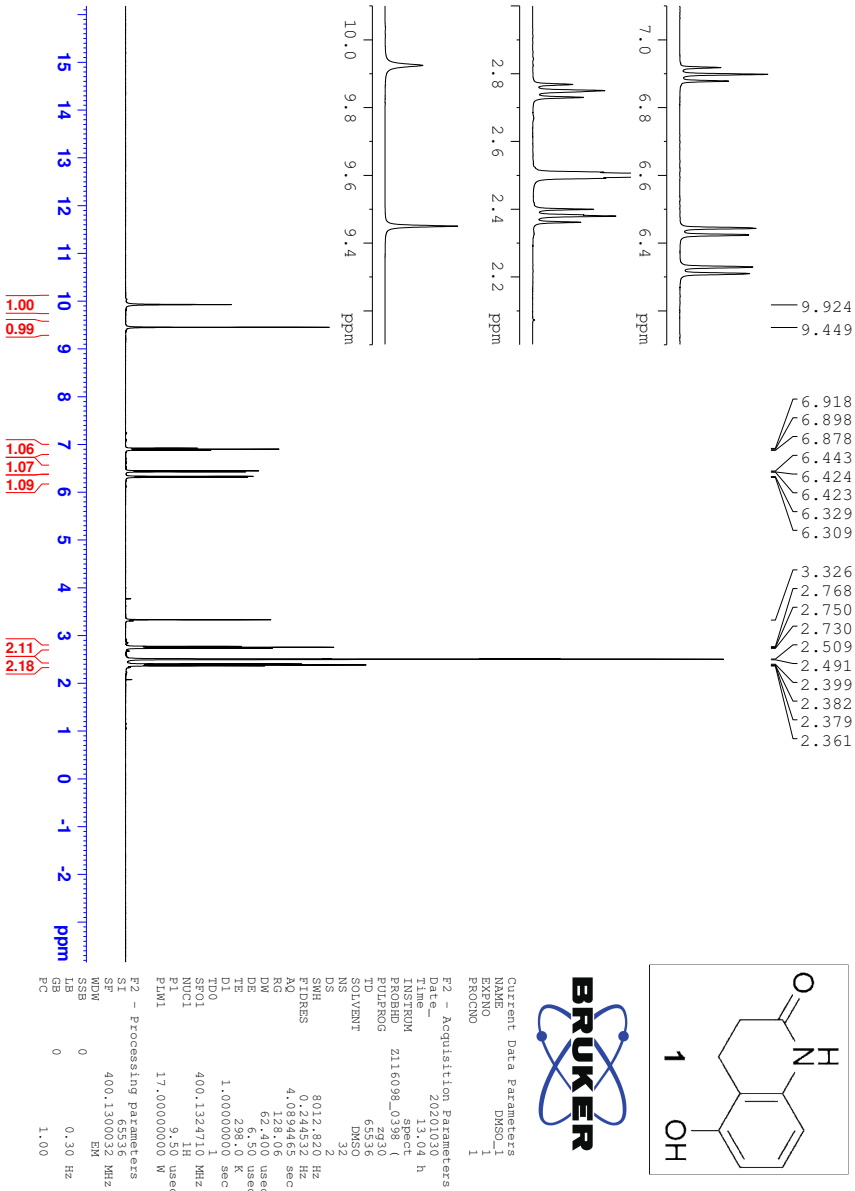

Figure A.1: ^{1}H NMR (400 MHz, $DMSO_{d6}$) spectrum of starting material **1**.

B Characterization of chlorohydrin 2a

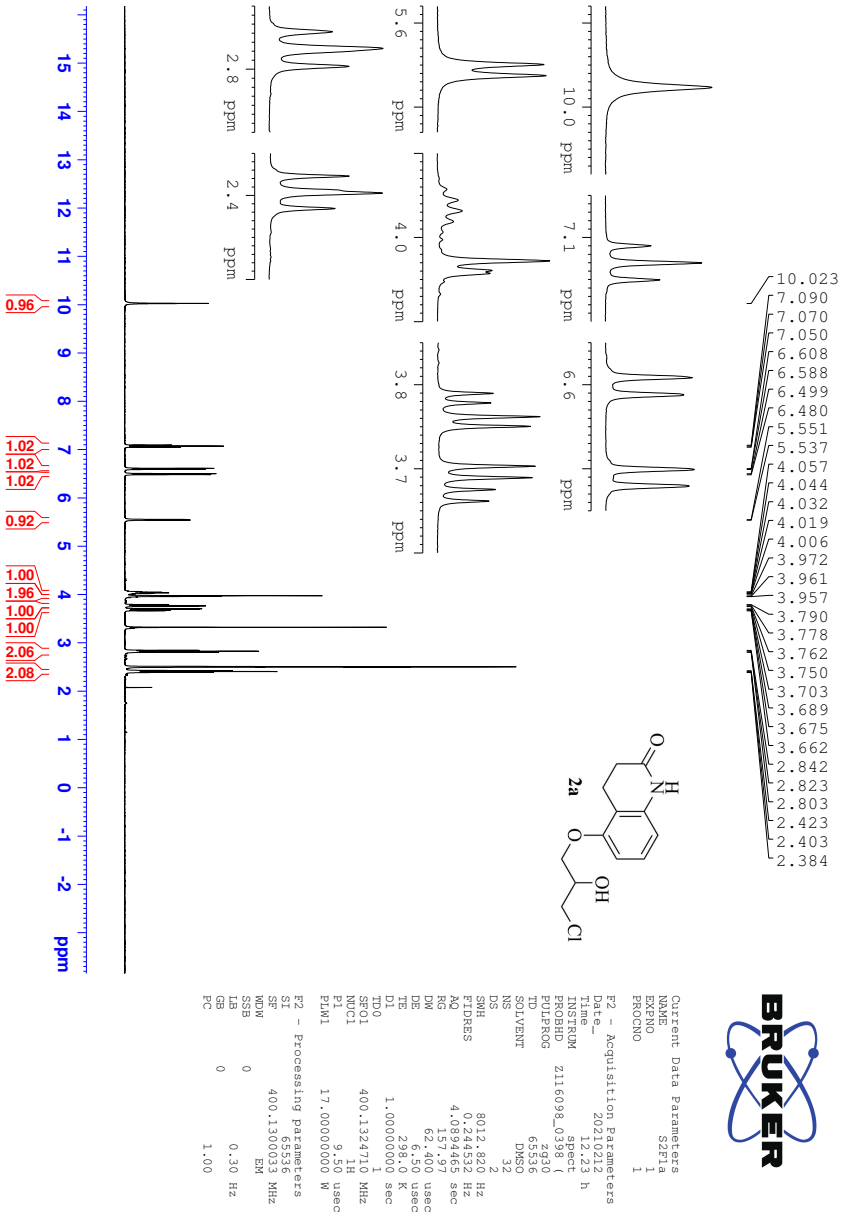

Figure B.1: ^{1}H NMR (400 MHz, DMSO$_{d6}$) spectrum of chlorohydrin **2a**.

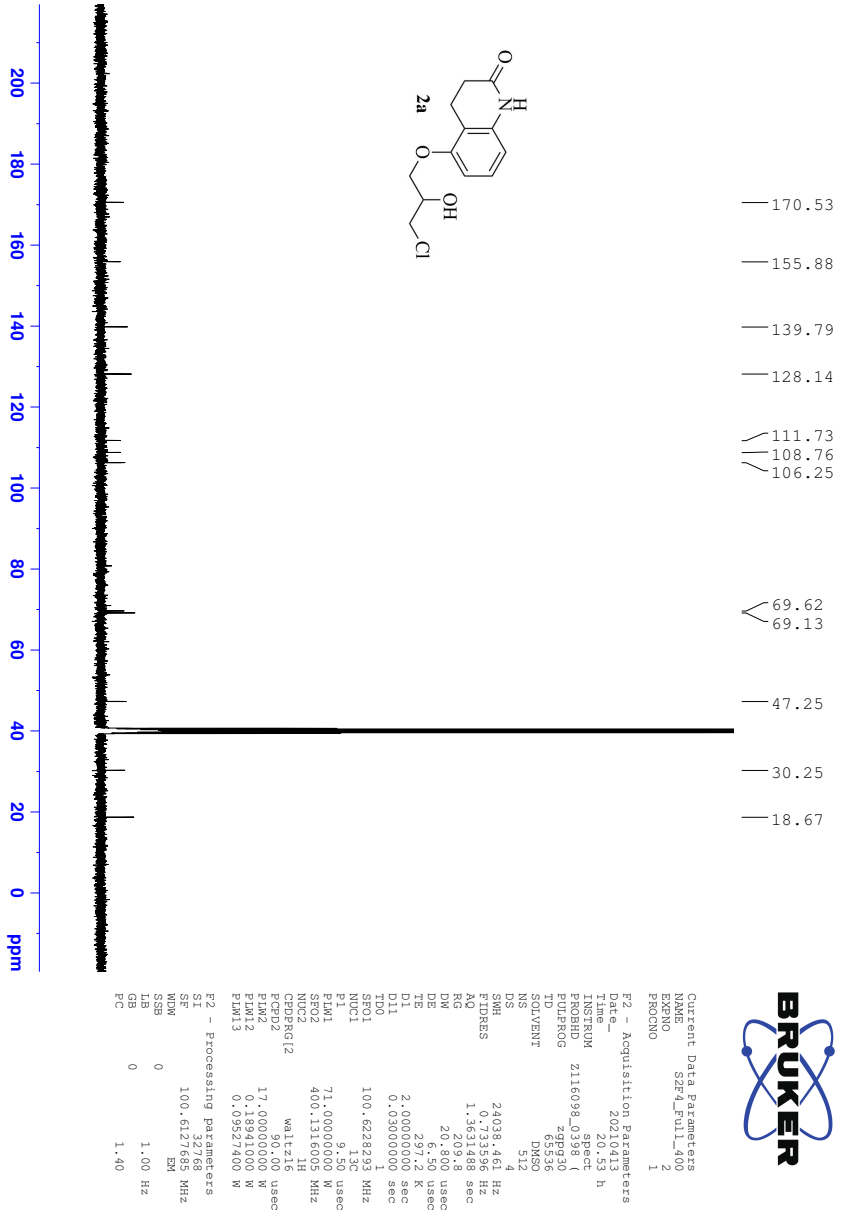

Figure B.2: ^{1}C NMR (400 MHz, DMSO$_{d6}$) spectrum of chlorohydrin **2a**.

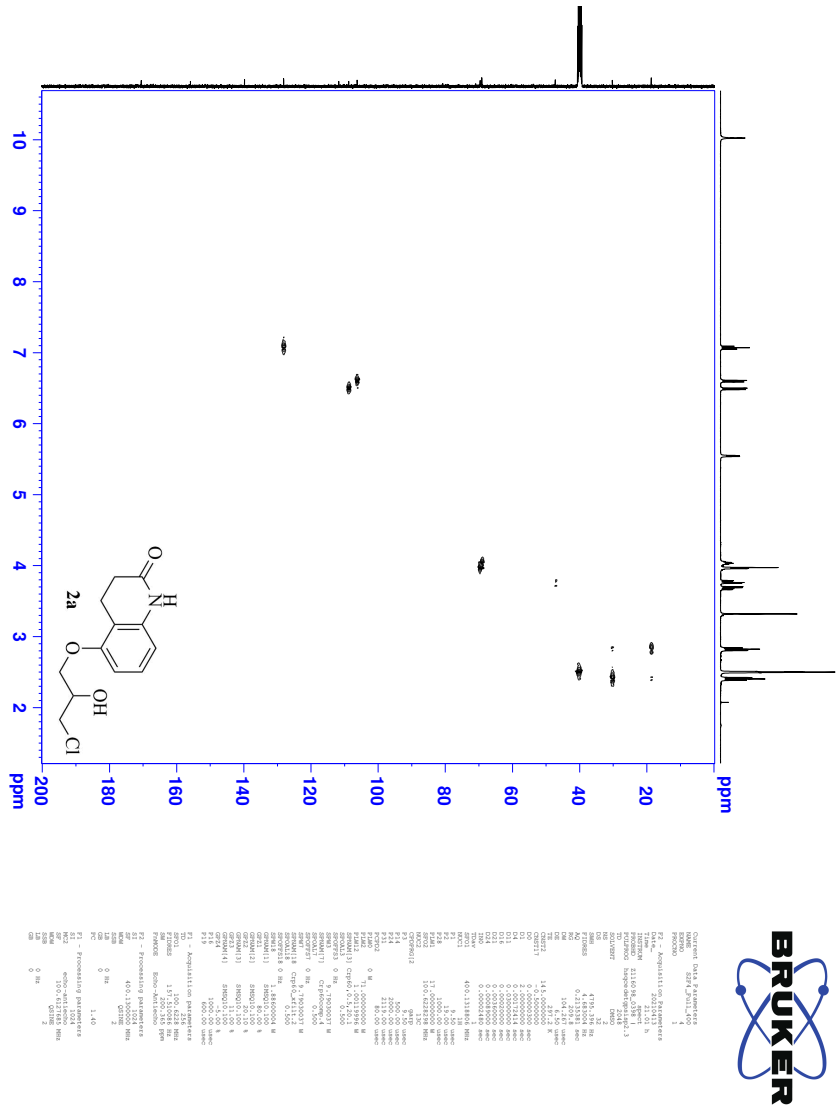

Figure B.3: HSQC (400 MHz, $DMSO_{d6}$) spectrum of chlorohydrin **2a**.

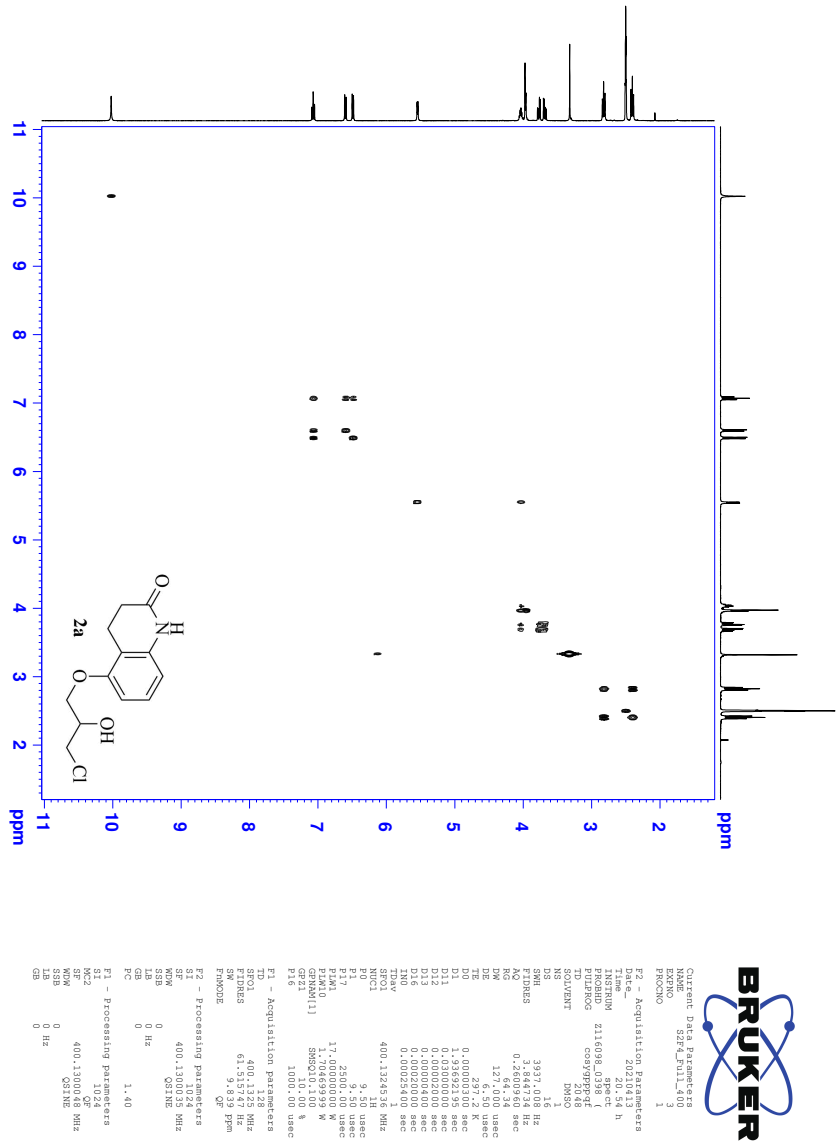

Figure B.4: COSY (400 MHz, $DMSO_{d6}$) spectrum of chlorohydrin **2a**.

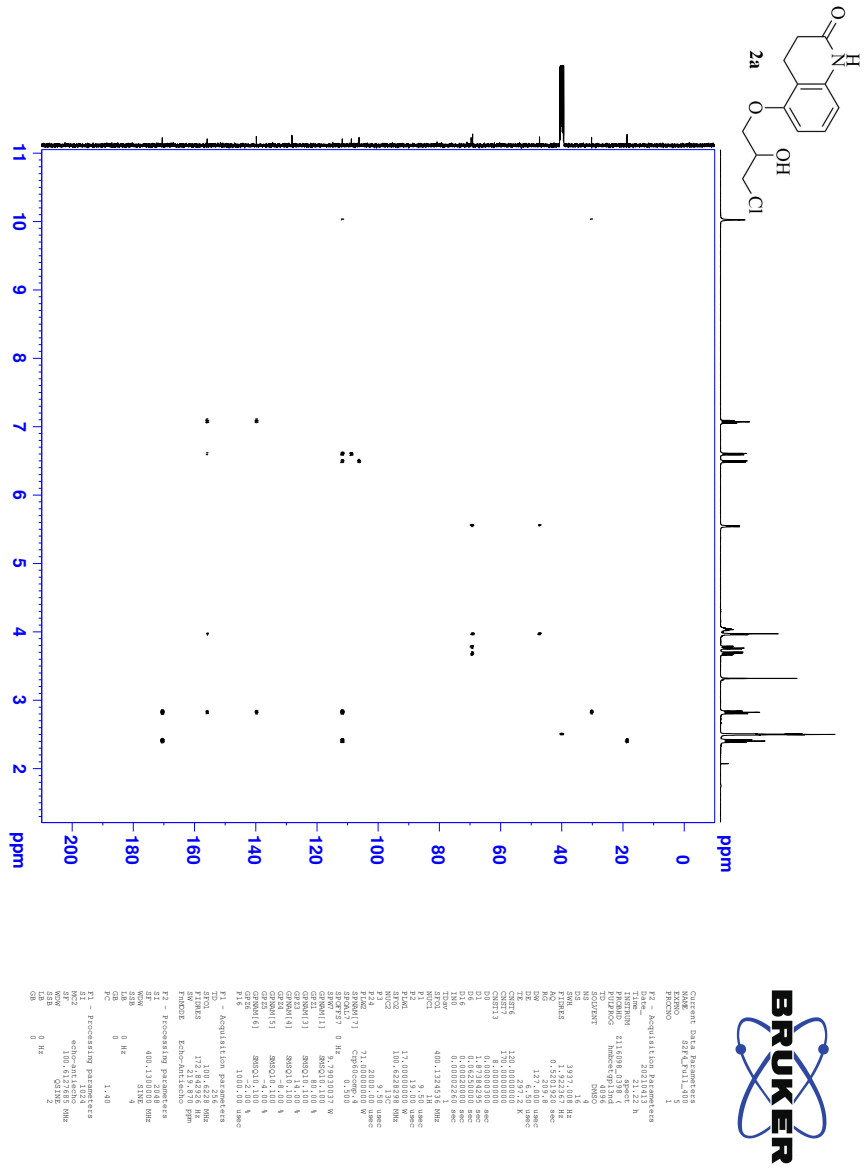

Figure B.5: HMBC (400 MHz, $DMSO_{d6}$) spectrum of chlorohydrin **2a**.

Elemental Composition Report **Page 1**

Single Mass Analysis
Tolerance = 3.0 PPM / DBE: min = -10.0, max = 50.0
Element prediction: Off
Number of isotope peaks used for i-FIT = 6

Monoisotopic Mass, Even Electron Ions
1038 formula(e) evaluated with 2 results within limits (all results (up to 1000) for each mass)
Elements Used:
C: 0-100 H: 0-100 N: 0-10 O: 0-10 Cl: 0-2
2021_333 110 (1.040) AM2 (Ar,35000.0,0.00,0.00); ABS; Cm (105:110)
1: TOF MS ES+

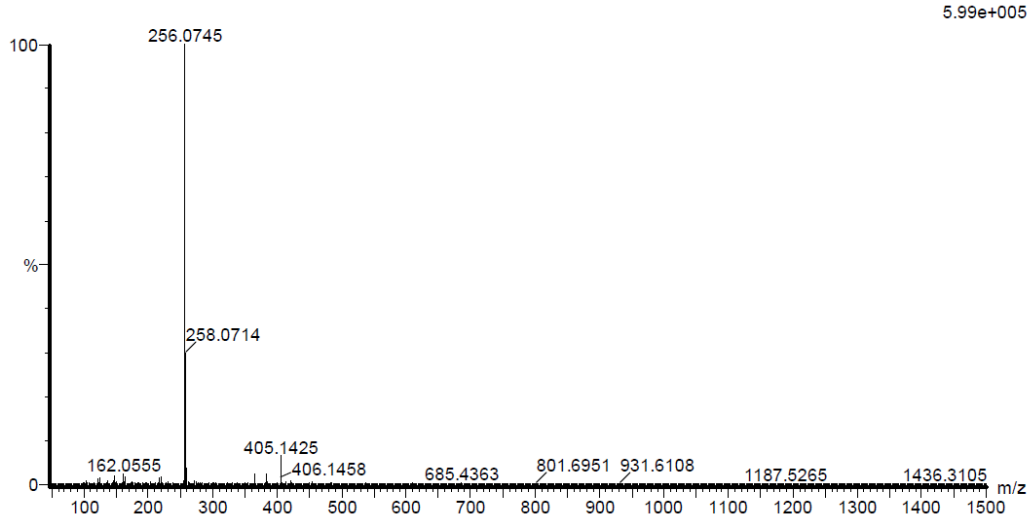

Minimum:				-10.0				
Maximum:		5.0	3.0	50.0				
Mass	Calc. Mass	mDa	PPM	DBE	i-FIT	Norm	Conf(%)	Formula
256.0745	256.0741	0.4	1.6	-2.5	2232.7	29.946	0.00	C H14 N5 O10
	256.0740	0.5	2.0	5.5	2202.7	0.000	100.00	C12 H15 N O3 Cl

Figure B.6: HRMS (TOF-ASAP$^+$) spectrum of chlorohydrin **2a**.

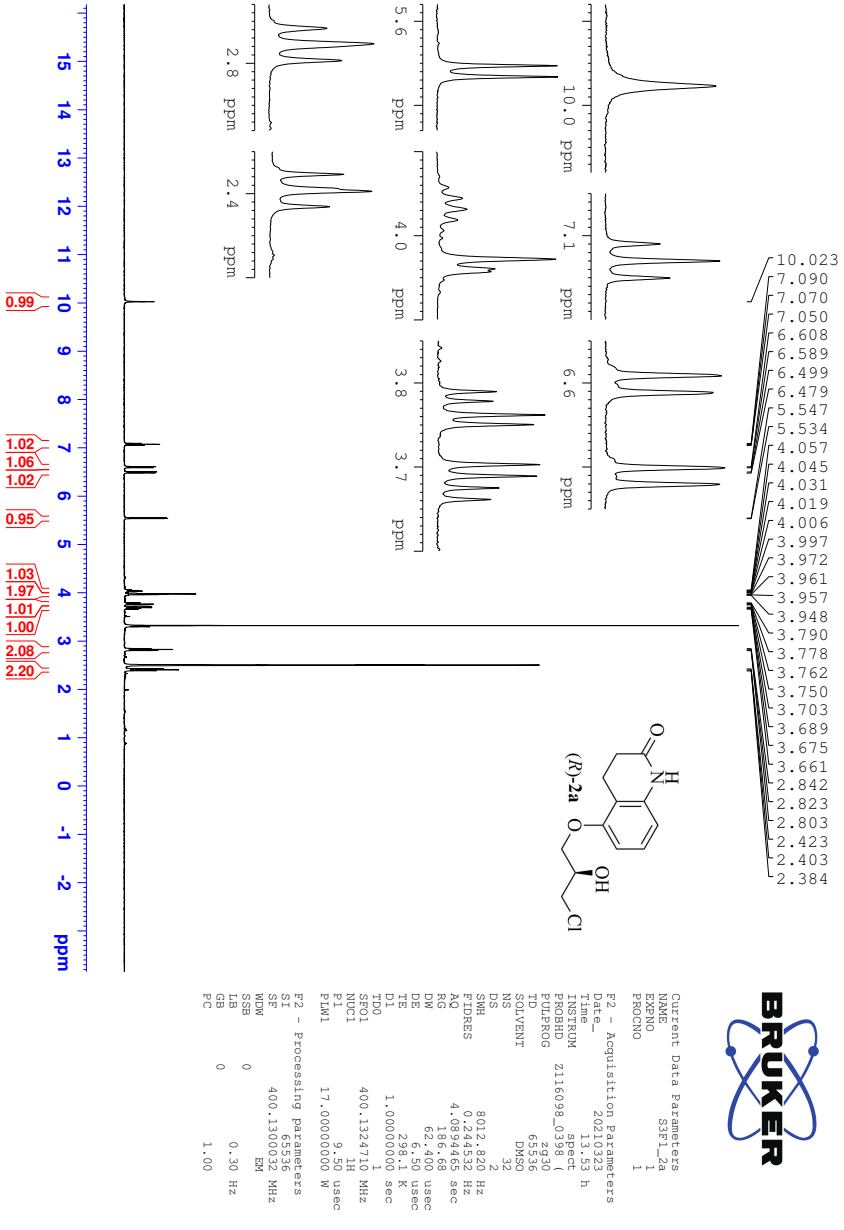

Figure B.7: ^{1}H NMR (400 MHz, DMSO$_{d6}$) spectrum of chlorohydrin (*R*)-**2a**.

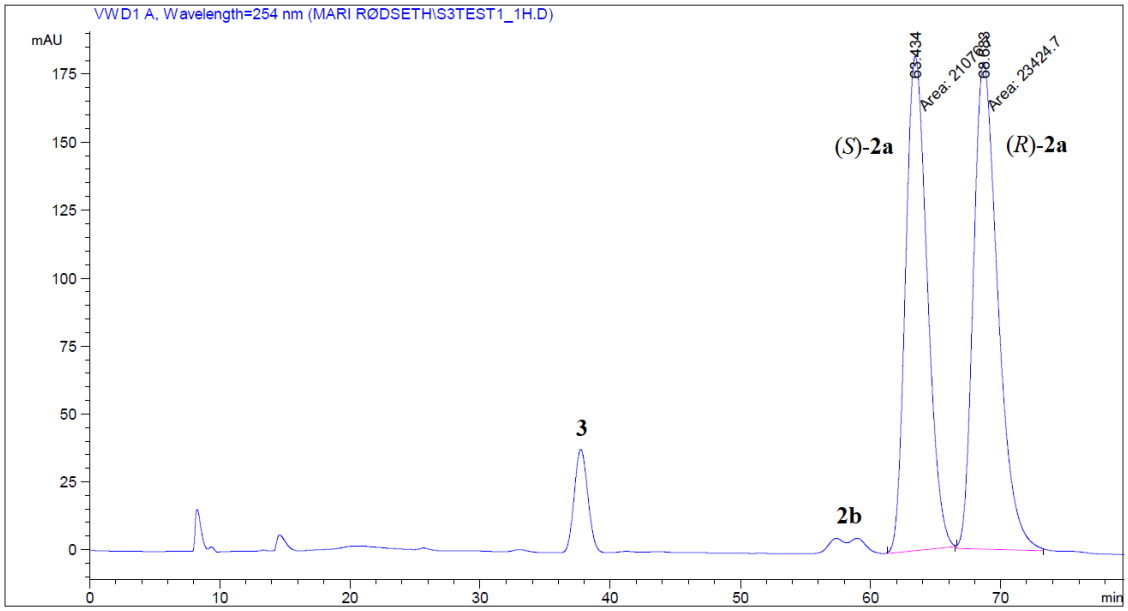

Figure B.8: Chiral HPLC (Chiralcel OD-H, *n*-hexane:ethanol:trifluoroacetic acid [90:10:0.1], 0.4 mL/min) chromatogram of racemic chlorohydrin **2a**.

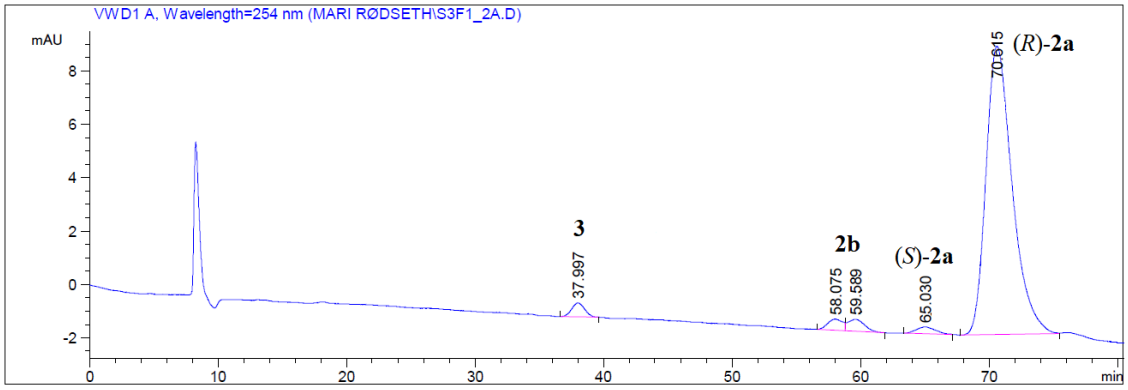

Figure B.9: Chiral HPLC (Chiralcel OD-H, *n*-hexane:ethanol:trifluoroacetic acid [90:10:0.1], 0.4 mL/min) chromatogram of chlorohydrin (*R*)-**2a** in 97% *ee*.

C Characterization of epoxide 2b

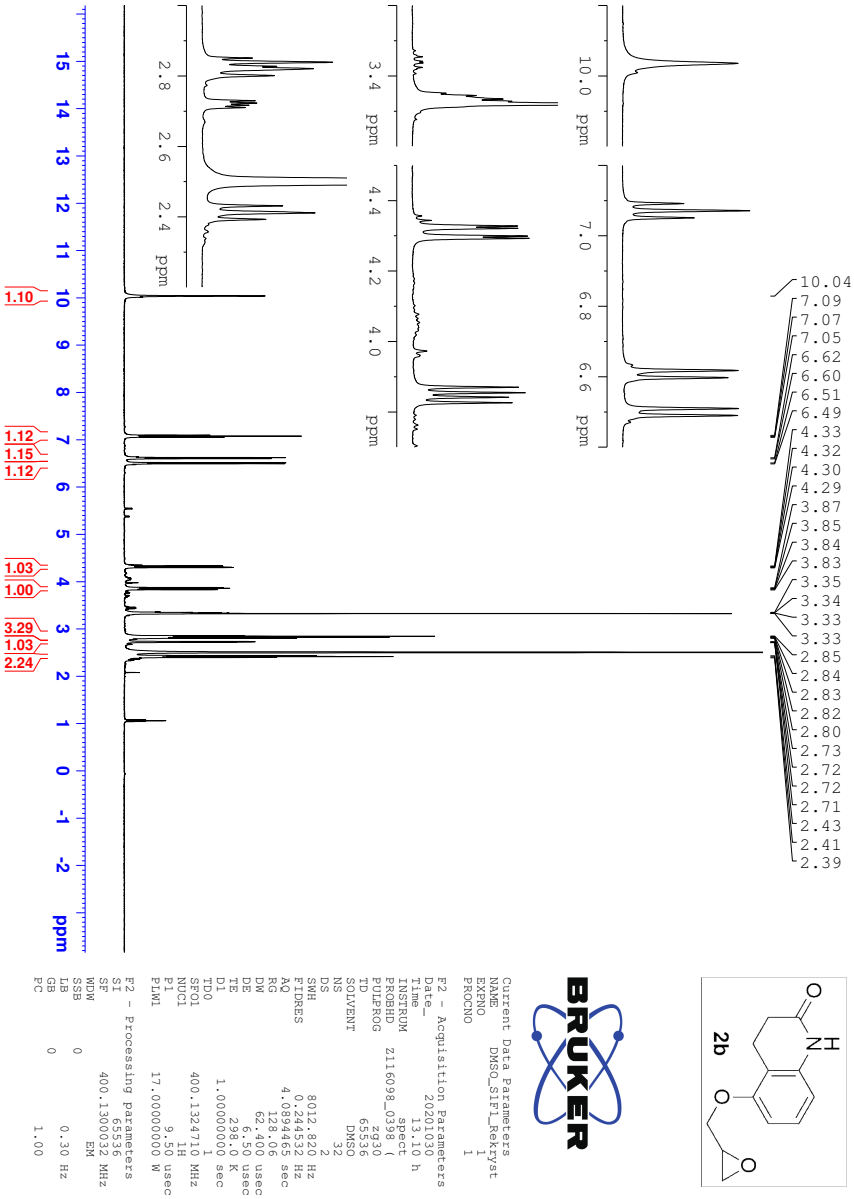

Figure C.1: ^{1}H NMR (400 MHz, DMSO$_{d6}$) spectrum of epoxide **2b**.

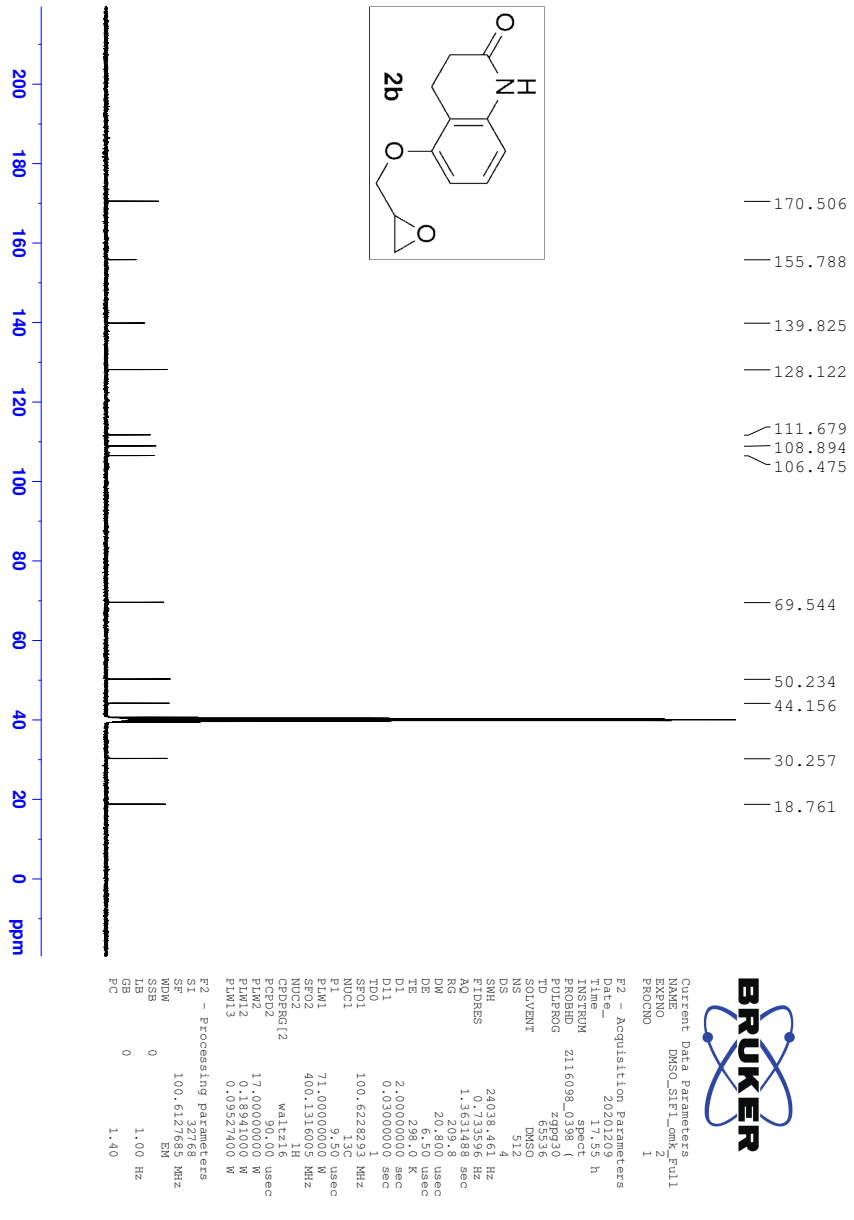

Figure C.2: ^{1}C NMR (400 MHz, DMSO$_{d6}$) spectrum of epoxide **2b**.

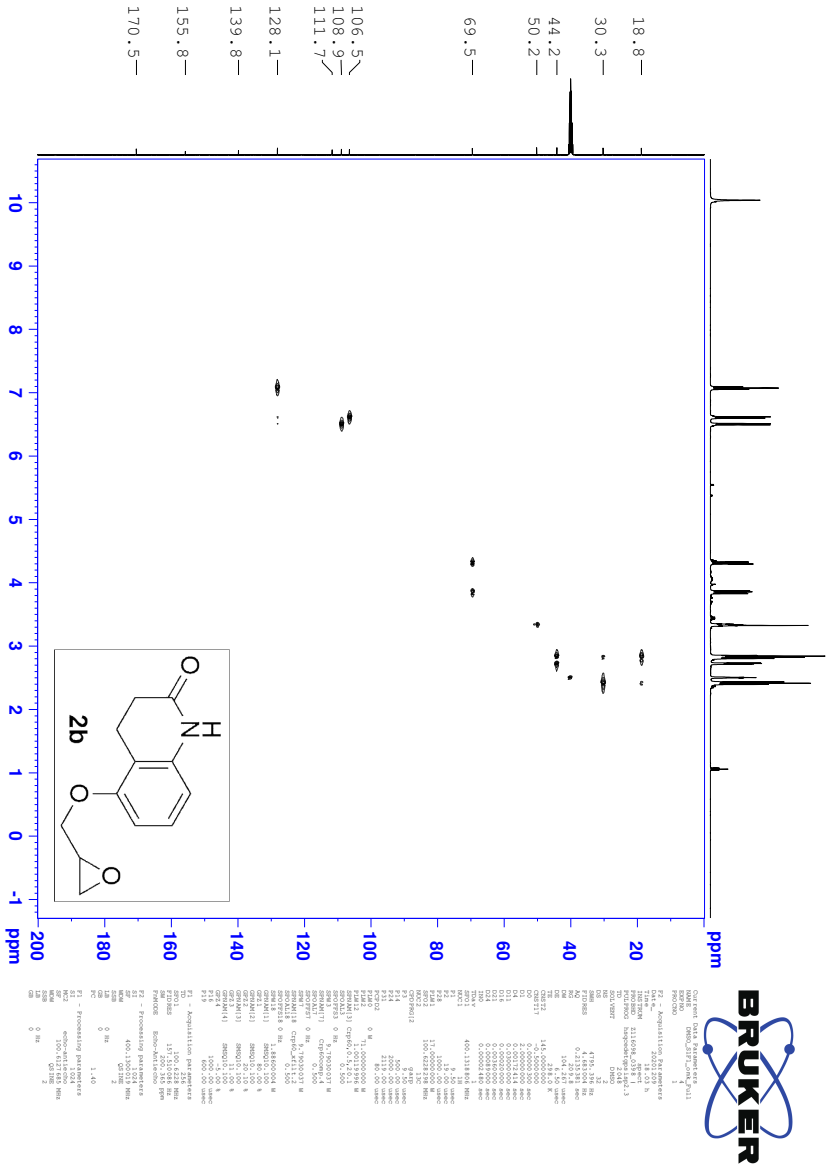

Figure C.3: HSQC (400 MHz, $DMSO_{d6}$) spectrum of epoxide **2b**.

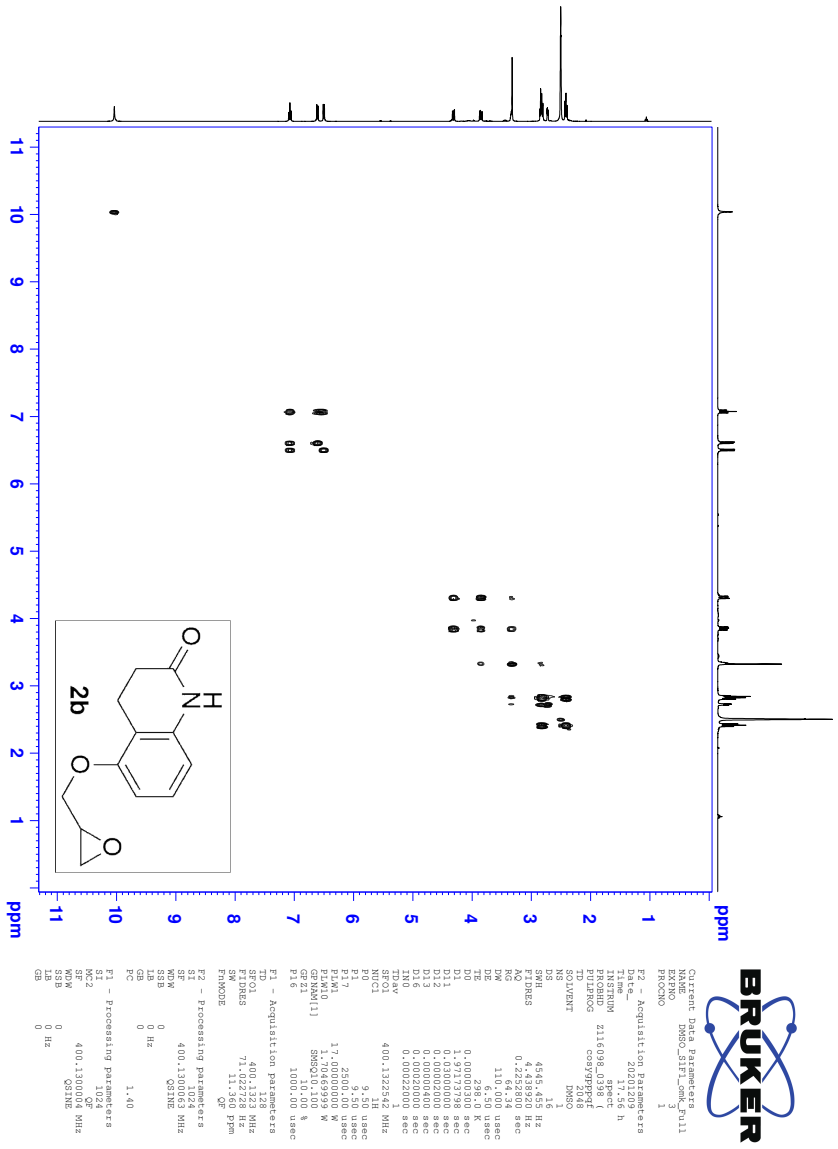

Figure C.4: COSY (400 MHz, $DMSO_{d6}$) spectrum of epoxide **2b**.

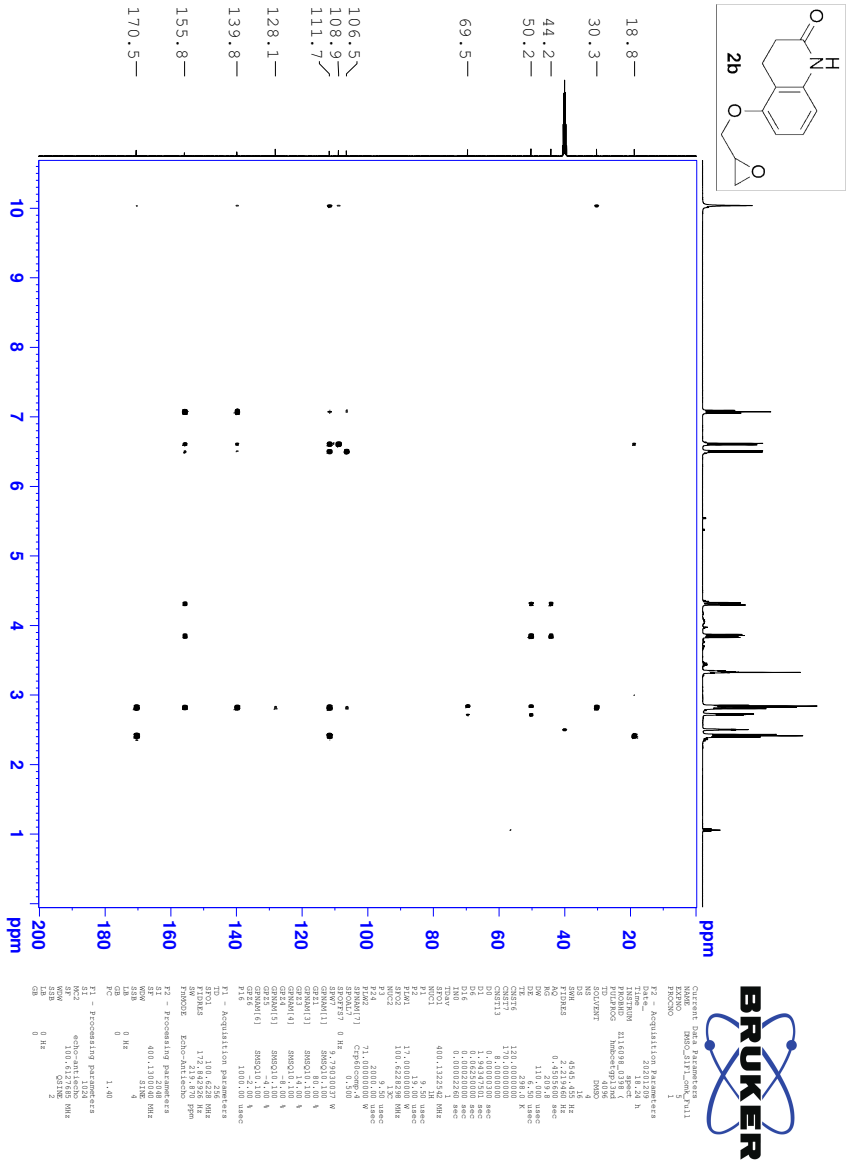

Figure C.5: HMBC (400 MHz, $DMSO_{d6}$) spectrum of epoxide **2b**.

Elemental Composition Report **Page 1**

Single Mass Analysis
Tolerance = 2.0 PPM / DBE: min = -50.0, max = 100.0
Element prediction: Off
Number of isotope peaks used for i-FIT = 6

Monoisotopic Mass, Even Electron Ions
1041 formula(e) evaluated with 1 results within limits (all results (up to 1000) for each mass)
Elements Used:
C: 0-100 H: 0-100 N: 0-8 O: 0-8 Na: 0-1
SVG_20201029_S1F1 137 (2.540) AM2 (Ar,35000.0,0.00,0.00); Cm (137:140)
1: TOF MS ES+

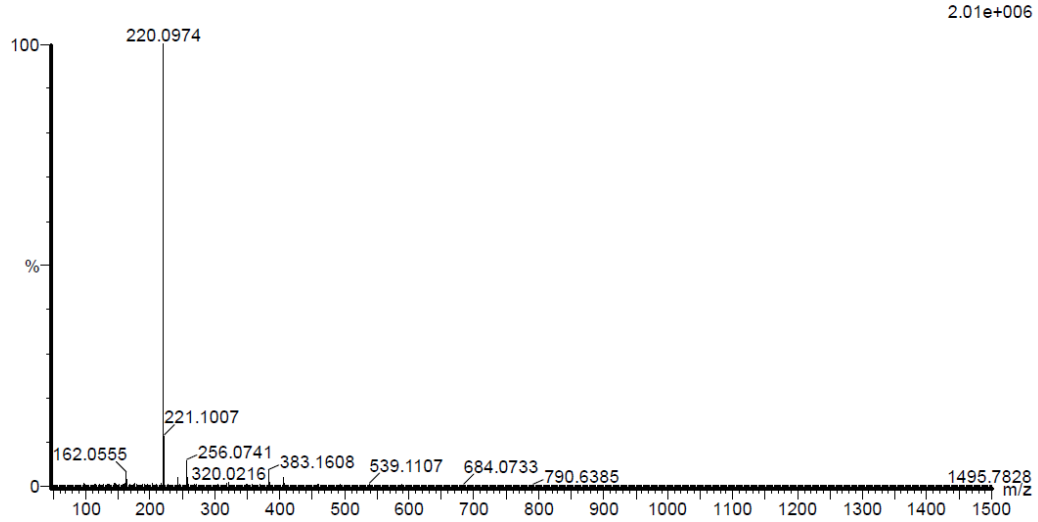

Minimum:				-50.0				
Maximum:		5.0	2.0	100.0				
Mass	Calc. Mass	mDa	PPM	DBE	i-FIT	Norm	Conf(%)	Formula
220.0974	220.0974	0.0	0.0	6.5	3077.1	n/a	n/a	C12 H14 N O3

Figure C.6: LC-HRMS (TOF-ASAP$^+$) spectrum of epoxide **2b**.

D Characterization of dimer 2c

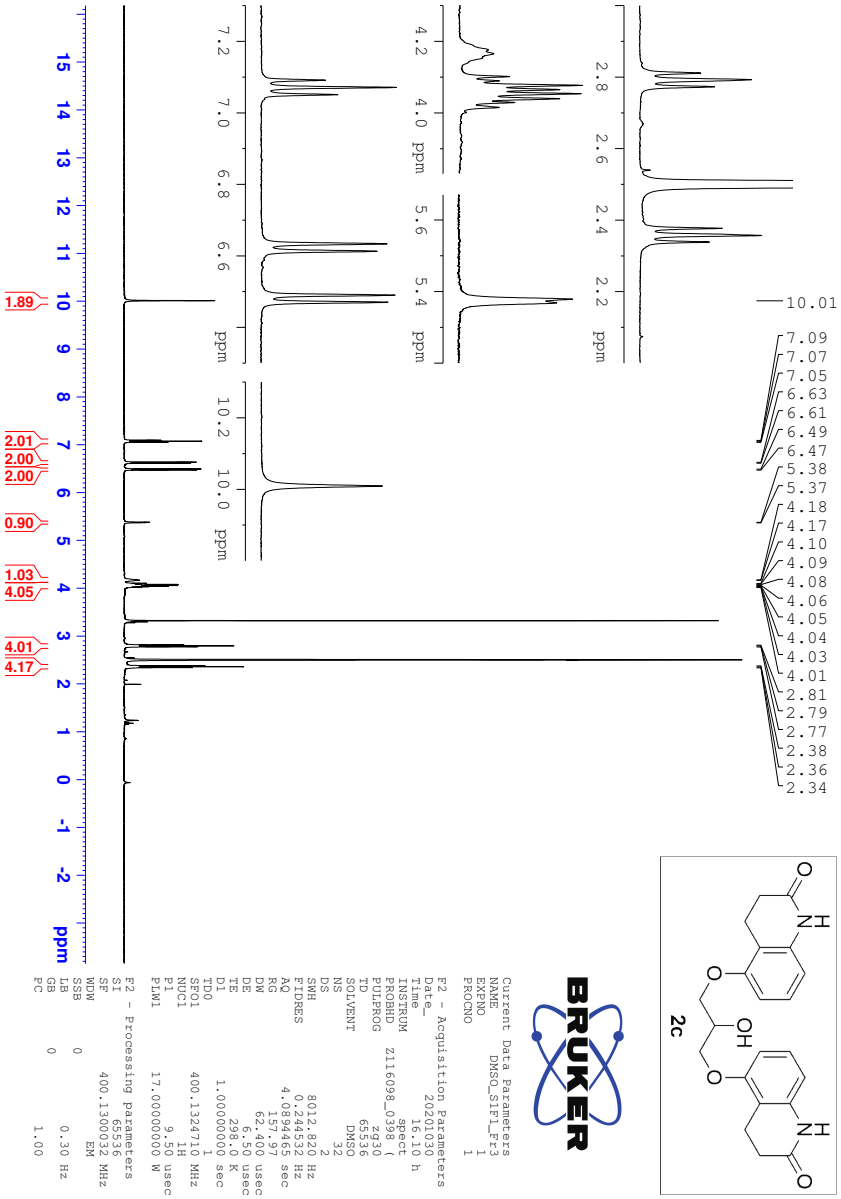

Figure D.1: ^{1}H NMR (400 MHz, DMSO$_{d6}$) spectrum of dimer **2c**.

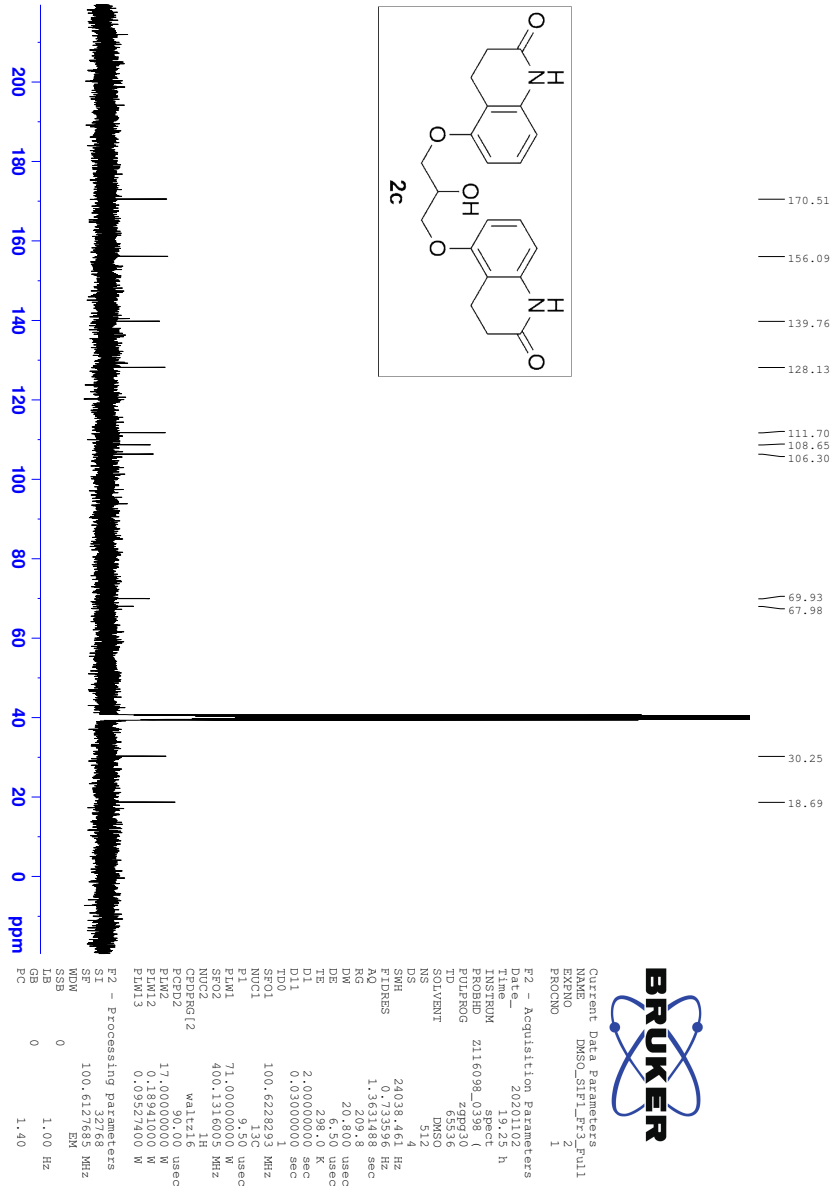

Figure D.2: ^{1}C NMR (400 MHz, DMSO$_{d6}$) spectrum of dimer **2c**.

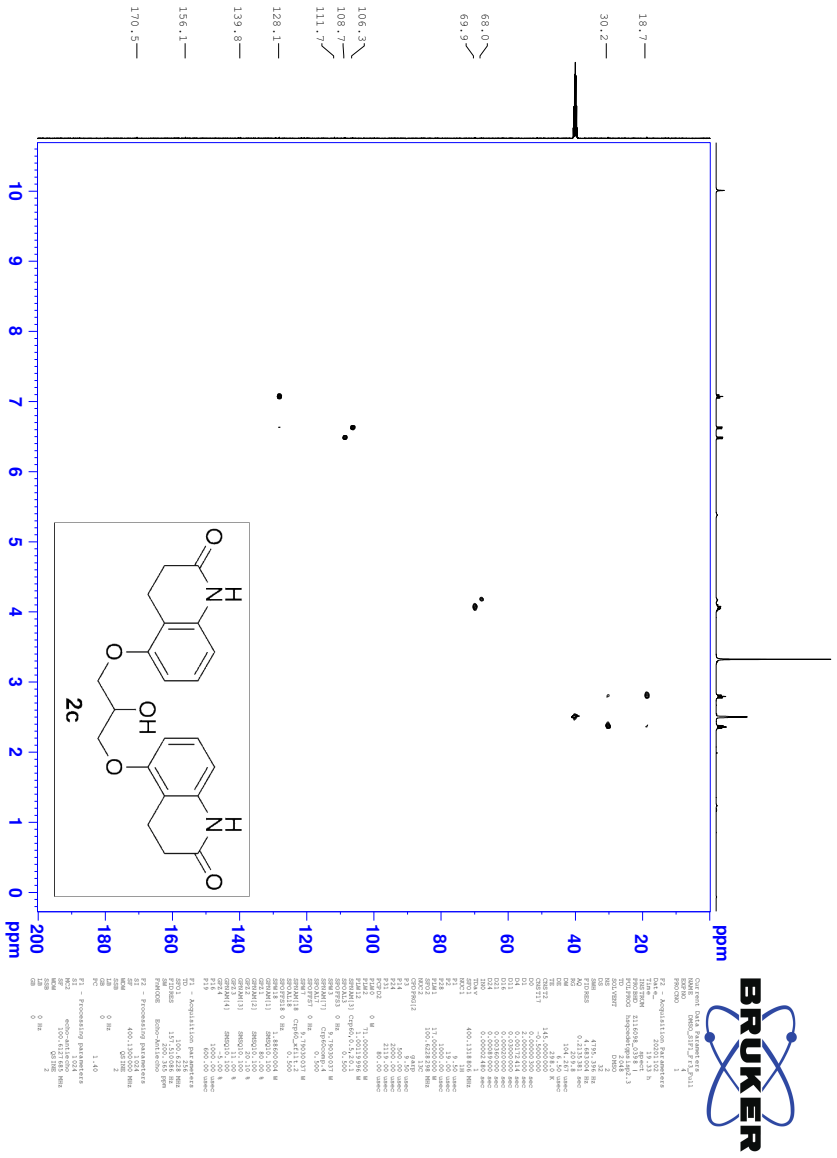

Figure D.3: HSQC (400 MHz, $DMSO_{d6}$) spectrum of dimer **2c**.

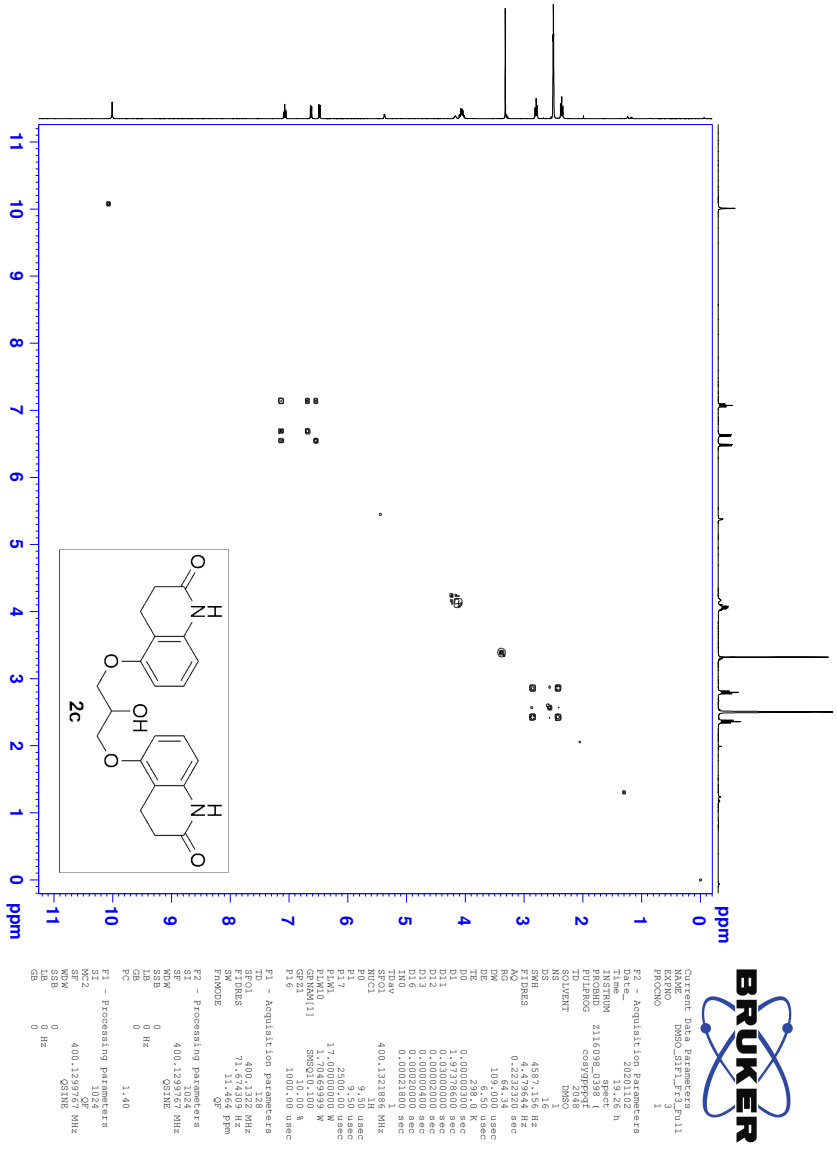

Figure D.4: COSY (400 MHz, $DMSO_{d6}$) spectrum of dimer **2c**.

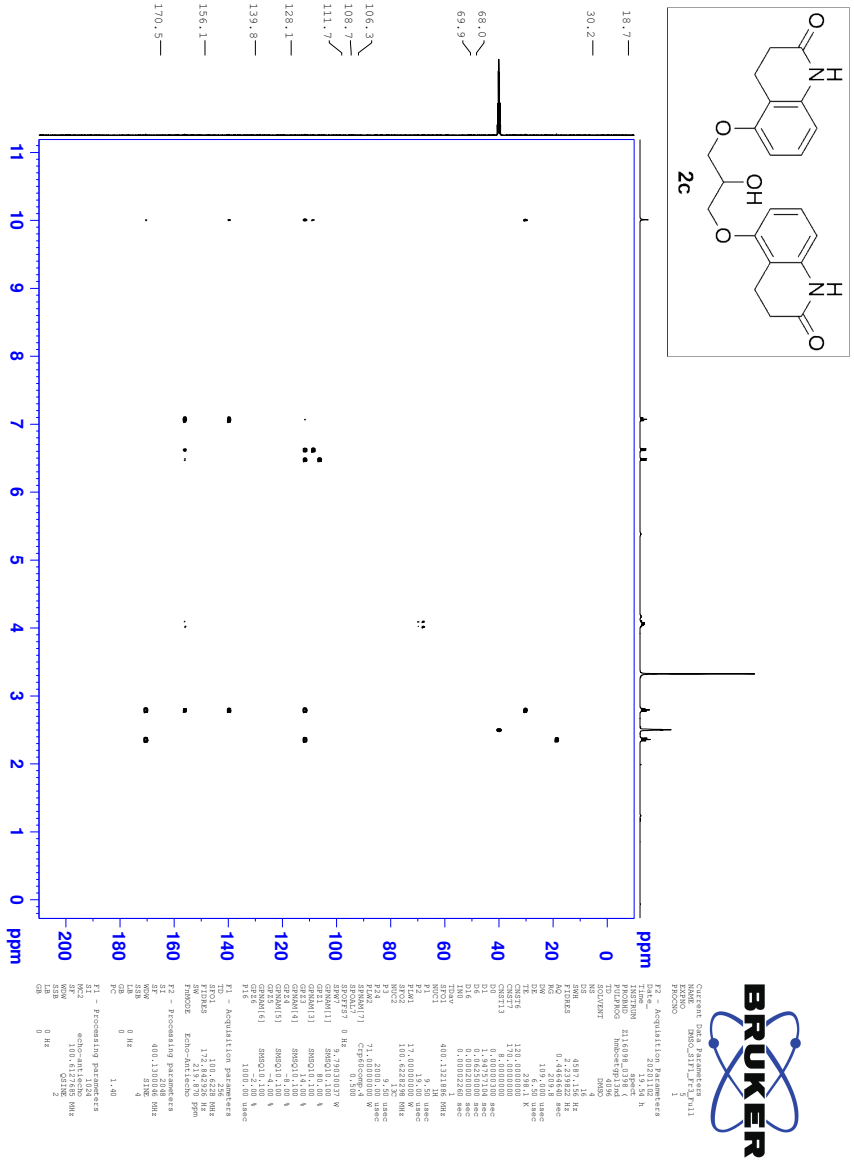

Figure D.5: HMBC (400 MHz, $DMSO_{d6}$) spectrum of dimer **2c**.

Elemental Composition Report **Page 1**

Single Mass Analysis
Tolerance = 2.0 PPM / DBE: min = -50.0, max = 100.0
Element prediction: Off
Number of isotope peaks used for i-FIT = 6

Monoisotopic Mass, Even Electron Ions
1392 formula(e) evaluated with 2 results within limits (all results (up to 1000) for each mass)
Elements Used:
C: 0-100 H: 0-100 N: 0-8 O: 0-8 Na: 0-1
SVG_20201029_S2F3 174 (3.220) AM2 (Ar,35000.0,0.00,0.00)
1: TOF MS ES+

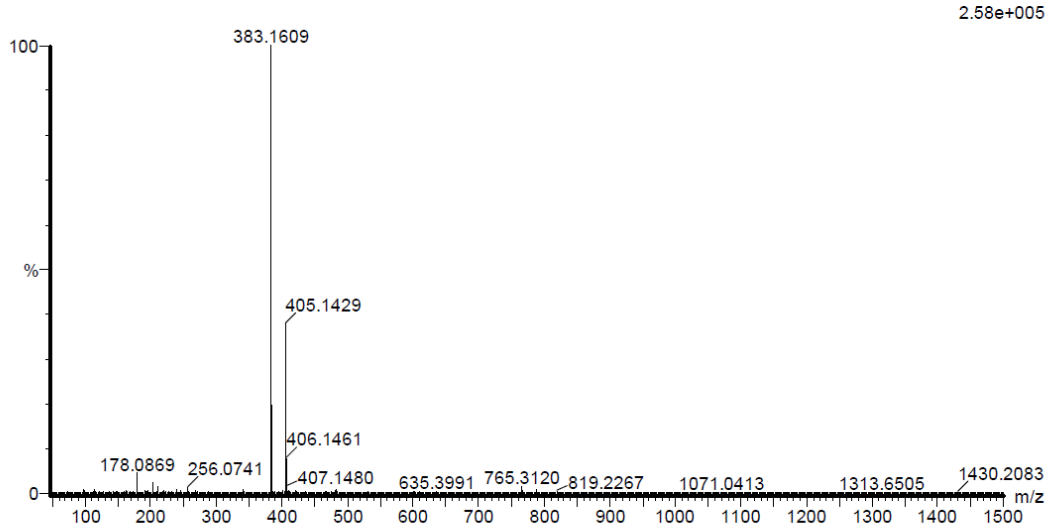

Minimum:				-50.0				
Maximum:		5.0	2.0	100.0				
Mass	Calc. Mass	mDa	PPM	DBE	i-FIT	Norm	Conf(%)	Formula
383.1609	383.1607	0.2	0.5	11.5	1448.3	0.035	96.54	C21 H23 N2 O5
	383.1615	-0.6	-1.6	0.5	1451.6	3.364	3.46	C8 H24 N8 O8 Na

Figure D.6: LC-HRMS (TOF-ASAP$^+$) spectrum of dimer **2c**.

E Characterization of fluorohydrin 2d

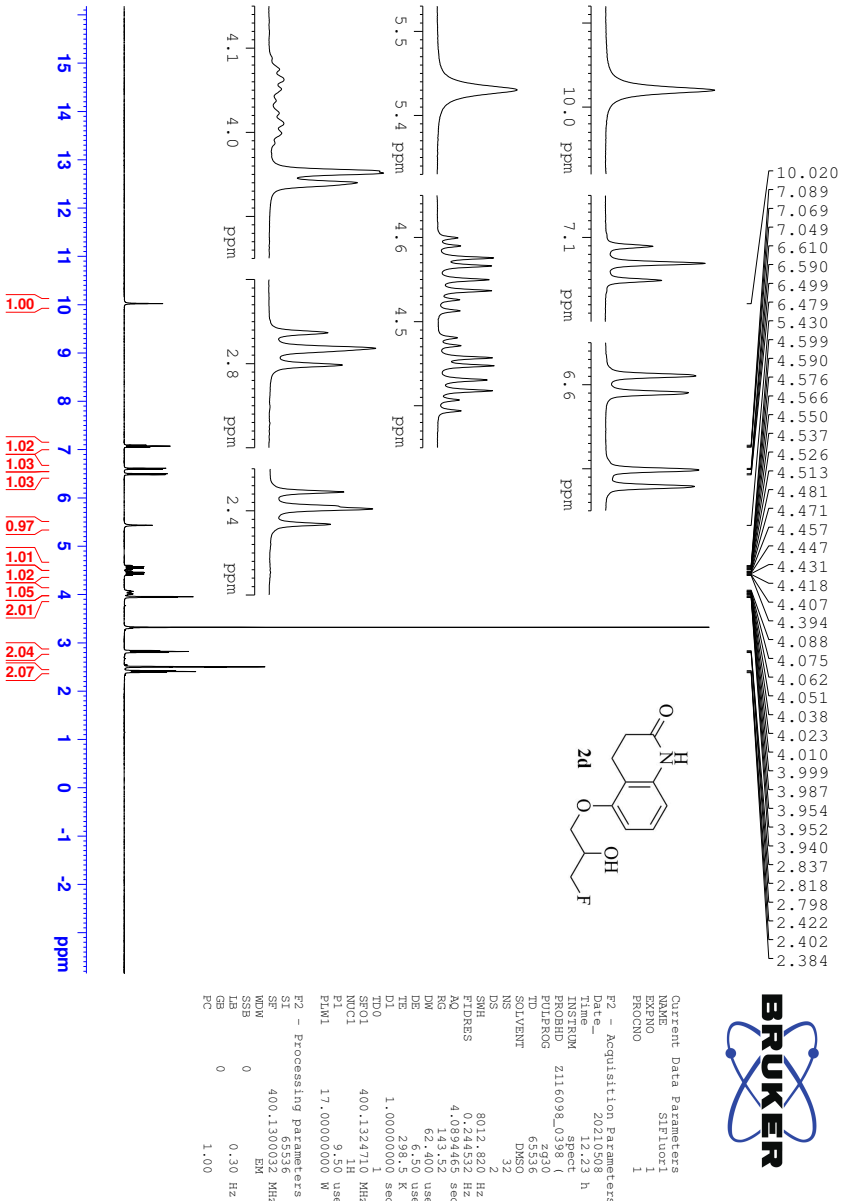

Figure E.1: ^{1}H NMR (400 MHz, DMSO$_{d6}$) spectrum of fluorohydrin **2d**.

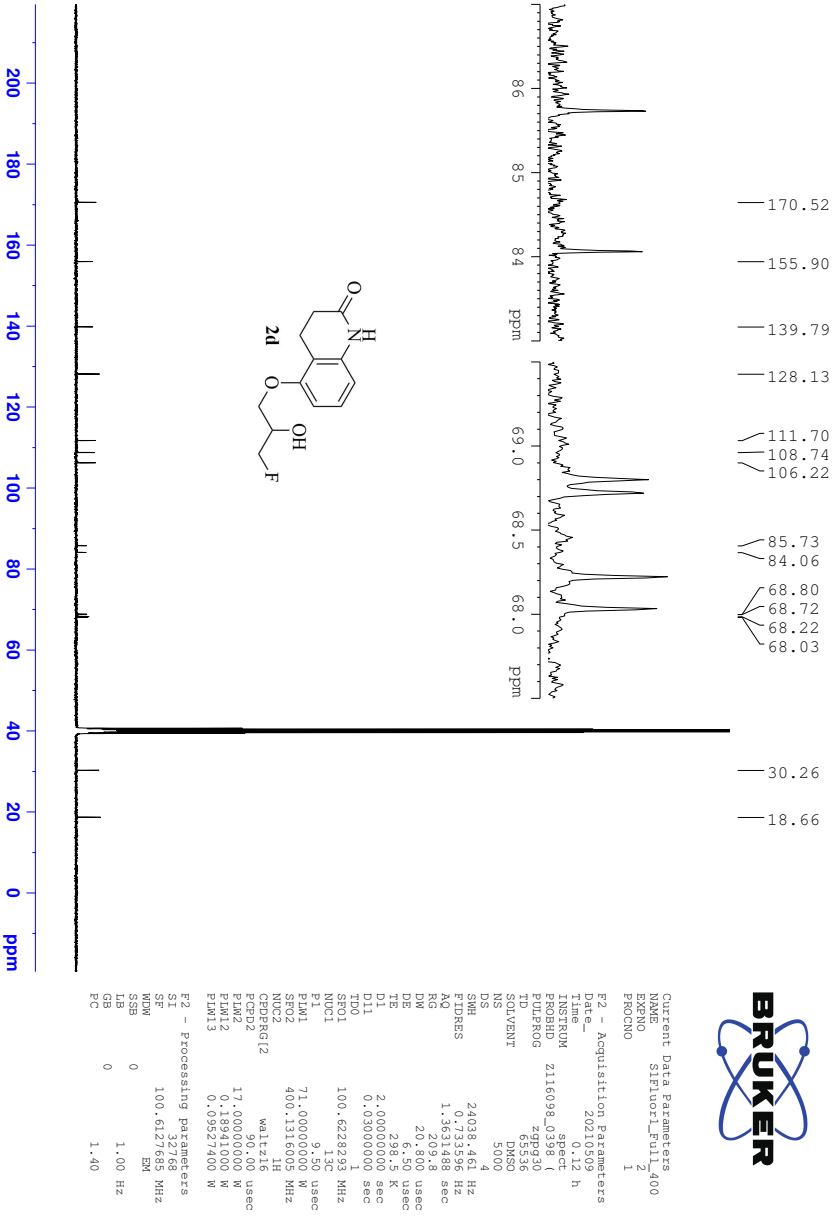

Figure E.2: ^{1}C NMR (400 MHz, DMSO$_{d6}$) spectrum of fluorohydrin **2d**.

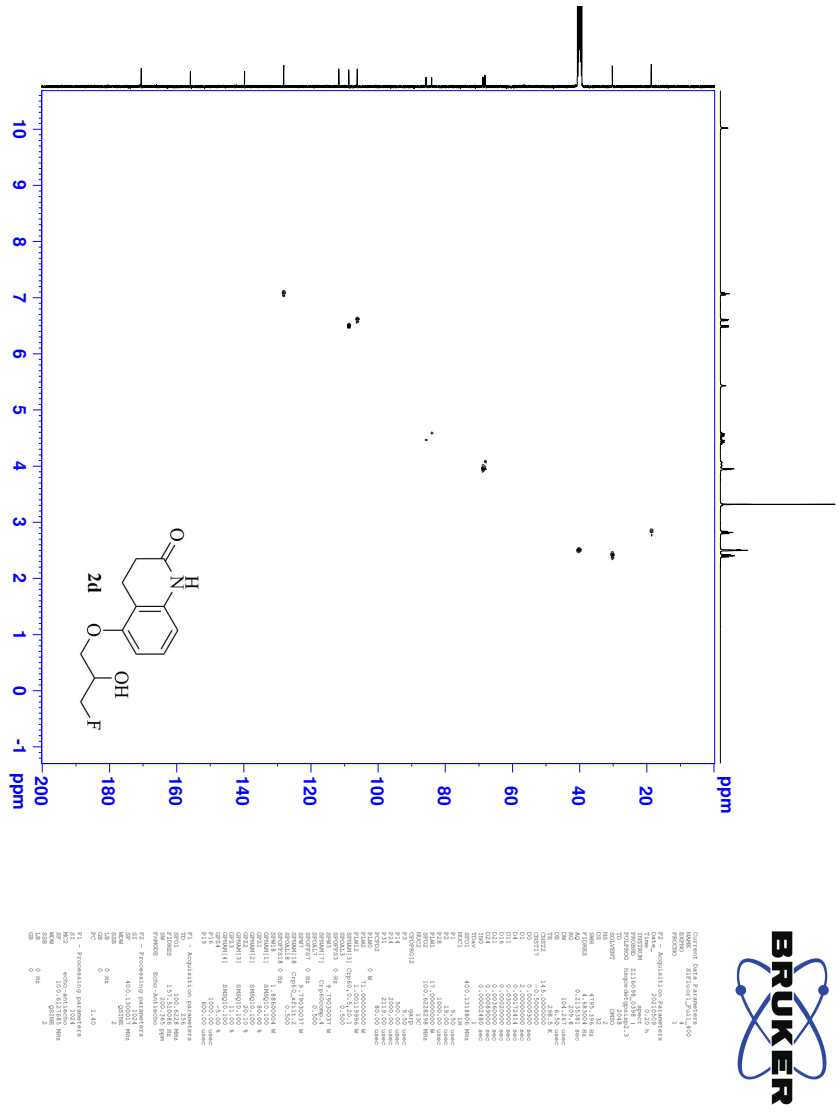

Figure E.3: HSQC (400 MHz, $DMSO_{d6}$) spectrum of fluorohydrin **2d**.

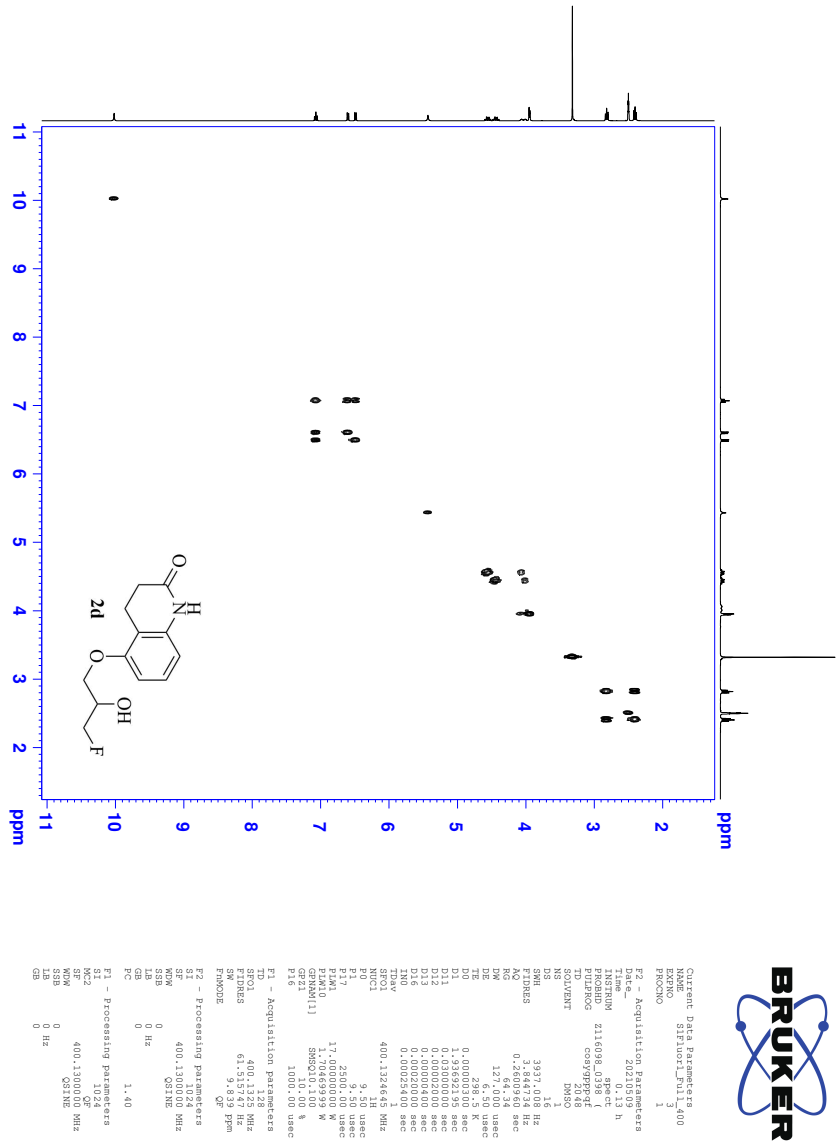

Figure E.4: COSY (400 MHz, $DMSO_{d6}$) spectrum of fluorohydrin **2d**.

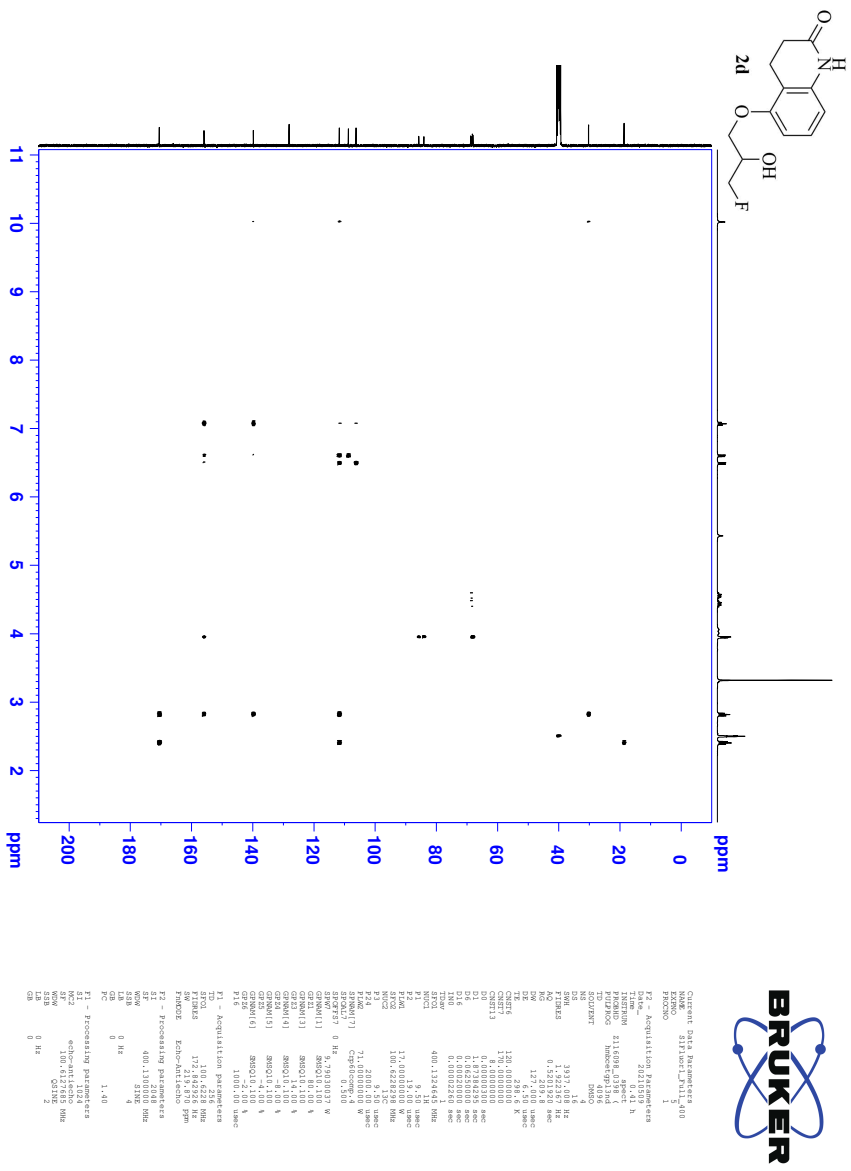

Figure E.5: HMBC (400 MHz, $DMSO_{d6}$) spectrum of fluorohydrin **2d**.

Elemental Composition Report **Page 1**

Single Mass Analysis
Tolerance = 2.0 PPM / DBE: min = -10.0, max = 50.0
Element prediction: Off
Number of isotope peaks used for i-FIT = 6

Monoisotopic Mass, Even Electron Ions
1286 formula(e) evaluated with 2 results within limits (all results (up to 1000) for each mass)
Elements Used:
C: 0-100 H: 0-100 N: 0-10 O: 0-10 F: 0-3
2021_332 68 (0.648) AM2 (Ar,35000.0,0.00,0.00); ABS; Cm (64:68)
1: TOF MS ES+

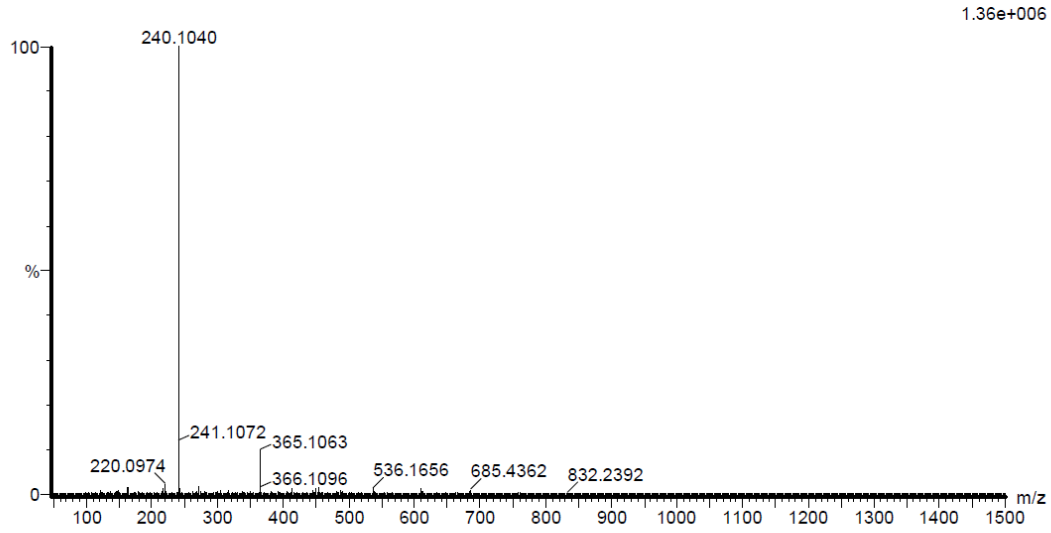

Minimum:				-10.0				
Maximum:		5.0	2.0	50.0				
Mass	Calc. Mass	mDa	PPM	DBE	i-FIT	Norm	Conf(%)	Formula
240.1040	240.1036	0.4	1.7	5.5	2330.0	0.001	99.94	C12 H15 N O3 F
	240.1043	-0.3	-1.2	-3.5	2337.5	7.480	0.06	C3 H18 N3 O9

Figure E.6: HRMS (TOF-ASAP$^+$) spectrum of fluorohydrin **2d**.

F Characterization of ester (*S*)-3

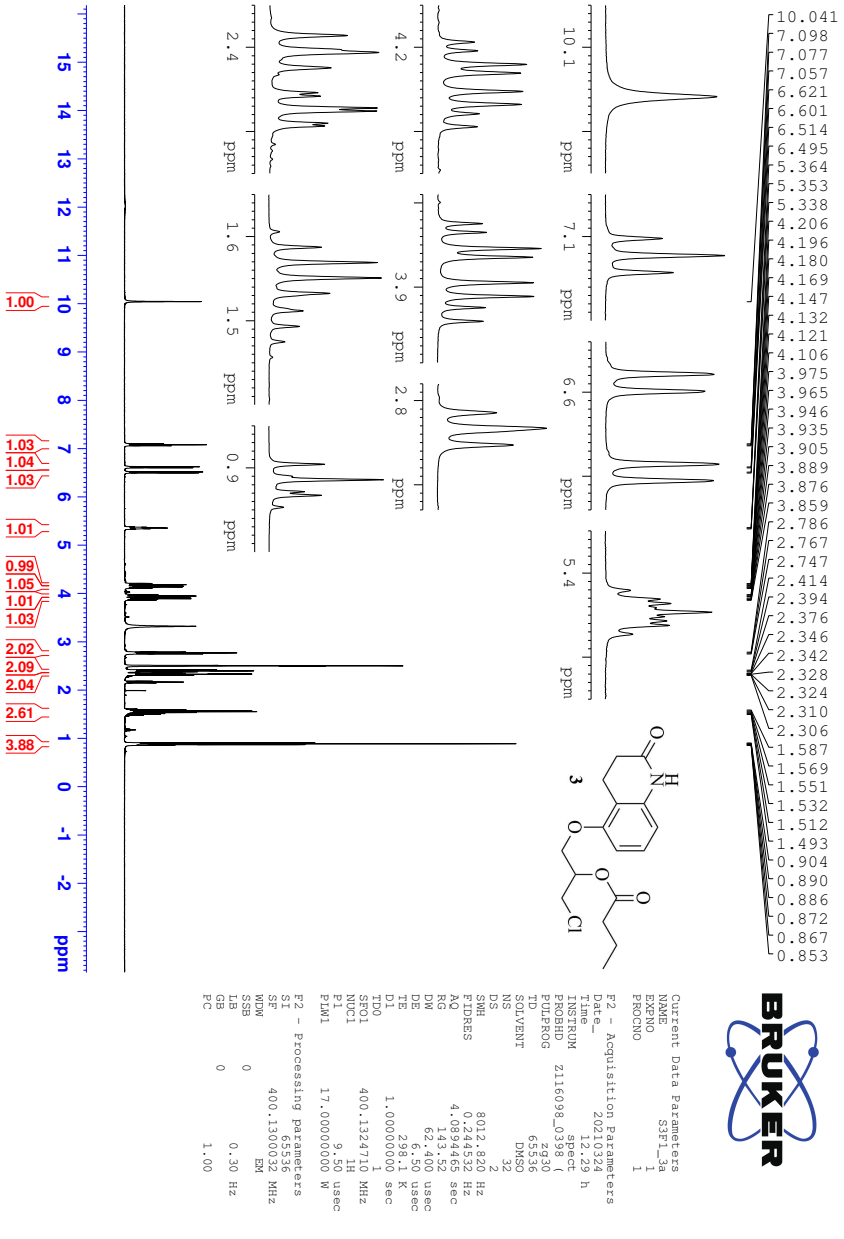

Figure F.1: ^{1}H NMR (400 MHz, DMSO$_{d6}$) spectrum of ester (*S*)-**3**.

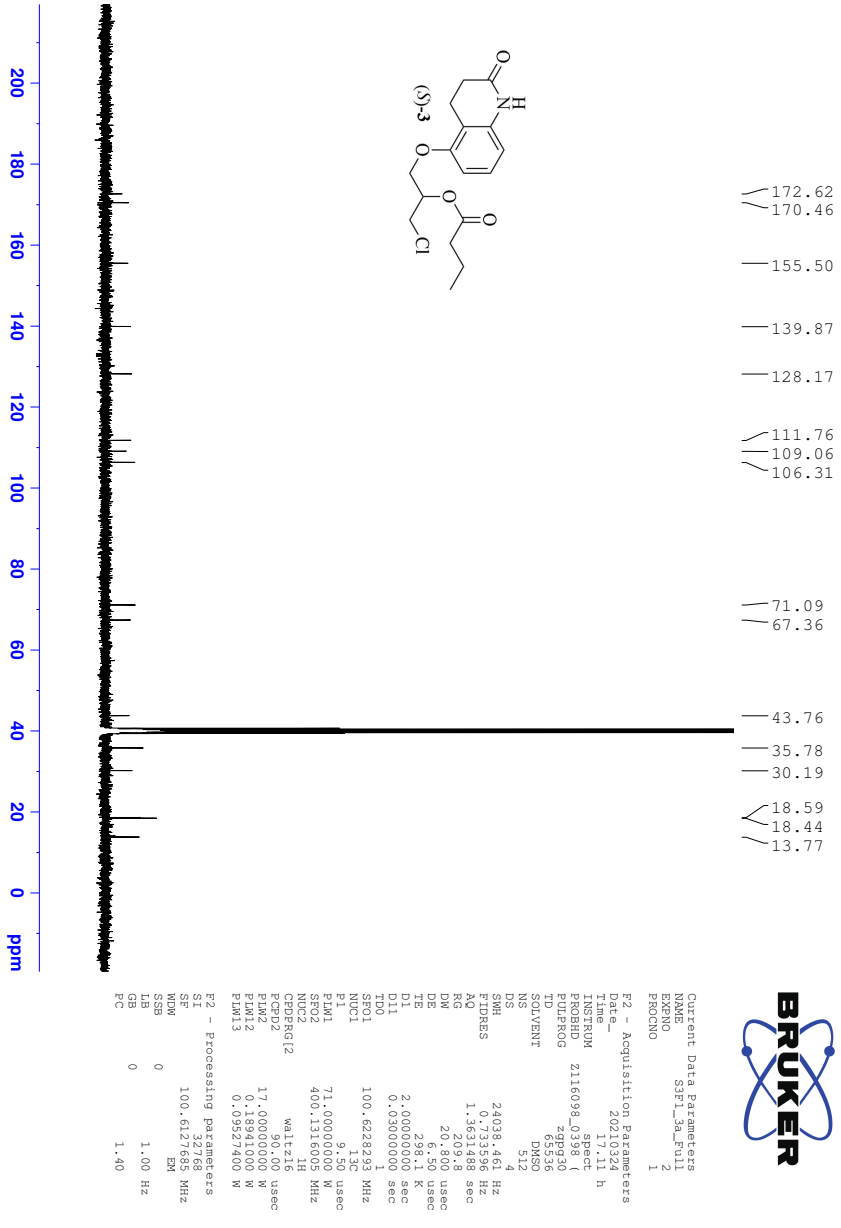

Figure F.2: ^{1}C NMR (400 MHz, DMSO$_{d6}$) spectrum of ester (*S*)-**3**.

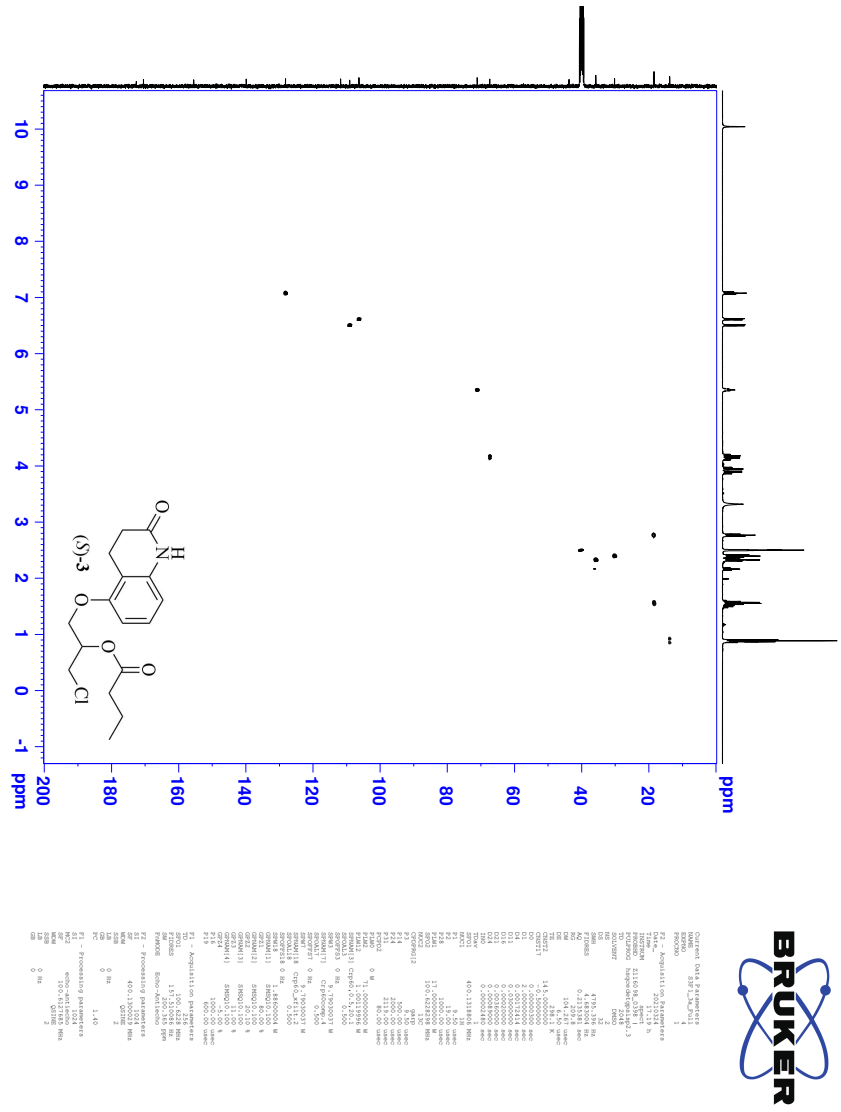

Figure F.3: HSQC (400 MHz, $DMSO_{d6}$) spectrum of ester (*S*)-**3**.

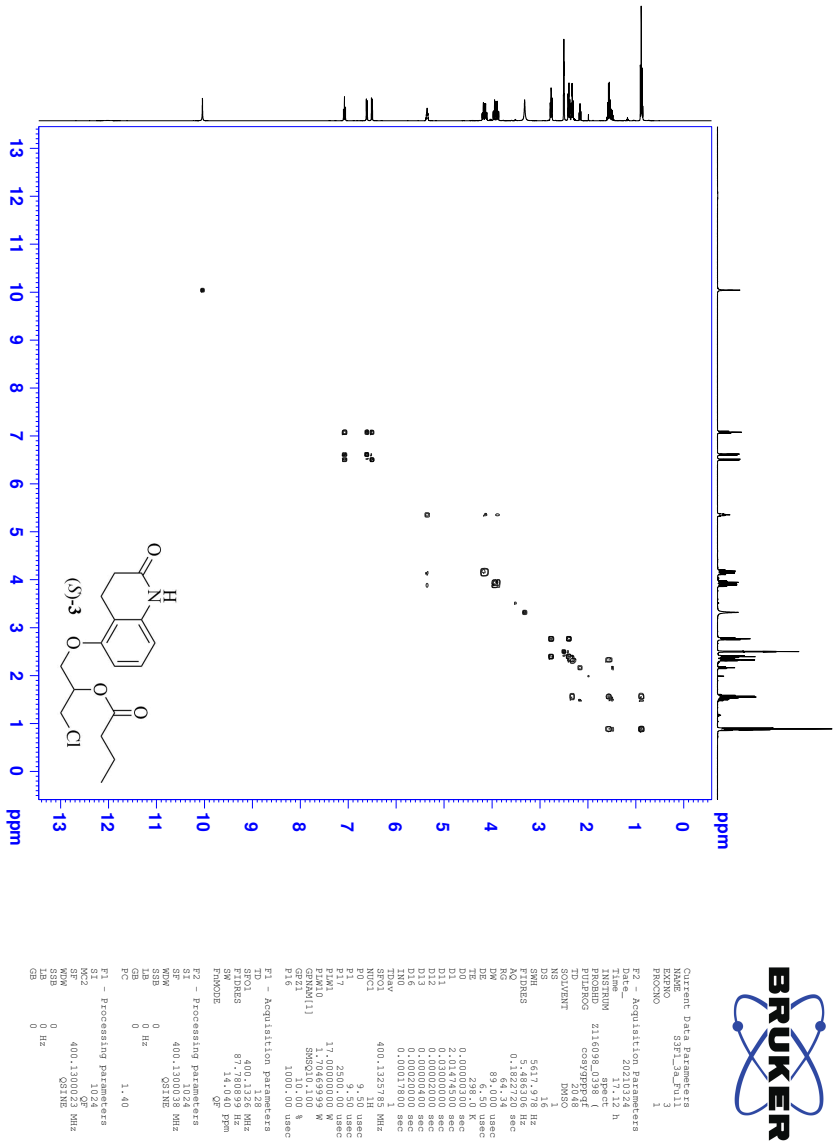

Figure F.4: COSY (400 MHz, $DMSO_{d6}$) spectrum of ester (*S*)-**3**.

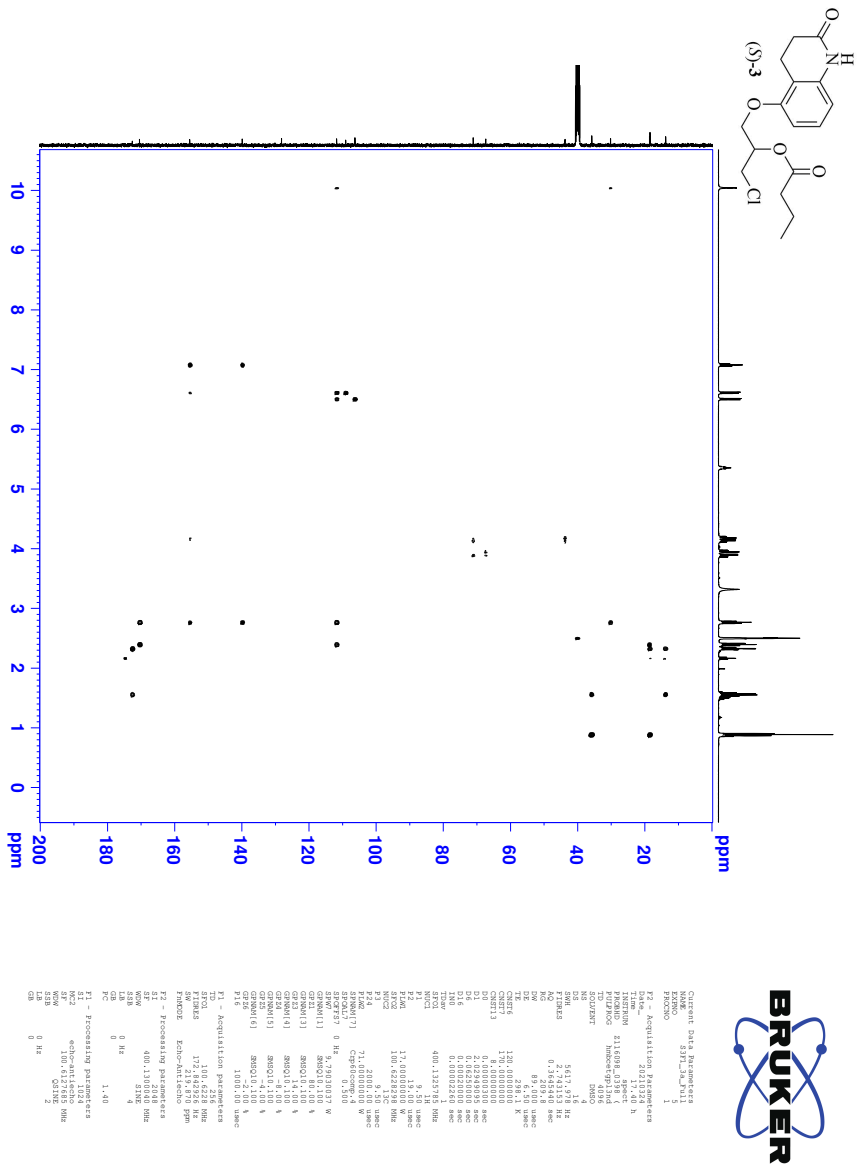

Figure F.5: HMBC (400 MHz, $DMSO_{d6}$) spectrum of ester (*S*)-**3**.

Elemental Composition Report **Page 1**

Single Mass Analysis
Tolerance = 2.0 PPM / DBE: min = -10.0, max = 50.0
Element prediction: Off
Number of isotope peaks used for i-FIT = 6

Monoisotopic Mass, Even Electron Ions
1482 formula(e) evaluated with 1 results within limits (all results (up to 1000) for each mass)
Elements Used:
C: 0-100 H: 0-100 N: 0-10 O: 0-10 Cl: 0-2
2021_334 98 (0.927) AM2 (Ar,35000.0,0.00,0.00); ABS; Cm (98:101)
1: TOF MS ES+

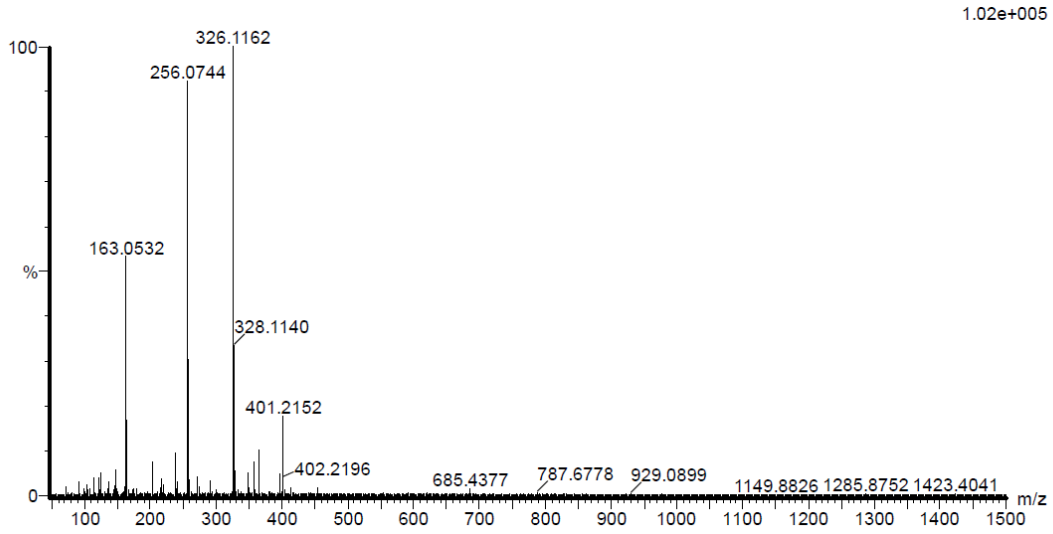

Minimum:				-10.0				
Maximum:		5.0	2.0	50.0				
Mass	Calc. Mass	mDa	PPM	DBE	i-FIT	Norm	Conf(%)	Formula
326.1162	326.1159	0.3	0.9	6.5	1474.4	n/a	n/a	C16 H21 N O4 Cl

Figure F.6: HRMS (TOF-ASAP$^+$) spectrum of ester (*S*)-**3**.

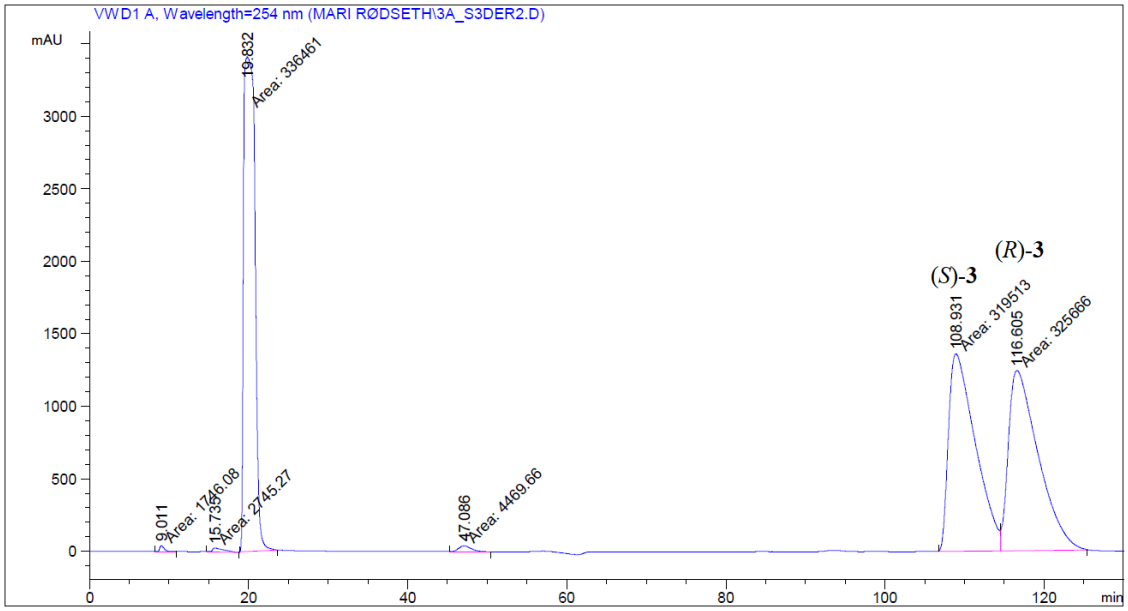

Figure F.7: Chiral HPLC (Chiralcel OD-H, *n*-hexane:*iso*-propanol:diethylamine [95:5:0.4], 0.4 mL/min) chromatogram of racemic ester **3**. Poor separation was attributed to the high concentrations of the sample and a change in solvent.

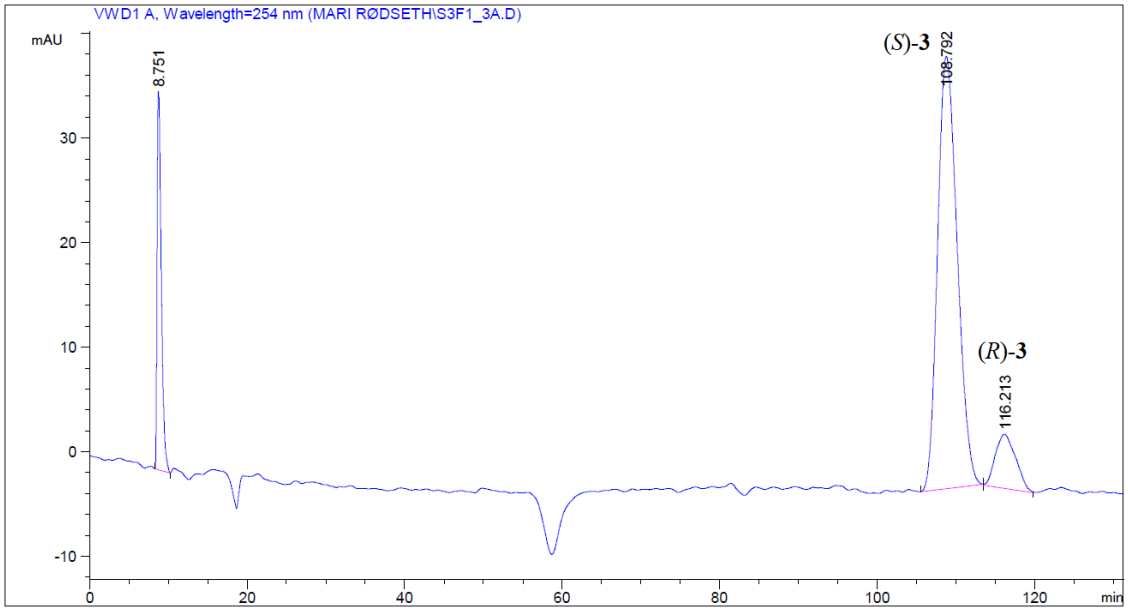

Figure F.8: Chiral HPLC (Chiralcel OD-H, *n*-hexane:*iso*-propanol:diethylamine [95:5:0.4], 0.4 mL/min) chromatogram of ester (*S*)-**3** in 77% *ee*.

G Characterization of carteolol (4)

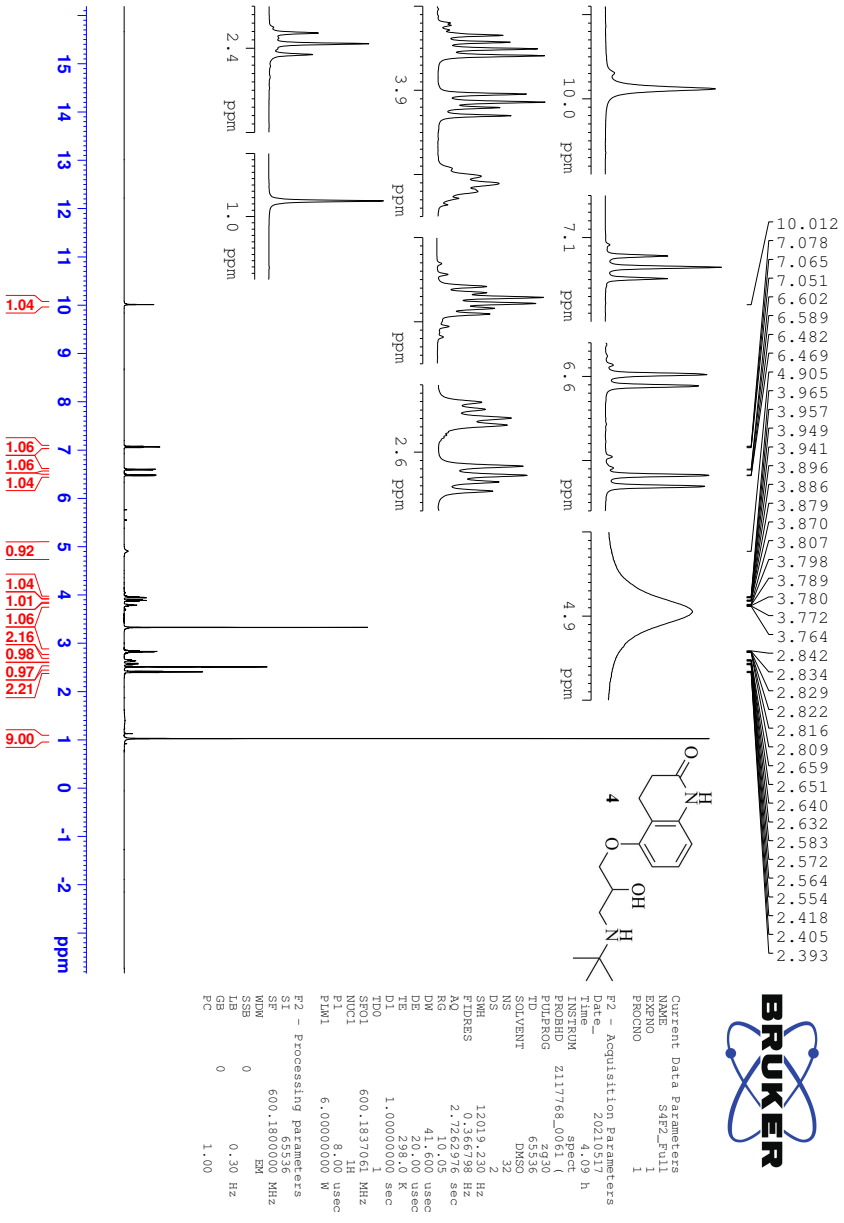

Figure G.1: ^{1}H NMR (600 MHz, DMSO$_{d6}$) spectrum of **4**.

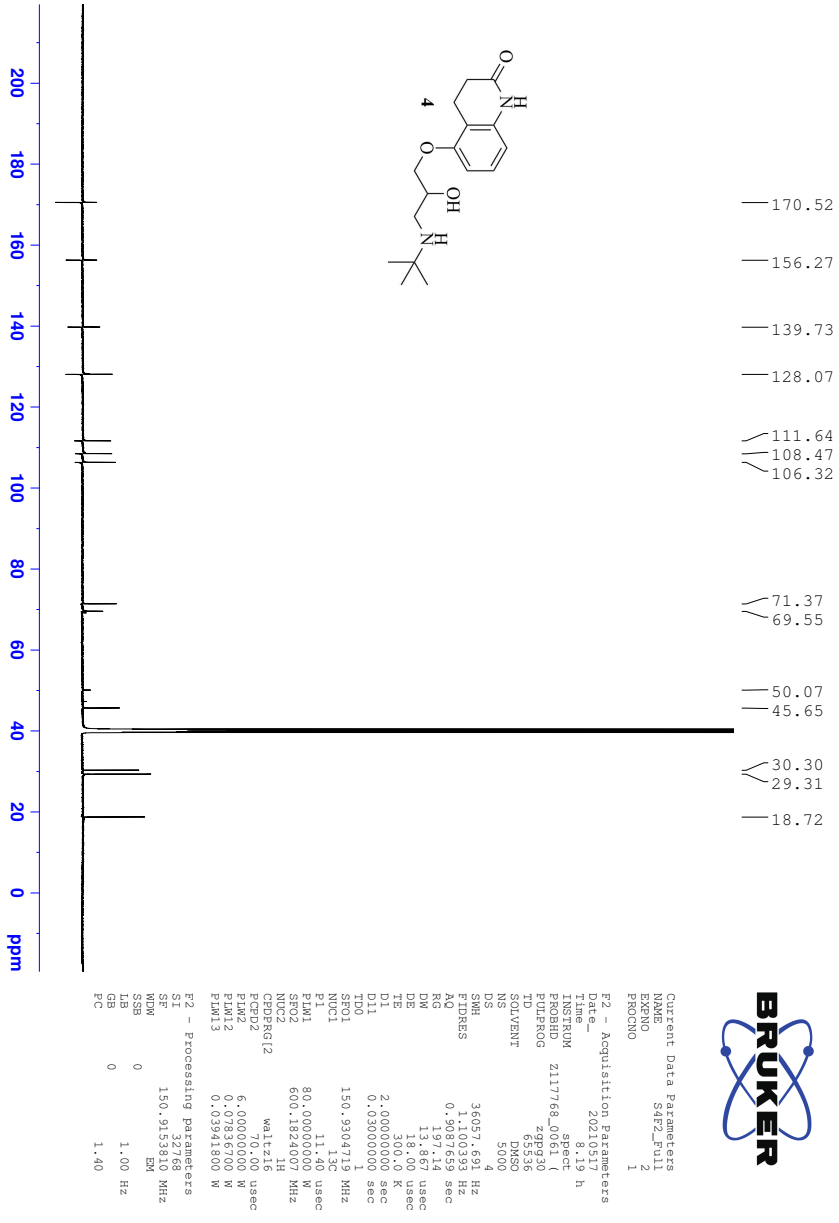

Figure G.2: ^{1}C NMR (600 MHz, DMSO$_{d6}$) spectrum of **4**.

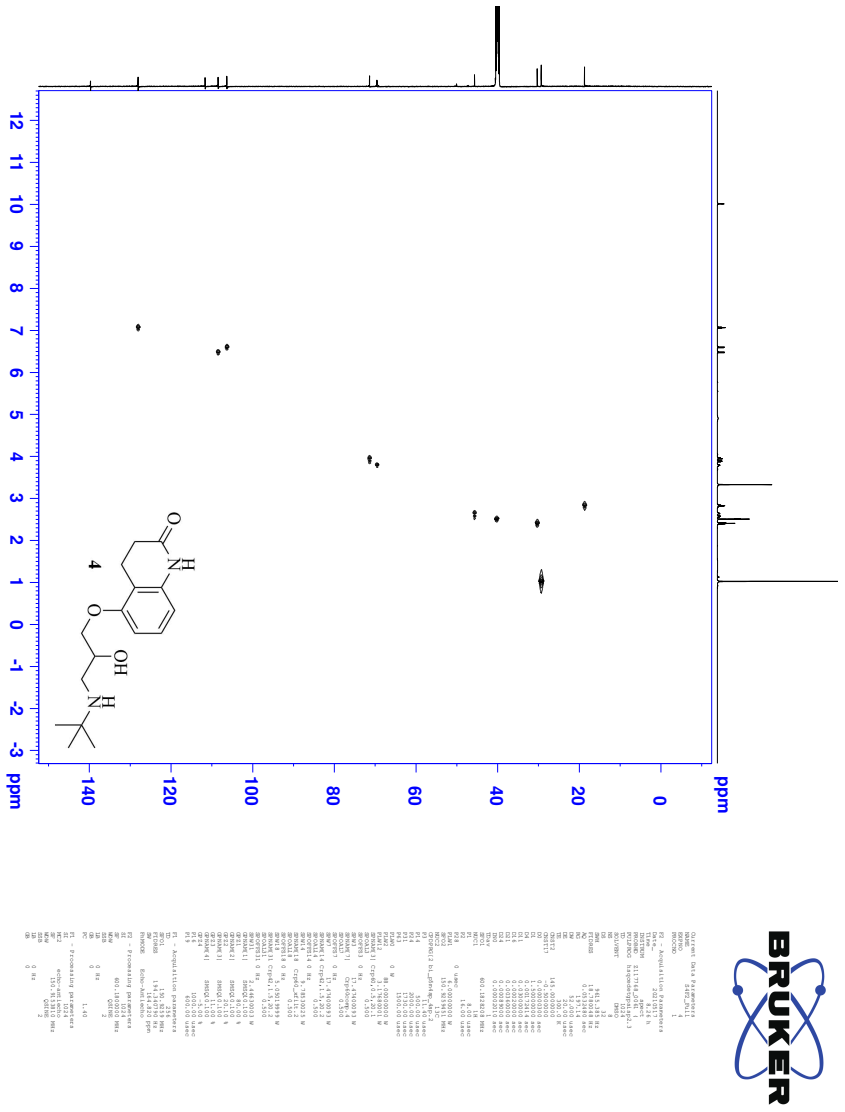

Figure G.3: HSQC (600 MHz, $DMSO_{d6}$) spectrum of **4**.

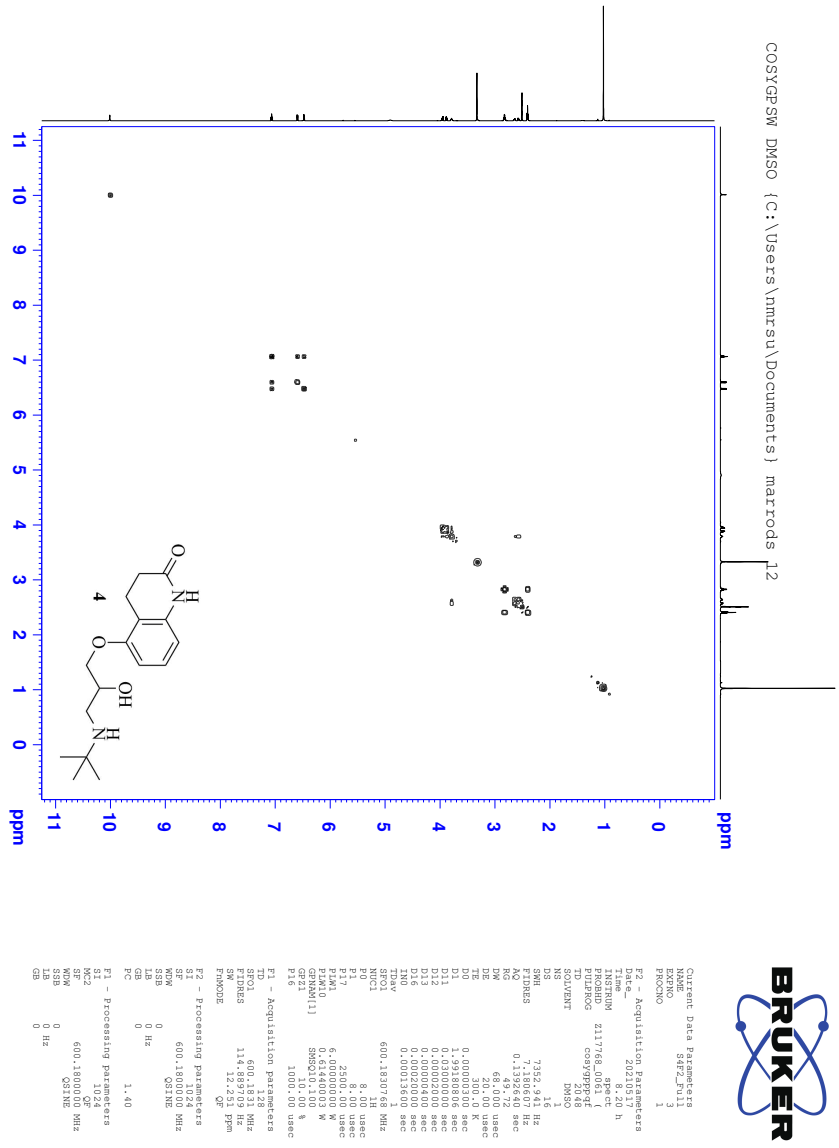

Figure G.4: COSY (600 MHz, $DMSO_{d6}$) spectrum of **4**.

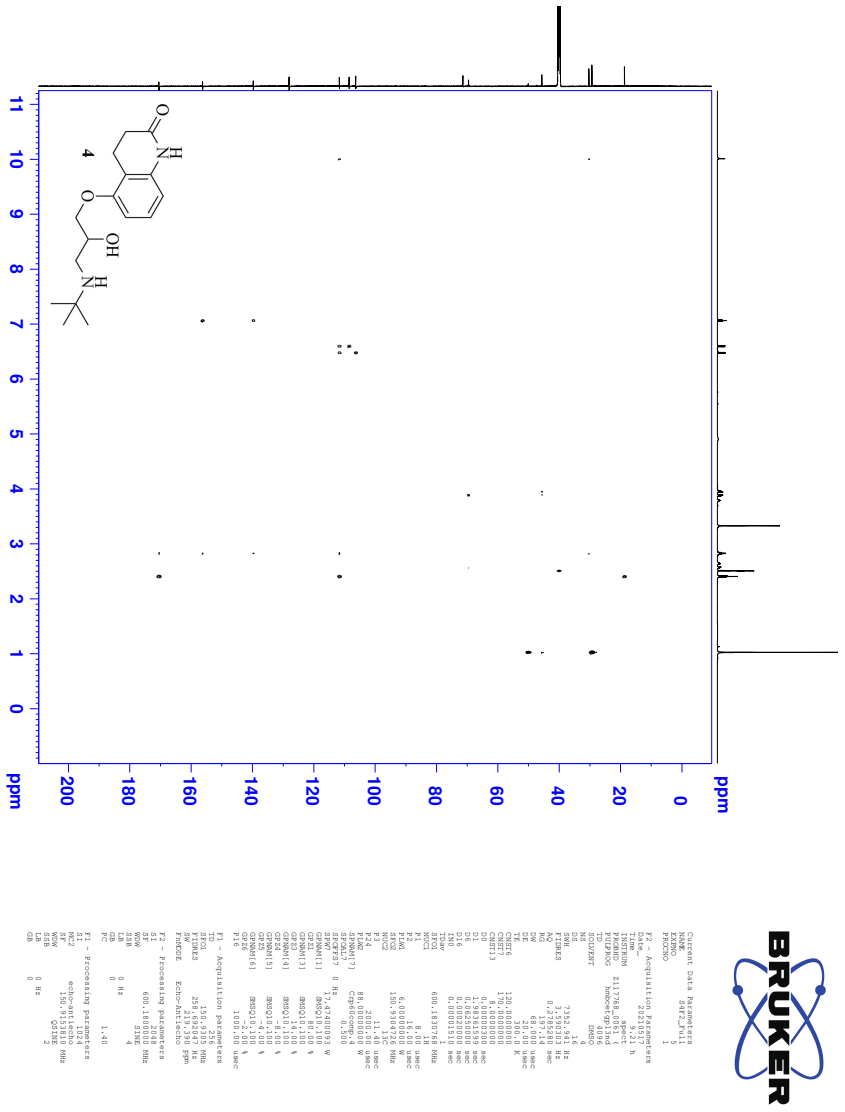

Figure G.5: HMBC (600 MHz, $DMSO_{d6}$) spectrum of **4**.

Elemental Composition Report **Page 1**

Single Mass Analysis
Tolerance = 2.0 PPM / DBE: min = -10.0, max = 50.0
Element prediction: Off
Number of isotope peaks used for i-FIT = 6

Monoisotopic Mass, Even Electron Ions
1291 formula(e) evaluated with 1 results within limits (all results (up to 1000) for each mass)
Elements Used:
C: 0-100 H: 0-100 N: 0-10 O: 0-10 Cl: 0-2
2021_335 74 (0.708) AM2 (Ar,35000.0,0.00,0.00); ABS; Cm (74:79)
1: TOF MS ES+

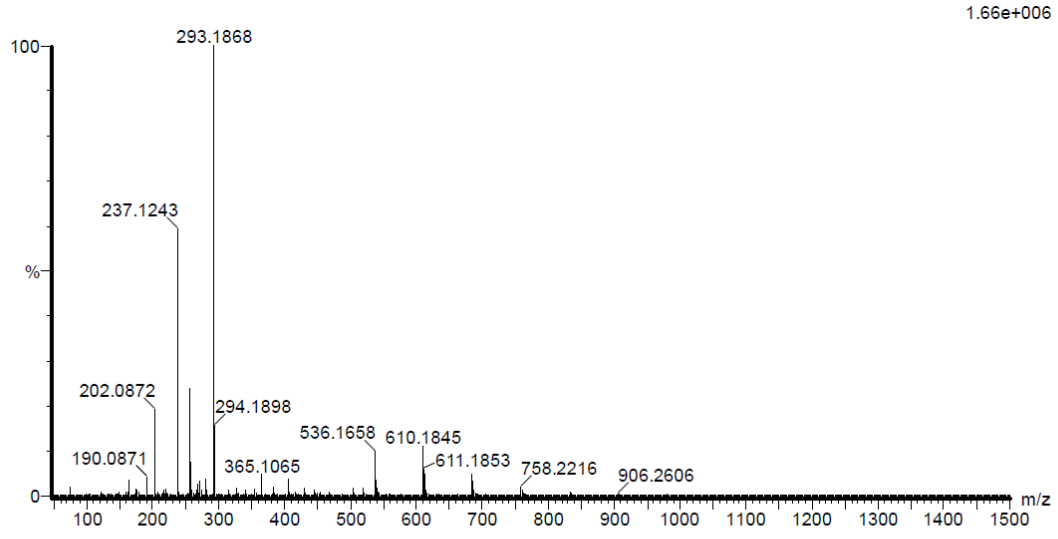

Minimum:				-10.0				
Maximum:		5.0	2.0	50.0				
Mass	Calc. Mass	mDa	PPM	DBE	i-FIT	Norm	Conf(%)	Formula
293.1868	293.1865	0.3	1.0	5.5	1983.7	n/a	n/a	C16 H25 N2 O3

Figure G.6: HRMS (TOF-ASAP$^+$) spectrum of **4**.

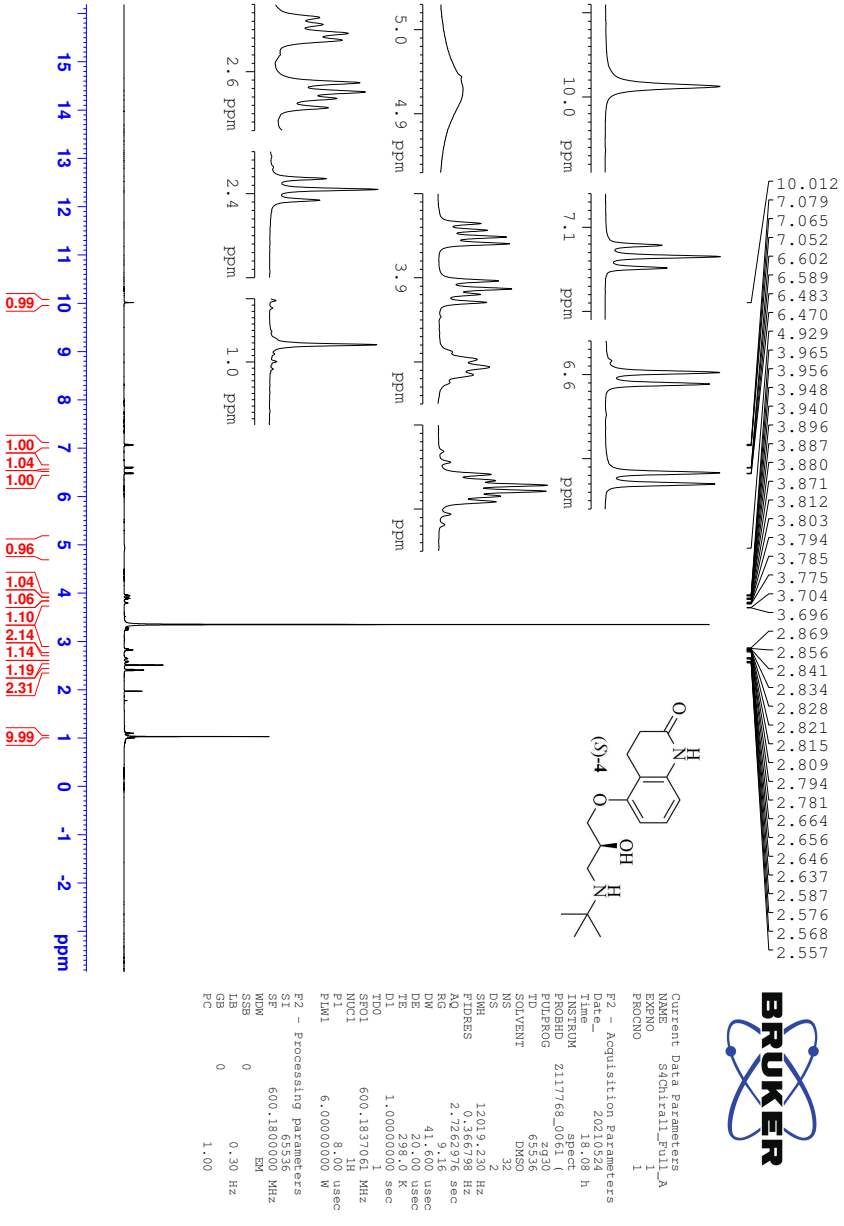

Figure G.7: ^{1}H NMR (600 MHz, DMSO$_{d6}$) spectrum of (*S*)-**4**.

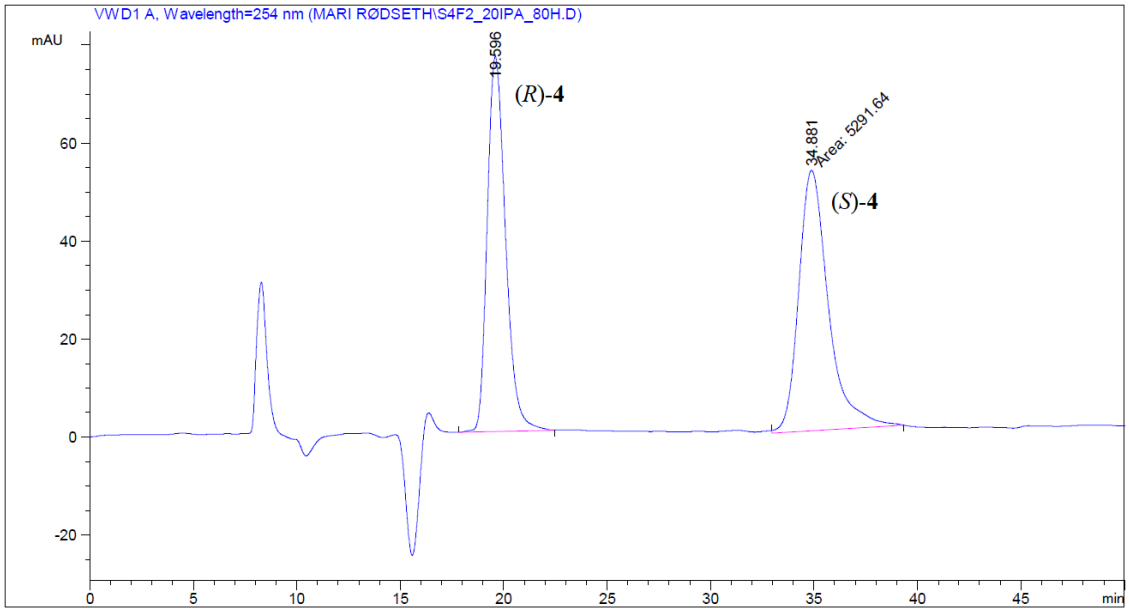

Figure G.8: Chiral HPLC (Chiralcel OD-H, *n*-hexane:*iso*-propanol:diethylamine [80:20:0.4], 0.4 mL/min) chromatogram of racemic **4**.

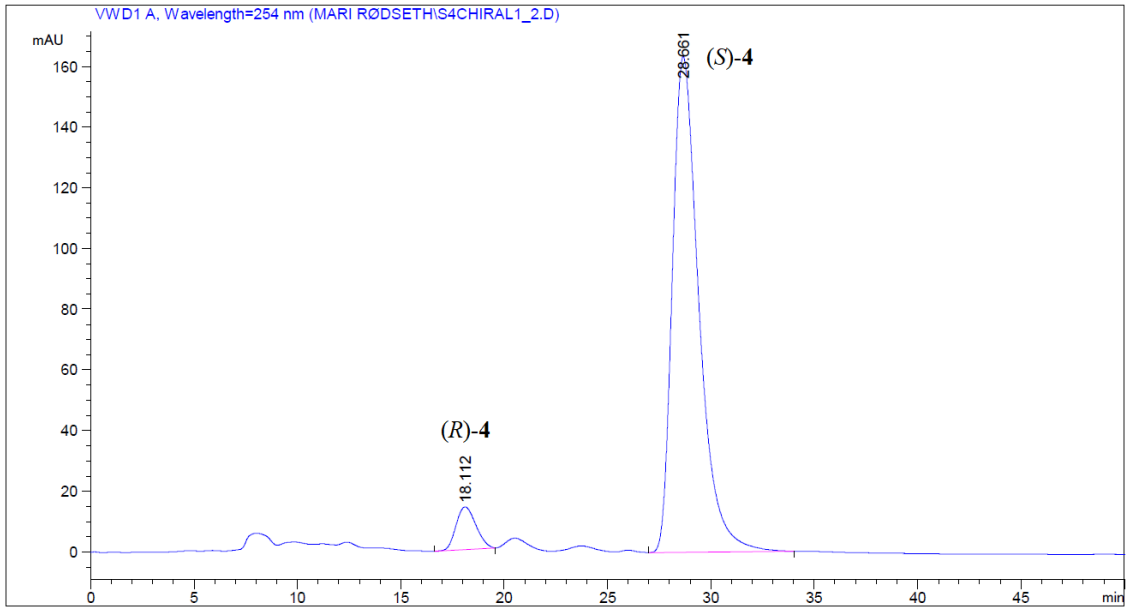

Figure G.9: Chiral HPLC (Chiralcel OD-H, *n*-hexane:*iso*-propanol:diethylamine [80:20:0.4], 0.4 mL/min) chromatogram of (*S*)-**4** in 88% *ee*.

Mari Rødseth

Chemoenzymatic synthesis of (S)-carteolol

NTNU
Norwegian University of
Science and Technology